POLITECNICO DI MILANO

Department of Civil and Environmental Engineering

Master of Science in

Civil Engineering for Risk Mitigation

Hydro-geological process chain for building a flood scenario

Supervisor:

Ing. Laura LONGONI

Co-supervisor:

Dr. Alessio RADICE

Submitted by:

Vladislav IVANOV Matr. 797006

Academic Year 2013 – 2014

Acknowledgements

I would like to express my warm thanks to Dr Alessio Radice, Ing. Laura Longoni and Ing. Davide Brambilla for their exceptional guidance during the preparation and completion of this submission.

Contents

Abstract (English)

Flash flood events in mountain environments are often related to the transport of large amounts of sediment from the slopes through the stream network. As a consequence, significant morphological changes may occur in rivers during a single, short-duration event, with possibly significant effect on the water elevation. An appropriate hazard evaluation would therefore require the thorough modelling of the flood-related phenomena and of their interconnection. In this respect, this thesis will be focused on an attempt of integrated modelling of event-scale water and sediment transport processes for the reference case of the Mallero basin in the Italian Alps. The approach will include the development of a Gavrilovic sediment supply model as well as a hydro-morphological model of the river bed evolution during a 100-year event. Simple hydrological analysis will be also used wherever necessary. Particular attention will be paid to the interface between the geological and hydraulic processes, where the models lack consistency between their respective spatial and temporal scales. The resulting scenario will produce, as a quantitative outcome, an outflow hydrograph into a town crossed by the river in its downstream part. Results will be discussed in terms of the validity of the separate models as well as of the approach for their integration.

Abstract (Italian)

Gli eventi alluvionali in ambiti montani sono spesso associati al trasporto, nei corsi d'acqua, di notevoli quantità di sedimenti, prevenienti dai pendii delle valli. Quindi, anche nella breve durata di un singolo evento la morfologia del fiume può cambiare considerevolmente, con possibili ricadute negative sui livelli idrici. Una valutazione accurata del pericolo alluvionale richiede dunque la modellazione di tutti i fenomeni coinvolti nell'evento di piena, con le relative interconnessioni. Questa tesi presenta un tentativo di realizzare una modellazione integrata del flusso idrico e del trasporto di sedimenti per un evento alluvionale del torrente Mallero (Valtellina). L'approccio modellistico include lo sviluppo di un modello di erosione del suolo tramite l'equazione di Gavrilovic, nonché un modello morfologico di evoluzione del fiume relativamente a un tempo di ritorno di 100 anni. Dati idrologici di riferimento sono usati a supporto dei vari modelli. Si pone particolare attenzione sull'interfaccia tra i modelli di natura geologica e quelli idraulici, dal momento che le scale spazio-temporali di supporto delle due categorie di strumenti sono notevolmente diverse. Il risultato dello scenario è rappresentato da un idrogramma di portata in uscita dal fiume, verso la città che esso attraversa nel tratto di valle. I risultati sono discussi considerando la validità delle stime ottenute e della strategia di integrazione dei modelli.

Abstract (Bulgarian)

Внезапни наводнения в планинските райони са често свързани с транспортирането на големи количества земна маса чрез мрежа от потоци. В резултат, значителни морфологични промени могат да настъпят в реките, в рамките на едно краткотрайно интензивно събитие, с възможност за значителено покачване на водното ниво. По тази причина, адекватна оценка на опасността от наводнение, би изисквала задълбочено моделиране на съответните процеси и тяхната взаимовръзка. В това отношение, тази теза ще се фокусира върху опит за цялостен модел на воден поток, придружен с пренос на значителни седиментни маси за кратко, интензивно събитие свързано с водосборният басейн на река Малеро в италианските Алпи. Подходът ще включва изчисляването на ерозивен седиментен принос по модела на Гаврилович, както и хидроморфологичнен модел на еволюцията на речното легло по време на събитие с период на повторение от 100 години. Особено внимание ще бъде отделено на взаимодействието между двата модела, където липсва съгласуваност в съотвените им времеви и пространствени характеристики. Като количествен резултат, полученият сценарий, ще доведе до наводнение в град, намиращ се в долната част от басейна на реката. Резултатите ще бъдат оценени по отношение валидността на отделните модели, както и подхода за тяхното интегриране.

Introduction

Flash floods have the potential to induce major physical as well as socio-economic damage to our society. They are natural phenomena and as such, their occurrence cannot be directly prevented. As a recent example, an enormous flood destroyed a suburb of the second largest city in Bulgaria – Varna, in July 2014 after 150 mm of rain fell for less than twenty four hours. Although it did not happen in a mountain region, a considerable mass of debris and mud was swept and deposited in the lower part of the stream, exactly where the inhabited area is situated. 11 people died and many others were injured and left without shelter. Even more recently, in November 2014, Northern Italy was struck by torrential rainfalls, resulting in massive floods and the collapse of numerous landslides. A total of 11 casualties have been recorded in a month in addition to the destroyed structures and infrastructure in the regions of Lombardia, Tuscany, Liguria and Emilia-Romagna. It is therefore evident that the consequences of disasters of such nature should not be dealt with after they happen, but avoided in the safest way possible. Since the nature cannot be controlled, prediction becomes crucial. In this respect, working towards the modelling of a flood event becomes significant and can be eventually used as a mitigation tool in support of civil protection, land use planners, emergency managers, and the implementation of an early warning system.

Flood events in mountain basins often involve large volumes of sediment transported by the streams. As it happens, sediment may be already present in the river or conversely, supplied during the event. However, in a mountain river basin, numerous sources of sediment supply are available such as localized debris flows, fault zones, unstable shallow landslides. These sources, however, may be significantly scattered over the area of a large river basin. Therefore, the presence of a widespread phenomenon, such as soil erosion could be the prevailing source of solid mass into the streams.

Not until the last couple of decades, there has risen a concern and a clear idea that soil erosion and its consequences, in the face of changes in river morphology, can lead to flood related hazard. Proper river management has been recognized as necessary for the prevention of river bed obstruction and possible limitation in channel conveyance and flood pain storage. In addition, in 2007 the European Parliament created a European Floods Directive, stating that sediment transport is a relevant factor when a flood hazard assessment is performed.

This process however has always been regarded as a long term process that spans over decades in order to show a noticeable effect on the river morphology and in this sense to eventually increase hazard probability. Since intrinsically soil erosion is indeed a long term process, modelling has been carried out with the assumption that river bed is stationary or quasi-steady, which may be reasonable when there is a clear distinction between timescales of morphologic evolution and a

flood event (Radice et al. (2012)). Although this is usually the case in lowland, mountain environments offer various features which are crucial for the behavior of an upland stream as opposed to lowland one. These have been pointed out by Klaassen (1997) as: 1) a small basin leads to a swift time response of the system to intense and localized rainfall events; thus, flow hydrographs are typically steep and short; 2) the slopes generate high flow velocities; 3) sediment transport phenomena can be very intense, as is the case during flash floods. Therefore, a large portion of eroded material, can be transported downstream within a couple of days or even hours with a single wave. Thus, the difference in timescales could become negligible or even non-existent. Therefore an important conclusion can be drawn, that a coupled approach between morphological changes due to sediment transport and flood risk analysis should always be undertaken, when dealing with any flood scenario. Research in this issue has recently been carried out, among others, by Ballio and Menoni (2009), Brambilla et al. (2011) Radice et al. (2012), Radice and Rosatti (2012), at Politecnico di Milano. It is however due to the complexity of the problem that certain obstacles in the modelling chain still exist such as the inconsistency of time and spatial scales between the different phenomena and the large portion of uncertainty underlying semi-empirical formulas and mathematical models. Therefore, this thesis will represent a significant follow-up, aiming to establish an interface between the two different models and to produce a phenomenological process chain describing a flood. The analysis will be developed on the basis of the field case of the Valmalenco valley and its main stream – the Mallero river, located in the province of Sondrio, northern Italy. A return period of 100 years will be considered. An emphasis will be put on the validity of the results obtained by the different models as well as the approach for their integration.

The following work will start with a description of the Mallero basin in Chapter I. Its characteristics in terms of both hydraulic and geological aspects will be presented along with a reminder of the flood event that struck the surrounding region during the summer of 1987 and provoked the onset of numerous studies, some of which will be briefly reviewed in this first chapter. Chapter II will be devoted to the estimation of sediment yield in the basin considering the widespread erosion phenomena as a predominant source of solid mass into the streams, therefore neglecting the effect of localized sources and major unstable landslides. Thus, the Gavrilovic method will be applied on a sub basin level as it is often considered the most suitable for mountain catchments. Further, Chapter III will deal with the problem of the morphological evolution of Mallero. After a reorganization of the existing river geometry, a morphological model will be produced and calibrated to recorded bed and water surface elevation levels of the reference event of 1987. The calibration will be in terms of friction coefficients and sediment grain size distribution along the river stream. This model will serve as a benchmark for the subsequent Chapter IV where the integration of the two previous models will

be attempted. In order to overcome the inconsistency between the models several assumptions will be made and their validity shall be discussed in terms of the results obtained. As a final result of the process chain, a flood with an outflow into the town of Sondrio will be created along with an estimation of its time variation, peak discharge and cumulated volume of flood water.

Chapter I. Case study – Mallero basin

This chapter will present a thorough description of the area of study. The problem of hydro-geological risk will be related to the basin and the reasons to link morphological evolution and soil erosion will be laid out. An important feature will be the description of the notorious event of 1987 which threatened the town of Sondrio. This has been a natural "alarm" and the reason for many investigations in the matter, including this one. Some of the work carried out on the topic at Politecnico di Milano in the past years will be briefly reviewed.

1. Characteristics of the basin

The hydrologic basin of Mallero river is situated in the southern flanks of the Alps in the northern part of Italy where it borders with Switzerland. It is a mountainous basin spreading over the Valmalenco valley with its highest point at around 4000 meters above mean sea level and ending at 298 meters at Sondrio. . The area of the catchments is around 320 km^2 in total and its main river stream, Mallero, is some 24 km long. While at the downstream end the river is characterized by a mild slope varying in the range 0.1%-1.2%, upstream the slopes are rather steep, ranging from 4% to 40% locally (mean values around 8%). The river receives water supply from its tributaries the largest of which are Lanterna, Torreggio and Antognasco (Figure I-1). There are several urban settlements along the stream, the biggest and most important of which is the town of Sondrio. It is located close to the confluence between Mallero and Adda rivers, around 150 km northwest from the city of Milano. The town lies on an evident sharp river bend (Figure I-1) after which there are four bridges connecting its western part with the eastern one (Figure I-5). The river channel inside the town has rather regular, almost rectangular shape with widths ranging from 20 to 60 m and banks elevated from 5 m to 8 m. In terms of granulometry, the median sediment size in the in-town part is in the range $2cm<d_{50}<11cm$, while upstream, sizes vary up to boulders of 200 cm, according to field investigation conducted by ITALTEKNA et al. (1989).

In order to obtain a more clear idea of the stream geometry, (Figure I-2) shows the longitudinal profile of the river bed along with the banks. The blue part of the bed represents the location of the town of Sondrio and the orange part is a river portion of about 3km upstream the town. These two portions combined will be the focus of this analysis which will be discussed in Chapter IV.

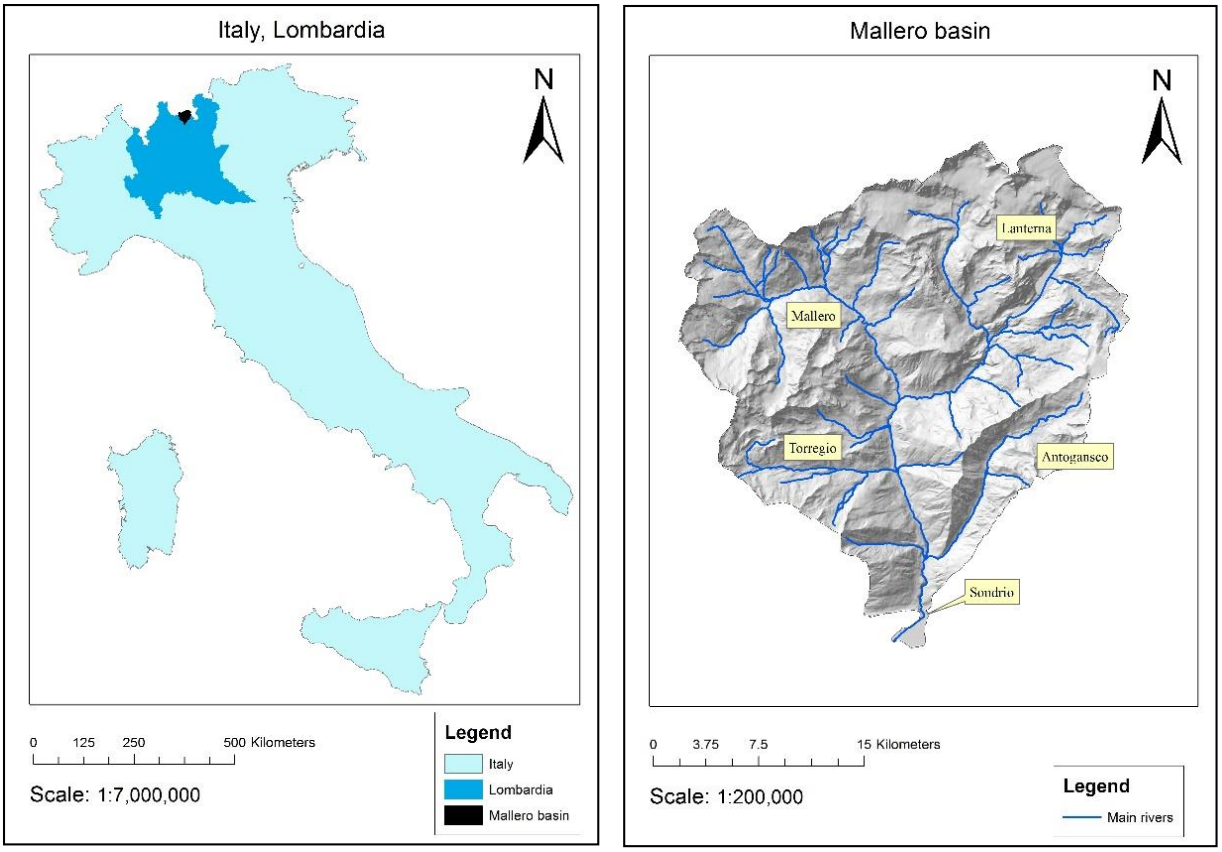

Figure I-1 Left – Mallero Basin; Right – Italy and Lombardia region

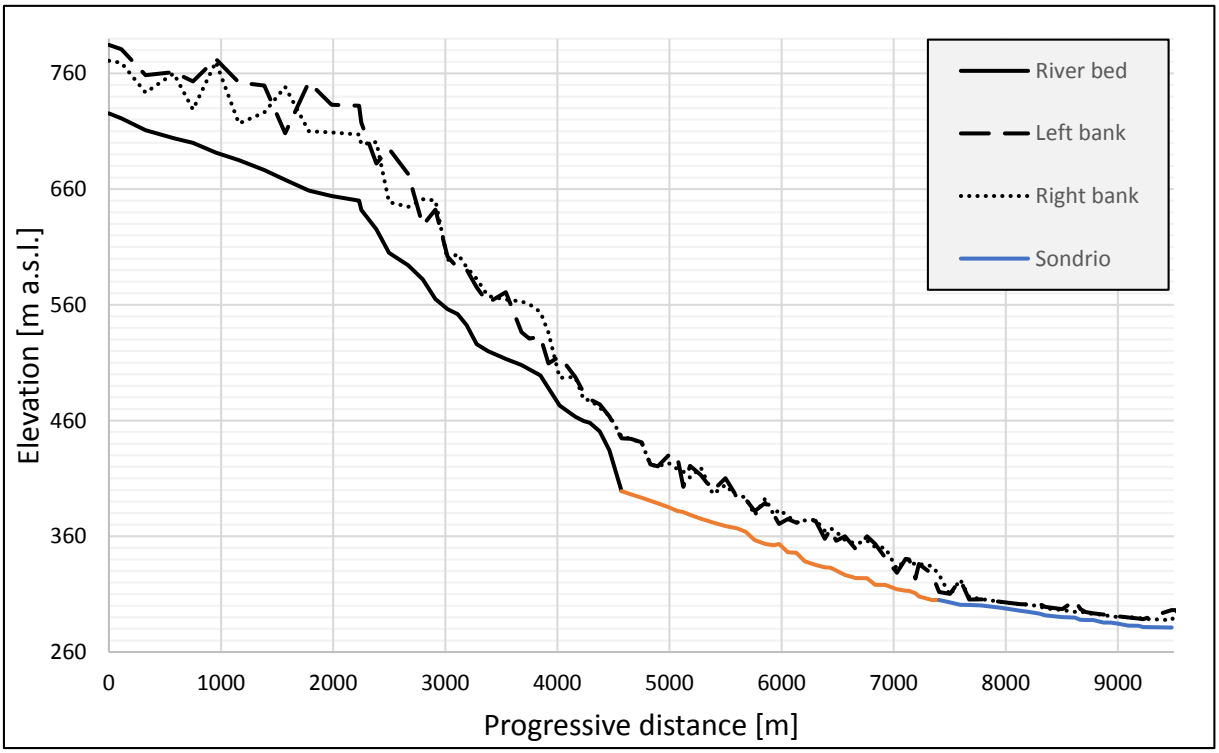

Figure I-2 Longitudinal profile of Mallero river, 9.5 km from the confluence with Adda river. Blue portion indicates the location of Sondrio. Blue and orange portions compose the part of the river that is the focus of the following chapters.

From a geological point of view, in the basin the Alpine thrusts give rise to significant lithological heterogeneity that includes various metamorphic and sedimentary rocks. The lower part of the valley is covered with glacial, fluvio-glacial, and colluvial deposits of variable thickness (Crosta, et al., 2003). At higher elevation Valmalenco is characterized by the outcropping metamorphic and magmatic formations with local debris cover. Glacial deposits cover a wide surface of steep slopes, at altitude between 2100 and 2400 m a.s.l., whereas at higher altitude only localized glacial deposits can be found (Francani, et al., 2011). The region is characterized by a variety of slides and unstable rock masses, the largest or which is the Spriana landslide. It is a partially reactivated ancient landslide and is located on the left bank of Mallero river (Figure I-3). The presence of the river at the foot of the landslide has an erosive action, triggering erosion and shallow land movements. Upstream of Spriana, in the Torreggio basin, an intense presence of rills at the foot of debris accumulation areas is related to shallow movements and landslides. This setting creates a considerable solid transport in Torreggio river and consequently in Mallero. In addition, three big landslides are present near the confluence with Mallero (Figure I-3).

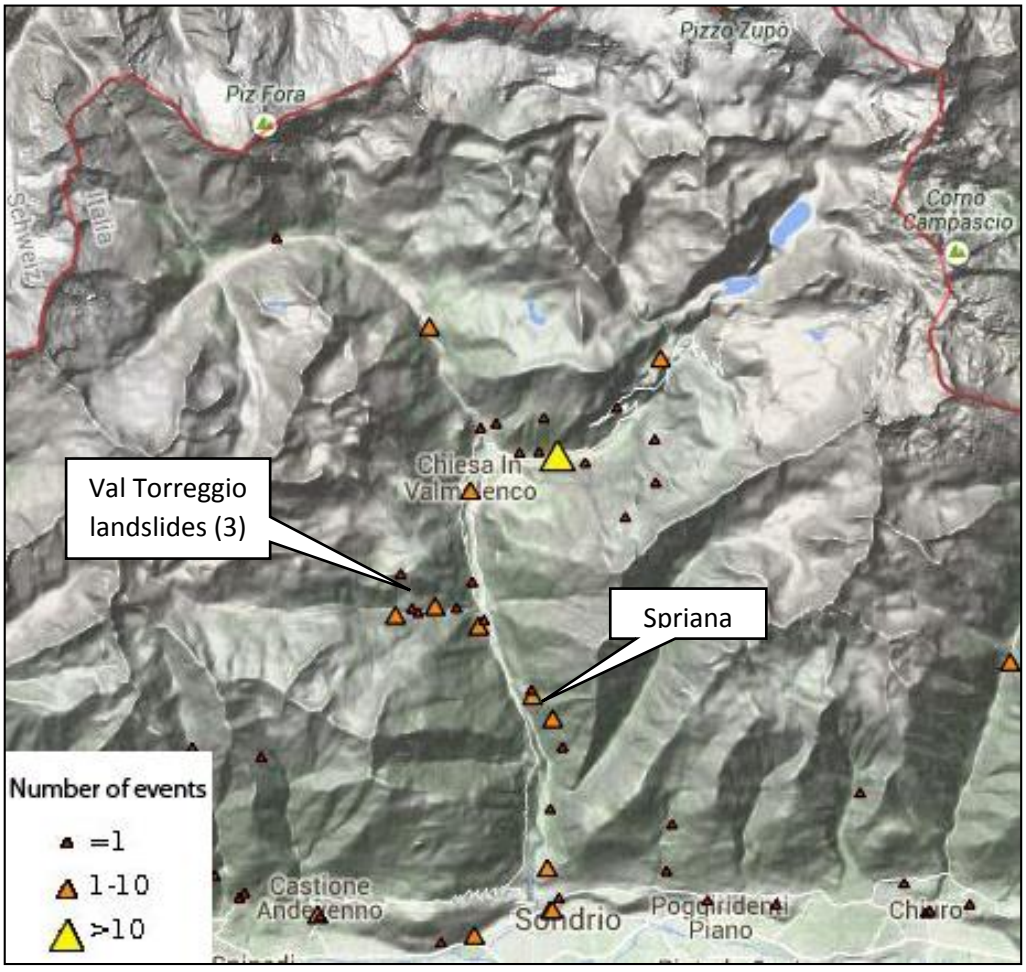

Figure I-3 Number of Landslide events in Valmalenco region. (Source: http://webmap.irpi.cnr.it/)

2. Past events

Numerous events have been recorded during the last century in the town of Sondrio. Records show that major floods have happened in 1911, 1927, 1951 and 1987 (Molinari, et al., 2013). Of these, it is reported that a specifically intense one was the one in 1927 because it included enormous amounts of sediment. However, due to the technological limitations of the time it happened, there are no available records that could allow its in-depth investigation. As it happened more recently, the flood in Valtellina that occurred in 1987 is probably the most famous one and investigations have been carried out on its basis ever since. The event claimed 53 lives while thousands of people were evacuated from their homes located in the flooded plain of the Adda river, or on the alluvial fans, inundated by debris flows and debris torrents all over the valley. The total economic loss was estimated in excess of 2000 billion 1987/Lire (around €340 million as of 2014) (Guzzetti, et al., 1992). Although water did not actually flood the town of Sondrio, it was centimeters away to spill all over the streets as it can be seen on (Figure I-6). As recalled, among several others, by Filippetti and Zoppi (2012), due to collision of cold mass of air coming from the Arctic with a mass of very hot and humid one over the Alps, the air pressure dropped sharply but the temperatures remained high (0 degree isotherm was recorded at 4000 m a.s.l.). This caused an extremely heavy precipitation and even glacier melting over short periods of time. A peak rainfall height was recorded of 305 mm in just one day (keeping in mind that average values vary around 1000 mm per year). It should be pointed out that in addition to the unusual phenomena, it had been raining also in the days before the event. Therefore, the level of saturation in the soil was highly elevated and in this sense, infiltration was hardly possible. The major part of the rainfall was immediately flushed downhill as runoff directly into the numerous rivers in the area. As already mentioned, the time of concentration of upland basins is in general short and in combination with the high saturation, it had become even shorter. The result was an enormous wave making its way through the narrow mountainous creeks along with accumulated mass of sediments and debris towards Adda, inevitably passing through the town of Sondrio. The Mallero, with its 3 large tributaries and many smaller ones (these waterways characterized by steep slopes and in combination with the exceptionally violent storm) led to a devastating effect not only from the hydraulic point of view but also due to the presence of the geologically delicate condition such as the one in the province of Sondrio, where the Alpine rock formations are highly deformed and fractured and favor a strong erosive activity in the area. In this sense, a colossal mass of eroded material was flushed downstream by the wave. As the change of slope from 3% to 1% just before the town of Sondrio is a premise for deposition, it is expected that the sediment would settle. As this is indeed what happened that day, the channel of the river in the in-town portion was almost completely congested by rock mass. Fortunately, there was still freeboard enough to accommodate the passing wave. This is mainly due to the fact that the

deposited rock mass arrived with the tail of the wave as explained, among others, by Radice et al. (2013).

Following the event, an investigation started in order to better understand the features of the disaster. A hydrograph was reconstructed on the basis of rainfall measurements, using a hydrologic Nash model for rainfall-runoff transformation. The estimated peak was about 500 m^3/s and the total duration of 60 hours (Figure I-4). Estimation of sedimentation was also conducted. It was estimated that around 3 million cubic meters of sediments had been involved of which 700 000 m^3 in the first 5 kilometers from the confluence with Adda. 220 000 m^3 were deposited in the in-town portion of the channel which led to the elevation of the river bed with 5 m near Garibaldi bridge, 3 m near Eiffel bridge, and 2 m near the railway bridge (Figure I-5). 350 000 m^3 were washed into Adda river. According to the technical study, the risk of flooding was both at the peak of the water wave and at its end when the bed aggradation was the largest and resulted in reducing the channel conveyance capacity by more than 75%.

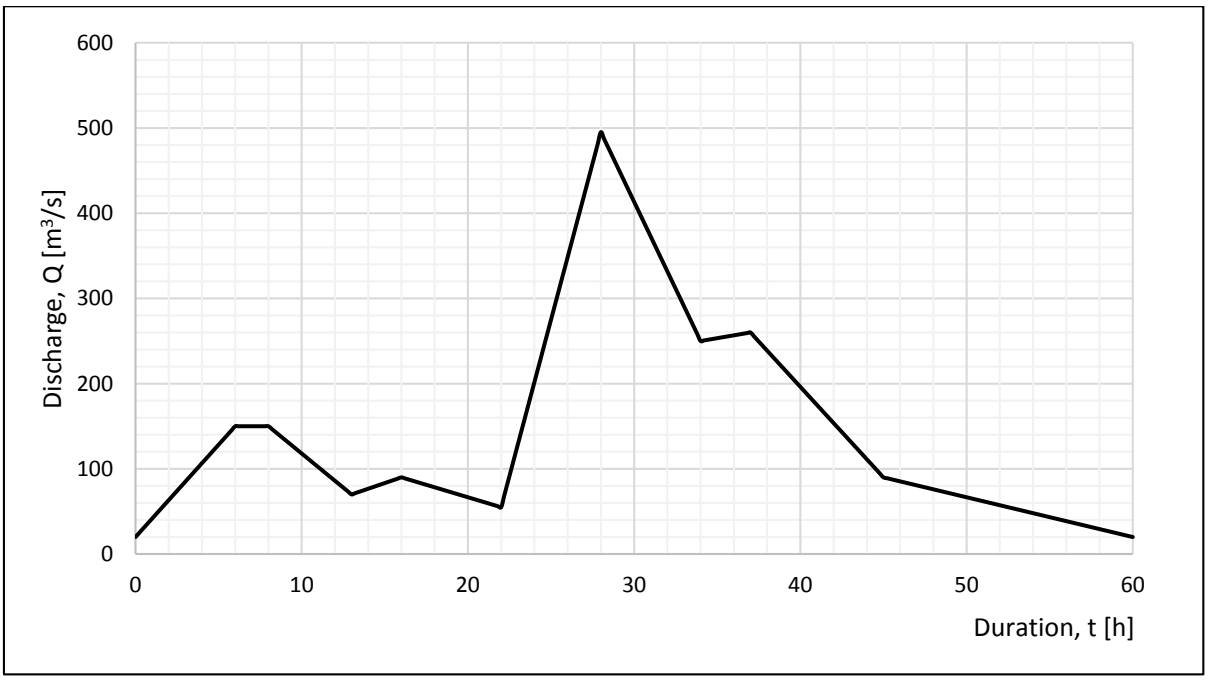

Figure I-4 Estimated flood hydrograph

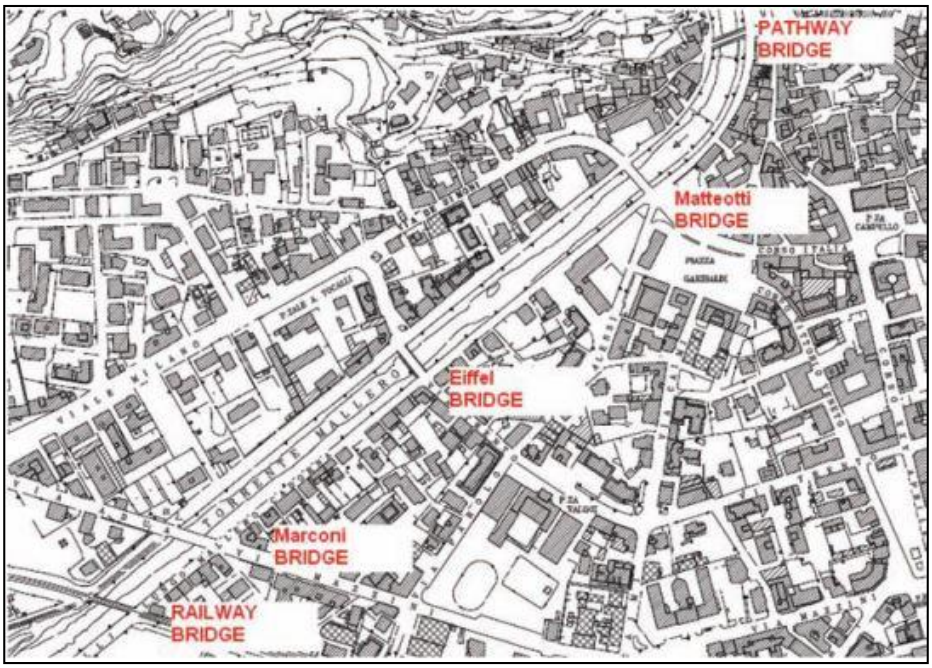

Figure I-5 Sondrio town center. (Ballio, F., Menoni, S., Molinari, D., 2013)

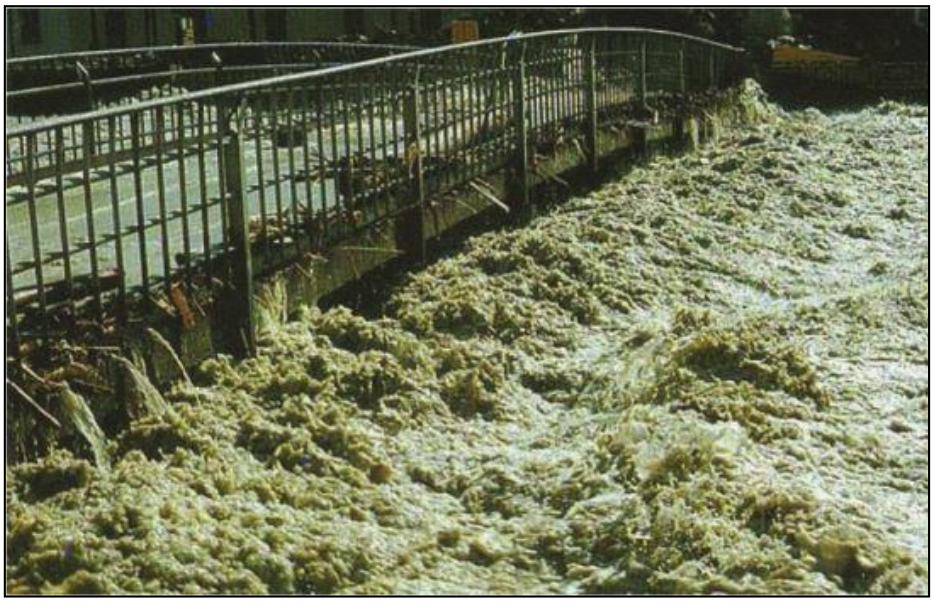

Figure I-6 Sondrio during the flood of 1987. (Ballio, F., Menoni, S., Molinari, D., 2013)

Figure I-7 Water surface elevation during the flood. (Filippetti, P., Zoppi,A., 2012)

3. Hydro-geological risk in Valmalenco

While floods in plain rivers are solely controlled by water flow, severe inundations in mountain streams are always related to extremely large inputs of sediment, followed by sudden deposition along the hydrographic network and consequent bank over-flow. In this respect, the following will associate the case-study site with the main phenomena that generate the risk of inundation for the town of Sondrio.

3.1. Geological aspect – soil erosion

When talking about Mallero basin, or any other Alpine valley, it is important to focus on main landslides which may lead to critical situation in case of collapse such as a possible dam formation and subsequent dam breach and flood wave. However, it is not enough to understand the full dynamics of the valley and its evolution because another very important feature of the mountain regions is the erosion process. As opposed to landslides or sinkholes, erosion is a widespread phenomenon and its integrated action over the entire area of the basin is what poses the threat. Mainly referring to sediment yield from slopes and river embankment erosion, this processes represent a risk for the city of Sondrio.

Figure I-8 Slopes in Valmalenco

As it can be seen on the pictures above, the valleys in Mallero basin contribute to the hill slope erosion process with such slopes where the soil is lose and can easily be entrained downhill even by its own weight. As an example, the presence of the Torreggio river at the foot of three landslides also has an erosive action since the landslide is reactivated. This results in solid transport downstream leading to the confluence with Mallero. Erosion in the area is also influenced by anthropic actions such as deforestation, extensive building of infrastructure as well as mining activities. Once open, quarries in the region offer bare soil, perfectly susceptible to the erosive actions of rainfall and wind.

3.2. Hydraulic aspect – morphological evolution

The high energy streams in the upland rivers are capable to initiate particle movement even of big boulders. Thus, erosion has elevated levels in the numerous creeks and larger rivers in the Mallero basin. Under the conditions of intense rainfall, the eroded material is flushed downstream and deposits

Figure I-9 Left - Mallero river near Torre di S. Maria. Right – weirs built to control the sediment yield (taken in October 2013)

around sharp changes of slope, bends, and where the transport capacity of the section is low in general. As previously discussed, the flow in the mountain streams is often supercritical and predisposes the river erosion and sediment transport along the path of the river. In addition, the mild slope of the bed in the town of Sondrio favors the deposition of sediments as a consequence of the decreased transport capacity of the flow.

After the event of 1987 various structures have been built, such as weirs and check-dams in order to limit the negative effect of sediment transport (Figure I-9).

In terms of monitoring the basin is supplied with several pluviometers, distributed over its area. On the basis of the rainfall depth recorded, the ’87 event hydrograph was reconstructed. According to Filippetti and Zoppi (2012) measurement of water depth in some sections during the period from 1992 to 1998 made it was possible to produce rating-curves relating water depth with the discharge

as well as the annual flow curves. The curves show that the maximum discharge measured at Eiffel bridge in this period is 160 m^3/s, while 100 m^3/s is exceeded only in 17 days for 6 years (1992- 1998). In addition, the ordinary discharge in Mallero is less than 10 m^3/s (which is very little value and no significant sediment transport can occur in this range of discharge). As discussed by Radice et al. (2013), in the absence of sediment aggradation, the town would not suffer from a significant flood hazard, since the peak of the 100-year discharge is 640 m^3/s and in Sondrio the limit capacity of the channel in the in-town reach is around 690 m^3/s. Therefore, there is no flood hazard for the town unless there is aggradation due to sediment transport.

4. Literature review

Here, a review of the research work carried out at Politecnico di Milano in the past years on the relevant topic will be discussed briefly in order to familiarize the reader with the progress achieved so far along with the issues surrounding this matter. The articles are non-necessarily related to Mallero in particular but cover similar cases and topics that are relevant for this study. A short summary will present the goal, the results and the evaluation of each of the articles. In addition, it is in the author's opinion that such a summary is the best way to structure and understand the key points of this hydro-geological assessment.

4.1. Ballio, F. et al. 2010, Evaluation of sediment yield from valley slopes: a case study.

The article investigates the results of the estimation of sediment yield production of the basin of Tartano valley in Northern Italy, since it is characterized by a significant presence of weak rocks. This is clearly a premise for the availability of large amounts of loose sediments. In order to validate the results, a comparison is made with volumes recorded at an artificial reservoir located at a downstream section of the valley.

Basin scale sediment yield evaluation is suitable for off-site processes. In the case of an on-site analysis, there are shortcomings: (i) spatial scale; (ii) temporal scale; (iii) no information of granulommetry (also relevant for off-site processes). These considerations provoke the study of a small scale (in both spatial and temporal aspects) investigation. With respect to spatial resolution, localized areas have been chosen considering an event with high intensity (return period). For the purpose, the valley is divided in 2 parts of which also 2 sub-parts with homogeneous cover are analyzed. With respect to time scale, the modified USLE (MUSLE) approach is used which accounts for the amount of sediment produced in one event.

The results of the basin scale analysis show variability between the different formulas, however, in comparison with the measured value, all of them correspond at least to the order of magnitude. From the scaled analysis it was discovered that both temporal and spatial scales influence greatly the results with significantly larger values of sediment yield shown for small sub-basin with homogeneous cover and a significant rainfall event.

4.2. Brambilla, D. et al. 2011, On analysis of sediment sources towards proper characterization of hydro-geological hazard for mountain environments.

Since several sediment sources are present in a mountain and modelling of sediment yield furnishes the necessary boundary condition for the modelling of sediment transport along a stream, in this study several sediment sources are separately analyzed with reference to the Tartano basin. Volumes obtained by soil erosion show that this process should not represent a problem for the sediment transport conditions within the rivers. On the contrary, a preliminary study of one lateral valley of the basin shows that the amount of debris supplied by the fault system to the rivers may be considerable. This implies that some sources have a negligible contribution to the solid volumes that are later transported by the streams. This allows for a simpler modelling, considering only sources that are expected to affect the sediment transport the most.

4.3. Brambilla, D. et al. 2011, Sediment yield from mountain slopes: a GIS based automation of classic Gavrilovic method.

This paper focuses on Gavrilovic method that is considered a standard for erosion evaluation in Alpine regions; this theory has proved to be effective and quite simple to be applied, but has a major drawback in the subjectivity of parameter determination. The method is used by means of a GIS software, leaving the only step, up to the decision of the operator, to be the determination of the coefficient of observed erosion. The capability of Gavrilovic method, linked to good processing power of modern CPUs and the availability of high resolution data for the whole Italian territory, proved to furnish reliable results. Final result of this work is an agile and light script that exploiting already existing databases and maps is able to return some indications about soil loss in a very quick and easy way. These data can constitute a valid, despite of its simplicity, result for preliminary assessment of erosion issues in Alpine region.

4.4. Mazza, F. 2011, et al., A hybrid method (Monte Carlo/probabilistic approach) to evaluate soil erosion in Alpine valleys.

The Gavrilovic model for soil erosion evaluation has been incorporated with a probabilistic approach in order to take into account the uncertainty related to input data. As usual approaches for soil erosion evaluation produce deterministic results, the subjectivity that originates from the choice of parameters and stochasticity of the natural processes are not accounted for. In this respect, the integration of a Monte Carlo probabilistic approach aims to introduce a degree of confidence in the obtained results. For the purpose the model has been applied to Tartano basin in the Italian Alps, for which data on sediment yield is available through measurements of deposited material in a reservoir downstream of the study site. The results define an interval of minimum to maximum volumes with a confidence level of 95%. In comparison, the results obtained with a deterministic approach fall within the limits of the interval. However they do not carry information about the uncertainty of the results. In this respect, the method deals with uncertainty in a manner that is understandable and useful for decision making.

4.5. Radice, A. et al. 2012, On integrated Sediment transport modelling for flash flood events in mountain environments

A complete process chain is attempted for a small basin in the Italian Alpine region – Rossiga valley. The chain includes: (i) hydrologic estimation of peak discharge, (ii) evaluation of the volumetric sediment supply into the stream, and (iii) computation of the morphologic evolution of the river bed. A key point is the simplicity of the models used that aims to create an integration between them and not sophisticated results. Focus is put on the feasibility of a joint modelling in the light of all the limitations imposed by the different nature of hill slope-devoted models and the sensitivity of the obtained results to some parameters, for an assessment of result reliability. An important concept that has been introduced in this work is the spatial separation between supply and transport through a break-point which is chosen within the catchments. Since the models are not designed to work in cooperation, there are flaws that need to be further polished if such an integration is to dominate in future hydro-geological risk assessment. One of the main flaws discovered is that the models do not furnish information about the temporal evolution of sediment volumes and about the granulometry of the supplied material. On the other hand, with the proper assumptions, results can be obtained with some variability depending on parameters that need to be evaluated within an engineering perspective.

4.6. Radice, A. and Rosatti, G., 2012, Sulla modelazione idraulico-morfologica dei corsi d'acqua: il torrente Mallero e la propagazione dell'incertezza legata all'alimentazione solida.

The paper discusses a specific characteristic of hydro morphological models. It is often necessary to introduce a sediment source term at the upstream end of the modelled stream in order to represent the transfer of sediment from the catchment to the river. Given the difficulties in assessing the expected sediment yield, the uncertainty in estimates can propagate along the riverbed and reduce the validity of the results on which the decision-maker should base their choices in terms of land management or risk assessment. For this reason an analysis based on the Mallero 1987 flood event was carried out in order to quantify the velocity of propagation of uncertainty associated with the sediment input term. The results show that the duration of this particular event are sufficiently short for the deposition of solid material in Sondrio not to be altered by variation of sediment yield upstream. Events with longer durations or a succession of floods, however, could render the system sensitive to the solid contribution. The main limitations of this modelling approach are discussed in terms of simplifications such as the single sized sediment transport calculation and the particular relation of the model to a specific event, that is, it was at the time of development not generalized.

4.7. Radice, A. et al. 2013, Management of flood hazard via hydro-morphological river modelling. The case of Mallero in the Italian Alps.

In this work, feasibility of incorporating sediment transport modelling into the evaluation of flood hazard is assessed with reference to the case of the Mallero River in northern Italy. A past flood event has been modelled by means of a fully coupled model of flow and sediment transport. Particular attention has been focused onto the town of Sondrio, located at the downstream end of the river. Results show that interpretation of the event dynamics and proper quantification of flood hazard for the town cannot be obtained without considering the morphologic evolution of the river bed due to sediment transport. In addition, reliability of the results of hydro-morphologic modelling has been proved by extensive sensitivity analysis, showing a weak dependence of the findings on external forcing. Some arguments are thus provided towards the incorporation of morphologic processes into hazard assessment, landscape protection, scenario modelling and emergency management. Since in the actual plan morphological evolution is not considered, with reference to civil protection authorities, there is a major flaw in the risk assessment procedure. The major point that should be considered by emergency planners is that in upland streams, hydro-dynamics and morpho-dynamics often have timescales with the same orders of magnitude.

4.8. Radice, A. and Elsayed, S.M. 2014, Hydro-morphologic modelling for different calamitous scenarios in a mountain stream.

The article explores the use of hydro-morphologic modelling to assess the level of hazard related to two scenarios: one simulates flood with intense sediment transport and the other a landslide with following dam-break wave. The main purpose is to indicate if these types of waves could be able to transport significant amounts of sediments to Sondrio, maximum elevation of the water surface and characterization of the time scales for the events. Results show that the two kinds of events may results in similar hydraulic hazard for the town of Sondrio, however the features of the events are evidently different: in the case of the flood wave, the hazard is due to aggradation of the river bed, made possible by the duration of the event being long enough to move significant volumes of sediments; for the dam-break, the role of sediments is not particularly significant, with the maximum water elevation being related to a larger discharge in comparison to that for the previous scenario. These results could be implemented as a tool in territorial management and civil protection.

5. Objective and outline of this work

The aforementioned case study along with the reviews of previous work carried out on the topic have put in evidence the significance of hydro-geological risk and in particular the need for a joint model that is able to encompass both main aspects of the problem.

As the catchments in Mallero basin are characterized by instabilities of various nature, hazardous conditions may be created merely by the geological condition in the area. Active landslides of various typology and dimensions threaten to collapse and induce damage to structures, infrastructure, facilities etc. However, the scope of this work is focused on the flood-related risk for the town of Sondrio. As historical records show (e.g. Valtellina, 1987), the hazardous conditions created for the Alpine town were not created simply by a geological hazard neither by a hydraulic one. It was their mutual contribution that determined the bed and water surface elevations in Sondrio. Therefore, hydraulic modelling requires the implementation of a sediment yield boundary condition in order to account for the combined effect of water discharge and morphological evolution of a river bed. In cases where measurements, representative of sediment yield volumes are available (e.g. back analysis of events, data from reservoir siltation), such boundary condition may be determined with more certainty while otherwise, geological modelling is necessary. In this respect, geological conditions in the region create multiple sediment sources characterized by different spatial and temporal scales which makes a global analysis hardly possible. Leaving aside the collapse of a major landslide (e.g. Spriana landslide) that would lead to a complete impediment of Mallero river and possibly create an earth dam-break hazard, sediment yield originates from widespread erosion as

well as from localized sources such as debris flows and fault systems. As discussed by Brambilla et al. (2011), different sediment sources may not be needed to model the total sediment yield for a particular region as one source may represent a negligible contribution with respect to another. While in basins with relatively small area, concentration of localized sediment sources may have a predominant effect on the total sediment yield, for the case of the entire Mallero basin, it is assumed that the widespread erosion process would represent the main source of sediment that could be entrained during an intense event. Although the validity of such an assumption should be verified by a comparative study, the lack of essential data renders this task impossible for the scope of this thesis.

The goal of the present work is to create a comprehensive, integrated modelling of morphologic river bed evolution as a consequence of short-duration intense events and the corresponding sediment supply considering both geological and hydraulic tools. The main objective of the model is to find a reasonable way to connect the two processes and to produce a complete process chain for building a flood scenario for the town of Sondrio. Model feasibility and limitations will be later discussed.

The following work will be presented as follows:

Geology

- A theoretical background will introduce the problem of soil erosion.
- The particular semi-empirical formula, used in the analysis will be explained.
- Starting from a data package, a soil erosion analysis for the whole Mallero basin will be carried out.
- A critical review of the results will evaluate their credibility and usefulness.

Hydraulics

- A theoretical background will explain the problem of sediment transport and morphological evolution.
- A hydro-morphological model will be produced and its parameters calibrated to the 1987 event. The model to be used as a basis for the following work.
- A Review and discussion of the results will be proposed

Integrated modelling

- Strategies for integrating the previous work into a complete chain will be proposed in order to overcome the scale inconsistency.
- A flood scenario will be proposed.
- Considering the scenario, an outflow in the town of Sondrio will be computed.
- Review and discussion of the results will conclude the model.

Chapter II. Modelling sediment yield by soil erosion

Considering that the Mallero basin is affected by the presence of numerous landslides and debris flow sources, the erosion process is probably not the most crucial one in terms of natural disasters. The collapse of a landslide with up to 20 million cubic meters of soil mass (e.g. Spriana landslide) may cause substantial damage by destroying its surroundings as well as to block the river and create an earth dam. However, as discussed by Radice and Elsayed (2012), although the type of hazard posed by an earth dam for the town of Sondrio is similar to that posed by soil erosion, the features of the events are quite different. In the case of dam break, the role of sediments is insignificant in comparison to the large discharge. Since the purpose of this work is to implement tools also for the prediction of bed aggradation, the landslide hazard will not be on focus, acknowledging its validity and importance for the case study. On the other hand, historical events such as the one from 1987 have shown the criticality of eroded material as a hazard that may lead to flood and considerable damage.

Following the natural sequence of processes, the sediment yield production would come first in the chain of events and therefore, the present chapter will be focused on its description and modelling.

1. Theoretical background

In order to understand the soil erosion process in more detail, its various types, and effects, a theoretical background will be proposed to the reader. This will be helpful also for the understanding of the reasoning behind choices and assumptions made in relation to the modeling process, described in the following sections.

Soil degradation is driven by environmental conditions as well as by land management practices. In the near future, soil degradation might be significantly increased by the combined effects of global climate and land use change. Referring to the mountain regions, the extreme topography and climate result in additional high instability, fragility and sensitivity of the soil cover (Meusburger, 2010).

Soil erosion is a two-phase naturally occurring process consisting of the detachment of individual soil particles from the soil mass and their transport by erosive agents such as running water and wind, each contributing to the loss of soil. When sufficient energy is no longer available to transport the particles, a third phase, deposition, occurs (Morgan, 2005). Considering the previous establishment of phase-like classification, each agent can be referred to one of the phases as shown in the table below.

1.1. Erosion by water

The rate and magnitude of soil erosion by water is controlled by the following factors:

Rainfall and Runoff intensity (erosivity of the agent)

Both rainfall and runoff factors must be considered in assessing a water erosion problem, despite their different functions in the overall process. The impact of raindrops on the soil surface can break down soil aggregates and disperse the aggregate material. Lighter aggregate materials such as very fine sand, silt, clay and organic matter can be easily removed by the raindrop splash and runoff water; greater raindrop energy or runoff amounts might be required to move the larger sand and gravel particles.

Table II-1Erosion agents after Morgan, R.P.C. (2005)

<table>
<tr><th colspan="3">Agent</th><th>Function</th></tr>
<tr><td colspan="3">Rain splash</td><td>Detaching, Transporting</td></tr>
<tr><td rowspan="3">Surface runoff</td><td rowspan="3">resulting in</td><td>Shallow flow (sheet flow/overland flow)</td><td rowspan="3">Transporting</td></tr>
<tr><td>Flow in small channels (rills)</td></tr>
<tr><td>Flow in gullies and rivers (more permanent)</td></tr>
<tr><td colspan="3">Wind</td><td>Detaching, Transporting</td></tr>
</table>

Soil movement by rainfall (raindrop splash) is usually greatest and most noticeable during short-duration, high-intensity thunderstorms. Although the erosion caused by long-lasting and less- intense storms is not as distinguishable or noticeable as that produced during strong storms, the amount of soil loss can be significant, especially when integrated over time. Runoff can occur whenever there is excess water on a slope that cannot be absorbed into the soil or trapped on the surface. The amount of runoff can be increased if infiltration is reduced due to soil compaction, oversaturation or freezing. Runoff may be greatest during spring months when the soils are usually saturated, snow is melting and vegetative cover barely represents any barrier for rainfall drops.

Intensity is generally considered the most important characteristic of rainfall when sheet and rill erosion are considered (Morgan, 2005). In order to quantify the intensity of a storm, erosivity indexes can be calculated as a function of duration, mass, diameter and velocity of raindrops.

1.1.1. Soil Erodibility

Soil erodibility is an estimate of the ability of soils to resist erosion (both detachment and transport), based on the physical characteristics of each soil. Erodibility varies with soil texture, aggregate stability, shear strength, infiltration capacity and organic and chemical content. Generally, soils with faster infiltration rates and higher levels of organic matter have a greater resistance to erosion.

Decreased infiltration and increased runoff can be a result of compacted subsurface soil layers. A decrease in infiltration can also be caused by a formation of a soil crust, which tends to "seal" the surface. On some sites, a soil crust might decrease the amount of soil loss from sheet or rain splash erosion, however, a corresponding increase in the amount of runoff water can contribute to greater rill erosion problems.

Past erosion has an effect on a soils' erodibility for a number of reasons. Many exposed subsurface soils on eroded sites tend to be more erodible than the original soils were, because of their poorer structure and lower organic matter.

1.1.2. Slope Gradient and Length

Naturally the steeper the slope of a field, the greater the amount of soil loss from erosion by water as in the case of Mallero basin. Soil erosion by water also increases as the slope length increases due to the greater accumulation of runoff. In addition, while on a flat surface raindrops splash soil particles randomly in all directions, on sloping ground more soil is splashed downward as a function of the slope steepness. Longer slope lengths result in increased erosion potential, due to increased velocity of water which permits a greater degree of scouring.

1.1.3. Vegetation

Vegetation acts as a protective layer or buffer between the atmosphere and the soil. Soil erosion potential is increased if the soil has no or very little vegetative cover of plants. Plant components such as leaves and stems, protect the soil from raindrop impact and splash, while the subsurface components - the root system tend to increase the mechanical strength of the soil.

The erosion-reducing effectiveness of plant covers depends on the type, extent and quantity of cover mostly in terms of height and density. Vegetation combinations that completely cover the soil, and which intercept all falling raindrops at and close to the surface are the most efficient in controlling soil erosion (e.g. forests, permanent grasses). In terms of runoff, greatest reduction in velocity occurs with dense, spatially uniform, vegetation covers. Sparse vegetation is less effective and may even lead to concentration in flow with localized high velocities between plants. It should be mentioned that the seasonal availability of the cover is also an important factor. Evergreen forests provide quite permanent protection, while deciduous trees are available only for half of the year.

1.2. Erosion by Wind

The rate and magnitude of soil erosion by wind is controlled by the following factors:

1.2.1. Erodibility of Soil

Very fine particles can be suspended by the wind and then transported to great distances. Fine and medium size particles can be lifted and deposited, while coarse particles can be blown along the surface (commonly known as the saltation effect). The abrasion that results can reduce soil particle size and further increase the soil erodibility.

1.2.2. Soil Surface Roughness

Soil surfaces that are not rough or ridged offer little resistance to the wind. However, over time, ridges can be filled in and the roughness broken down by abrasion to produce a smoother surface susceptible to the wind.

1.2.3. Climate

The speed and duration of the wind have a direct relationship to the extent of soil erosion. Soil moisture levels can be very low at the surface of excessively drained soils or during periods of drought, thus releasing the particles for transport by wind. This effect also occurs in freeze-thaw cycles of the surface during winter months.

1.2.4. Vegetative Cover

The lack of permanent vegetation cover in certain locations has resulted in extensive erosion by wind. Loose, dry, bare soil is the most susceptible. The absence of windbreaks (trees, shrubs, etc.) allows the wind to put soil particles into motion for greater distances thus increasing the abrasion and soil erosion.

1.3. On-Site Effects:

On-site effects take place within the basin (or sub-basin) under consideration. The implications of soil erosion on-site extend beyond the removal of valuable topsoil. With respect to agriculture, crop emergence, growth and yield are directly affected through the loss of natural nutrients within the soil. Soil quality, structure, stability and texture can be affected by the loss of soil. The breakdown of aggregates and the removal of smaller particles or entire layers of soil or organic matter can weaken the structure and even change the texture. Textural changes can in turn affect the water- holding capacity of the soil, making it more susceptible to extreme condition such a drought. On the other hand, on-site processes are related to changes in local morphology of slopes and water courses.

1.4. Off-Site Effects:

Off-site impacts of soil erosion are not always as apparent as the on-site effects. Problems arise from sedimentation downstream of a chosen investigation domain, which reduces the capacity of rivers and drainage ditches, increases the risk of flooding, blocks irrigation canals and shortens the design life of reservoirs. Many hydroelectricity and irrigation projects have been ruined as a consequence of erosion (Morgan, 2005). Sediment is also a pollutant. If contaminated on-site, eventual transport will have adverse effect downstream on soil as well as on water resources and natural habitat.

1.5. Modelling methods

Mostly with respect to the loss of valuable soil in agricultural land, many formulas have been developed based on empirical, conceptual or physics-based models. However, there is an extreme variability among the different models due to the philosophy and purpose for their creation. These include: type of erosion covered, most influencing factors (conceptual basis), data requirement, spatial and time scales. Most of the models, however, cover similar basin characteristics such as land use, slope steepness, amount of precipitation, runoff shear stress, soil cohesion, and surface roughness. These parameters are usually highly variable in time and space and interacting with each other. This renders any basin under consideration extremely complex to be analyzed and described by a mathematical equation. Many physical methods have been developed such as the most recent EUROSEM and SWAT. Although they can be very accurate, they are extremely complex and require an enormous amount of data. Thus they can be hardly applied to real case studies and research for their development has been terminated. Altogether, the limitations in our ability to model soil erosion and sediment yield at the basin scale are partly due to the high data requirements of each individual model and, maybe more importantly, due to the often poorly understood complex interactions between the different processes at the basin scale. In this sense, there is a need for alternative approaches for basin wide estimates of sediment yield. A number of empirical and semi-empirical methods are preferred due to their simpler application, more adequate data requirement and satisfactory results obtained in numerous cases with ranging areas and geographical locations. Among the most commonly used are the Gavrilovic method as well as the USLE (Universal Soil Loss Equation) and its variations – RUSLE (Revised USLE) and MUSLE (Modified USLE).

1.5.1. Review of models (USLE RUSLE MUSLE)

USLE equation predicts the mean quantity of soil erosion in relation to environmental conditions. It is a model tuned to calculate the mean losses of terrain, on long time periods, due to sheet and rill erosion. USLE does not consider deposition and gully erosion. Its revised form (RUSLE) has the same format with the difference that two of the topographic factors are combined into one. The MUSLE modification has been developed to incorporate the effects of a single intense event of short

duration. These equations, however, have been developed for soil loss estimation in agricultural land in the United States, which may pose a question mark on their applicability in mountain regions in Europe. The application of Gavrilovic method however, has been preferred one for such types of environment, since it has been developed in somewhat similar medium. In addition, the fact that practically all significant erosion processes are considered (sheet, rill, gully, bank) in its formulation makes it especially suited for estimating off-site effects of soil erosion (De Vente & Poesen, 2005).

1.6. Spatial scales

An analysis of the effect of scale variation carried out by Ballio et al. (2010) shows the effect of the presence of only few types of soil cover in a basin. Two sub-basins of areas 2.3 km^2 and 3.1 km^2 have been tested with USLE (Universal Soil Loss Equation) and RUSLE (Revised USLE) methods showing values of annual specific sediment yield considerably higher than those obtained on the basin scale as well as compared to sub-basin scale but with areas large enough to ensure the presence of several types of surface. As a general trend, shown in the work of de Vente and Poesen (2005), the specific sediment yield decreases with increase in the area of the basin. This estimation has been made on the basis of a number of case studies in Mediterranean regions.

1.7. Time scales

Under the same case study, the effect of time scale was also tested using the MUSLE (Modified USLE) method for event-induced sediment yield. Huge sediment yields have been obtained for two cases with different intensities (10 years and 100 years return period) in comparison with the yearly values. This effect was evident on the basin scale level as well as on the sub-basin scale. Thus, short-duration events with significant return period lead to concentrated in time sediment yields which may be dangerous.

2. Gavrilovic model for soil erosion evaluation

Following the previous considerations, a choice is made for this work to be carried out using the Gavrilovic model. The model is named after its creator, who proposed a semi-quantitative method for erosion and sediment yield estimates. It explicitly combines an erosion component and sediment delivery component (Gavrilovic, 1976). The method has been developed for application in torrential basins of south and south-eastern former Yugoslavia as the study has been carried out in the Morava basin, belonging to the Black-Sea drainage basin. Due to geographic similarities, the model has been successfully applied for cases in the Swiss and Italian Alps. The basic concept of the model is that the sediment volume transported by the stream depends on the sediment yield by soil erosion and the sediment deposition in the watershed (Ballio, et al., 2010). The following equations represent the relations used for erosion and sediment yield description.

$$G = W_{sp}.R \quad \text{Eq. (II.1)}$$

$$W_{sp} = T.H.\pi.Z^{2/3}.F \quad \text{Eq. (II.2)}$$

$$R = \frac{(l_p + l_a).\sqrt{O.D}}{(l_p + 10)} \quad \text{Eq. (II.3)}$$

$$T = \sqrt{0.1 + \frac{t}{10}} \quad \text{Eq. (II.4)}$$

$$Z = \Xi.\Pi.(\Phi + \sqrt{I}) \quad \text{Eq. (II.5)}$$

In which**, G [m^3/year]**: basin sediment yield, **R [-]**: sediment retention coefficient, **W_{sp} [m3/year]**: average annual gross erosion, **T [-]**: temperature coefficient, **t [^oC]**: annual average temperature**, H [mm/year]**: annual height of precipitation, **Z [m^2 $km^{-4/3}$ $mm^{-2/3}$]**: erosion coefficient, **F [km^2]**: area of the watershed, **O [km]**: perimeter of the watershed, **D [km]**: average elevation of the watershed, **l_p [km]**: length of principal waterway, **l_a [km]**: cumulated length of secondary waterways, **I [deg]**: average slope steepness of the watershed, **Ξ [-]**: coefficient of soil cover, **Π [-]**: coefficient of soil resistance, and **Φ [-]**: coefficient of type and extent of erosion.

The method calculates basin sediment yield per year depending on the main factors influencing the erosion phenomena as previously discussed in section 1.1.: type and severity of erosion (**erosivity**), **erodibility** factor, and a soil protection factor (**vegetative cover**). The values used for these factors are presented in Table II-2. In addition meteorological and geometrical features related to the basin are considered. These include annual precipitation, temperature, average slope and surface area. Basins with high spatial heterogeneity in these parameters should be further subdivided into smaller, more homogeneous basins. This will imply for the total amount of sediment yield to be a summation of the yield obtained from all the sub-basins (De Vente & Poesen, 2005). However, as it has been previously discussed in the work of Ballio et al. (2010) **this consideration may yield significantly larger sediment volumes.** The actual delivery of sediment, taking into account possible depositions, is calculated using morphometric characteristics of the basin such as the perimeter, total stream length relative to stream length of the principal waterway, average elevation, and surface area of the basin.

The Gavrilovic method is by far the most quantitative of all semi-quantitative methods developed. This is due to the fact that most of the variables in the model are quantitative descriptions of the catchment conditions, while the only descriptive variables are the coefficients for soil cover, soil resistance and type and extent of erosion (De Vente & Poesen, 2005).

2.1. Applicability and accuracy of the method

De Vente and Poesen (2005) quote several cases in their analysis, in which the Gavrilovic method has been applied in catchments other than the originally tested region. It is reported that Beyer Portner (1998) have estimated a variance $R^2 = 0.86$ in comparison with measured sediment yield values for five different basins with areas in the range 36 km^2 – 210 km^2 in the Swiss Alps. Further, Barazzoffi (1985) has applied it to four catchments in central Italy, again with variations of catchment areas. He obtained good results for the catchments with smaller areas, although with slightly adapted version of the method, where the coefficients of soil resistance were halved. This adjustment, however, was not reasonably explained, despite the fair results. On the other hand, using **the originally described method, sediment yield was overestimated.** The method showed good results also for a small

Table II-2 Descriptive factors used in the Gavrilovic method

Gavrilovic coefficients	
Coefficient of soil cover	Ξ
Mixed and dense forest	0.05-0.2
Thin forest with grove	0.05-0.2
Coniferous forest with little grove, scarse bushes, bushy prairie	0.2-0.4
Damaged forest and bushes, pasture	0.4-0.6
Damaged pasture and cultivated land	0.6-0.8
Areas without vegetal cover	0.8-1.0
Coefficient of soil resistance	Π
Hard rock, erosion resistant	0.2-0.6
Rock with moderate erosion resistance	0.6-1
Weak rock, schistose, stabilised	1-1.3
Sediments, moraines, clay and other rock with little resistance	1.3-1.8
Fine sediments and soils without erosion resistance	1.8-2.0
Coefficient of type and extent of erosion	Φ
Little erosion on watershed	0.1-0.2
Erosion in waterways on 20-50% of the catchment area	0.3-0.5
Erosion in rivers, gullies and alluvial deposits, karstic erosion	0.6-0.7
50-80% of catchment area affected by surface erosion and landslides	0.8-0.9
Whole watershed affected by erosion	1

catchment in Croatia (26.7 km^2), where Globevnik et al. (2003) compared the predicted result to sediment volumes extracted from a reservoir over a period of 11 years. Another application, this time for a considerably larger basin (7000 km^2) was carried out in Greece by Emmanouloudis et al. (2003), where a gross volume of erosion was computed, without taking into account the sediment

delivery ratio. The results agreed to a large extent with previous studies over sub-basins which are part of the basin under investigation. The last two cases have been implemented into a GIS environment, where the computation is carried out with simplicity. Another GIS aided case has been analyzed by Brambilla et al. (2011) in order to evaluate the usefulness of the automation process, which proved to be a success and in addition showed results similar to other evaluations on the same site. Recently, Ballio et al. (2010) have applied the method to a basin in northern Italy (49 km^2) and have compared the results with sedimentation volumes of a reservoir in a downstream section over a period of 7 year. In addition, a sensitivity analysis was done on the coefficients of soil erosion which led to the estimation of a range, for which the lower value was similar to the mean from the reservoir and the higher value resembled a year with elevated sedimentation rates. Nevertheless, the measured volume fell in the estimated range, which is a further proof of the applicability of the method to Alpine regions.

The case studies described above have shown satisfactory results over the years and over a number of basins with different areas. It is therefore considered by the author that the application of the Gavrilovic method for the case of Mallero basin will be reasonable and the results are expected to be within the margins of reality.

3. Methodology

Following the previous considerations, the Gavrilovic method will be applied to the Mallero basin case study and the calculation process will be presented here. For simplicity, a GIS based approach has been adopted in order to do most of the calculations in a synthetic way, depending on the availability of data. The soil erosion coefficient has been estimated, based on a DUSAF (*Destinazione d'Uso dei Suoli Agricoli e Forestali*) soil use map, where for each soil use type, a value for the three coefficients has been manually assigned. Since this process is left to the ability of the operator, it is a major source of uncertainty in addition to the reliability of the data that has been provided. All further calculations have been done using an Excel spreadsheet. A summary of the datasets is provided in the following table.

Table II-3 Datasets used in the computation

Name		Description	Format
DEM		Digital elevation model of the terrain	Raster (20 x 20m)
Basins 10km		Sub-basins division of the terrain	Vectorial
Basins 30ha		More detailed division of the terrain	Vectorial
Rainfall	Minimum	Annual rainfalls	Vectorial
	Mean		
	Maximum		
DUSAF2		Use of soil and land cover	Vectorial
DUSAF2		Description of the codes used	Text
Main rivers		Main water streams in the basin	Vectorial
Minor rivers		Secondary water streams in the basin	Vectorial
Contour lines		Elevation isolines	Vectorial

3.1. Computational procedure

Since the DEM provided (and all other data as a matter of fact) have originally covered larger area outside the extent of Mallero basin, it was necessary to delineate exactly the area belonging to the same hydrological basin i.e. all water streams contributing to flow in Mallero and consequently Adda river. As all further computations would be based on the basin itself, this was the first step undertaken in the analysis. A sequence of in-built functions of ArcMap 10.1 was applied to the DEM in order to obtain the proper watershed: 1) A “Fill” tool is first applied which sinks in a surface raster in order to remove imperfections. The output is again a similar raster, obviously without any imperfections; 2) A “Flow direction” tool is applied which creates a raster of flow direction from each cell to its steepest downslope neighbor. The input is the “Fill” raster and the output is a raster of values depending on the neighboring raster cell of each cell. 3) The “Flow direction” raster is used as input for the “Flow accumulation” tool which creates a raster of accumulated flow to each cell, as determined by accumulating the weight for all cells that flow into each downslope cell. The output is a raster with clearly visible cells in which flow will naturally accumulate due to the geometry of the basin. This result could be then cross-referenced with the sub-basin polygons and the limitations of the basin under investigation could be easily observed and all other unnecessary information – deleted. By means of “Clip” tool, the DEM was also edited so that only the Mallero basin was left. The same procedure was applied to the Rivers, Rainfall and DUSAF2 shape files. Further, a re-computation of the geometries of these files was needed since their original values had not changed after the clipping procedure. Having delineated the basin needed, the newly obtained dataset was

used for further manipulations. It was decided that the basin sub division of 10km^2 will be used instead of the 30ha one, resulting in the analysis of 13 sub-basins as shown on Figure II-1 below.

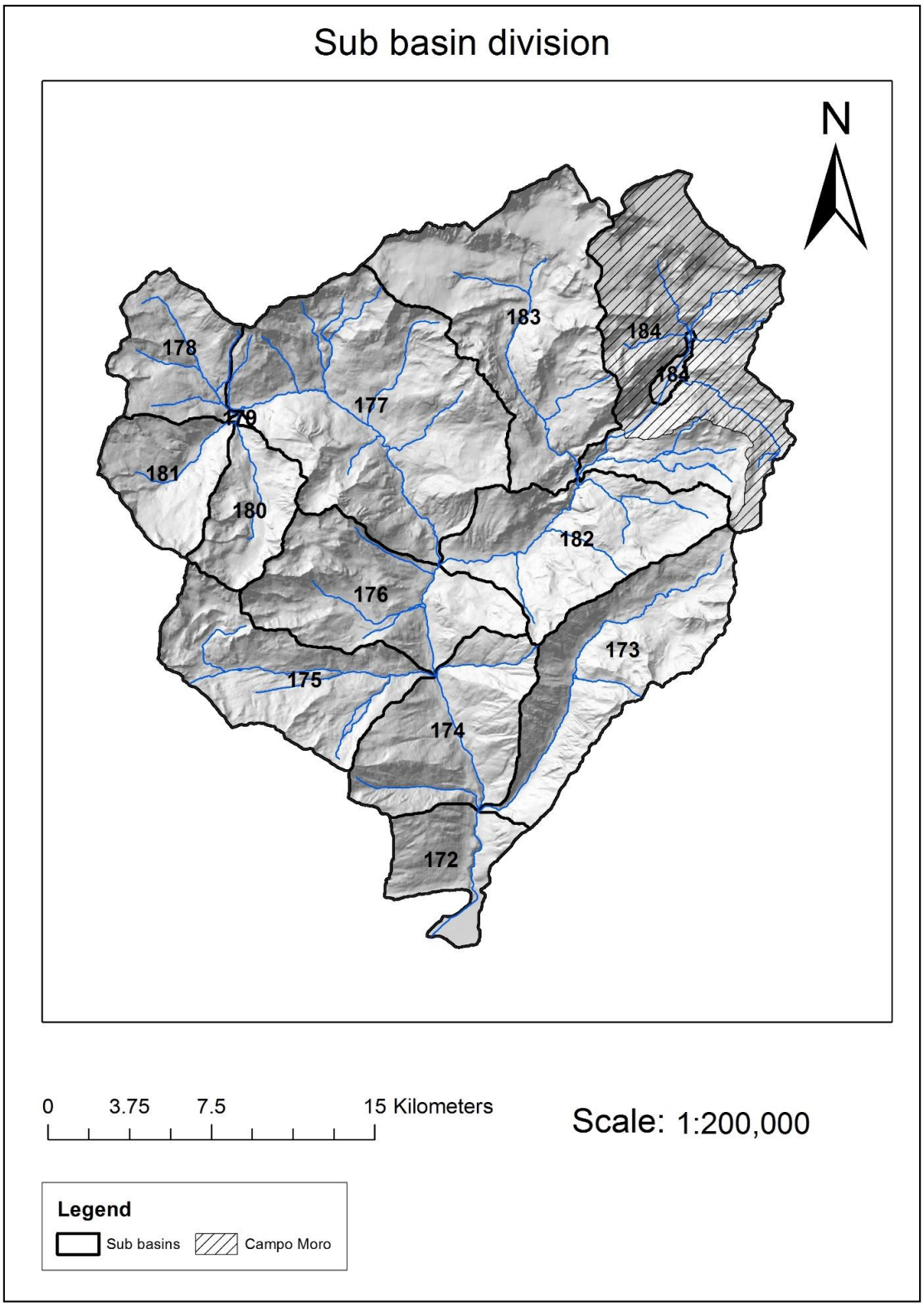

Figure II-1 Subdivision of the Mallero basin

3.1.1. Slope coefficient, I [deg] (figure)

The computation of this coefficient was quite straight forward by means of the Slope tools implemented in ArcMap using the DEM as input. It is calculated as the rate of change of elevation for each cell of the DEM. The output is a raster with slope in percentage for each raster cell. Using the "Zonal Statistics" tool, for each sub-basin, the mean slope value could be extracted in the form of a table.

3.1.2. Temperature coefficient, T [^{0} C]

Since temperature data was not provided, a request was submitted to ARPA Lombardia for temperature values for a period of 1 year. Unfortunately, only two stations were able to provide this data. Due to this low availability, further analysis had to be done.

Considering the environmental lapse rate lawEq. (II.6), the rate of decrease of temperature with increase in altitude is around 6.4^{o}C/km in normal conditions (UCLA, 2010).

$$\gamma = -\frac{\Delta T}{\Delta z} \qquad \text{Eq. (II.6)}$$

A linear relationship was established between the two data points obtained from ARPA Lombardia. Although these are barely enough to establish a trend, the equation relating the data points resulted in 6.6 ^{o}C/km decrease, which is quite close to the theoretical value. Therefore, it was decided that an approximation will be done for all the sub-basins on the basis of this relationship.

Table II-4Mean estimated temperature

Basin ID	172	173	174	175	176	177	178	179	180	181	182	183	184
Z_{mean} m	804	2166	1415	2209	1816	2078	2464	1716	2539	2531	1860	2664	2681
$T_{estimate}$ ^{o}C	8.79	-0.34	4.69	-0.63	2.01	0.25	-2.33	2.68	-2.84	-2.79	1.71	-3.67	-3.79

Here, however, another issue arises. From a mathematical point of view, the expression for the temperature coefficient (Eq. (II.4)) does not allow input of values of temperature, t, lower than -1^{o}C. In fact, even when t = -1^{o}C, the coefficient becomes 0 resulting in nil sediment yield. An attempt was made to find similar cases throughout literature, where a solution of this problem may be proposed. No success was achieved and for this reason, for all negative temperature values, a 0 value is adopted instead, considering that with such low mean annual temperatures, erosion will be far from active for long periods of time.

3.1.3. Annual rainfall, H [mm]

Three sets of rainfall data have been provided by Regione Lombardia – Minimum, Mean and Maximum annual rainfall in the form of isolines over the basin. Using the function "Topo to Raster", the lines were interpolated over the area of the basin and presented in a raster format. The three cases are shown in Figure II-3 – II-5. Again, using the "Zonal Statistics" tool mean values for each dataset were extracted in the form of a table.

3.1.4. Retention coefficient, R [-]

Geometrical features used for the computation of this coefficient were computed directly with "Zonal Statistic" tool and exported as table for further computation.

3.2. Choices made for the evaluation of the erosion coefficient, Z.

As previously discussed, the computation of this coefficient is still left to the operator's choice, abilities and mainly experience in the field. Here, the DUSAF2 map was used along with a description of the codes for each land use type. For each one, the three different coefficients were assigned based on the description provided and the table of descriptive factors recommended for the use of Gavrilovic method previously shown (Table II-2). As a reference point for the choice of the coefficients, additional literature was used (e.g. Brambilla et al., 2011, Mazza et al., 2011) where coefficients have been assigned in similar cases. Assigning the same values for similar land use types, the remaining coefficients were chosen by assigning lower or higher values in accordance with the recommendations set out in the table.

Since the need of single value for each of the three coefficients was needed for each sub-basin and the types of soil use are numerous in each of the thirteen, a weighted approach was chosen depending on the area that each soil type covers. Using the ArcMap tool "Tabulate Area", the number of pixels covered by a particular land use was extracted as a table. After a simple manipulation, the percentage of area covered by a specific land use type referred to the total area of each sub-basin was calculated. In this way, when the coefficients of soil erosion are assigned to the type of soil use, their effect will be weighted according to the fraction of area they occupy in each sub-basin. A summation of the weighted coefficients would yield a single value for each sub-basin. Explicit tables of computation can be found in Appendix A. As it is visible on Figure II-7, the soil use is characterized by a high level of heterogeneity over the area of the basin. In fact 51 different classes are defined representing different types of land use. This will of course inevitably affect the computations. However, it has been computed that a large portion (75%) of the land use is distributed among four classes. The remaining 25% comprise all other 47 classes and therefore their distribution is quite dispersed with values in the range of 0.003% - 5% of the total area. Therefore the

sediment yield will to a large extent be controlled namely by these classes. In this sense, here the major soil use/land covers will be presented and the choice of relevant coefficients will be discussed.

It is worth also mentioning that through a sensitivity analysis carried out by Ballio et al. (2010) the importance of each soil erosion parameter has been estimated. Each one was altered while keeping the other two constant. The results showed that a change of 5% in the coefficient of soil cover alters the result by 35%, while a change of 10% in the coefficients of soil resistance and type and extent of erosion alter the result by 19% and 5% respectively. It is therefore clear that the coefficient of soil cover has the greatest influence on the final result followed by the coefficient of soil resistance. Keeping this in mind, greater attention was paid for the accurate evaluation of this coefficient despite the degree of freedom provided by the ranges of their possible values.

332 - Debris accumulations and lithoid outcrops deprived of vegetation (37.4%)

- Coefficient of soil cover, Ξ = 0.95

Following the table recommended by Gavrilovic, this coefficient has been assigned with a value falling in the range of areas without vegetal cover.

- Coefficient of soil resistance, Π = 0.6

This type of land would be quite resistant to erosion. However, due to the presence of debris accumulations in this code, an intermediate value has been chosen.

- Coefficient of type and extent of erosion, Φ = 0.2

As little erosion is expected, a low value is chosen here also. Due to the same considerations as above, an upper limit value of the lower interval has been chosen.

3121 - Coniferous forests of medium and high density (19.5%)

- Coefficient of soil cover, Ξ = 0.15
- Coefficient of soil resistance, Π = 0.8
- Coefficient of type and extent of erosion, Φ = 0.05

This has been one of the reference cases, chosen from the work of Mazza et al. (2011) in order to calibrate similar types of soil cover. As an example, according to these values, the author has been able to define values for the case of *31111 - Deciduous forests of medium and high density* with slightly increased value for coefficient of soil cover (0.25) due to the unavailability of canopy during half of the year. In this sense also the value for type and extent of erosion will have a higher value (0.15).

333 - Sparse vegetation (10.25%)

- Coefficient of soil cover, Ξ = 0.6
- Coefficient of soil resistance, Π = 0.95
- Coefficient of type and extent of erosion, Φ = 0.4

As previously discussed, the protective features of this type of land cover are less effective and may even lead to concentration in flow with localized high velocities between plants.

335 - Glaciers and permanent snowfields (8.4%)

- Coefficient of soil cover, Ξ = 0
- Coefficient of soil resistance, Π = 0
- Coefficient of type and extent of erosion, Φ = 0

In the case of *335 – Glaciers and permanent snow fields*, it is obvious that erosion would be hardly possible. Therefore, nil values have been assigned to all the coefficients. As a matter of fact, as a result of the mathematical expression of the coefficient of erosion, Z, it is sufficient that either Ξ or Π be set to 0 in order to completely remove the effect of a specific land use.

All remaining assigned coefficients can be found in Appendix A.

Before proceeding further with the computations, two important considerations have to be made:

1) Part of sub-basin 184 contributes to the capacity of an artificial reservoir (bacino di Alpe Gera – hatched area in Figure II-1. In this respect, all sediment yield from this portion of the sub-basin will be trapped in the reservoir and will not be transported further downstream. For this reason, a computation has been made to assess the sediment yield only for this specific catchment and is then subtracted from the total volume;

2) As the first five kilometers of Mallero (starting from the confluence with Adda) will be considered for the integrated modelling, the sediment yield used as input will be limited to all the sub-basins above sub-basin 172. Therefore, volumes obtained for this particular area will be also subtracted from the total amount. In any case, this sub-basin does not have a major influence on the result due to the presence of the town of Sondrio, where residential areas have been assigned with nil coefficients of erosion and therefore do not present any sediment yield.

Computations have been made on the basis of sub-basin level, where for each sub-basin, indicated with an ID on the map (Figure II-1), a volume has been computed. Summation of all the volumes, multiplied by their respective routing coefficients (with the exceptions explained above) gives the

total sediment yield volume at the closing section (upstream of sub-basin 172) for a period of one year.

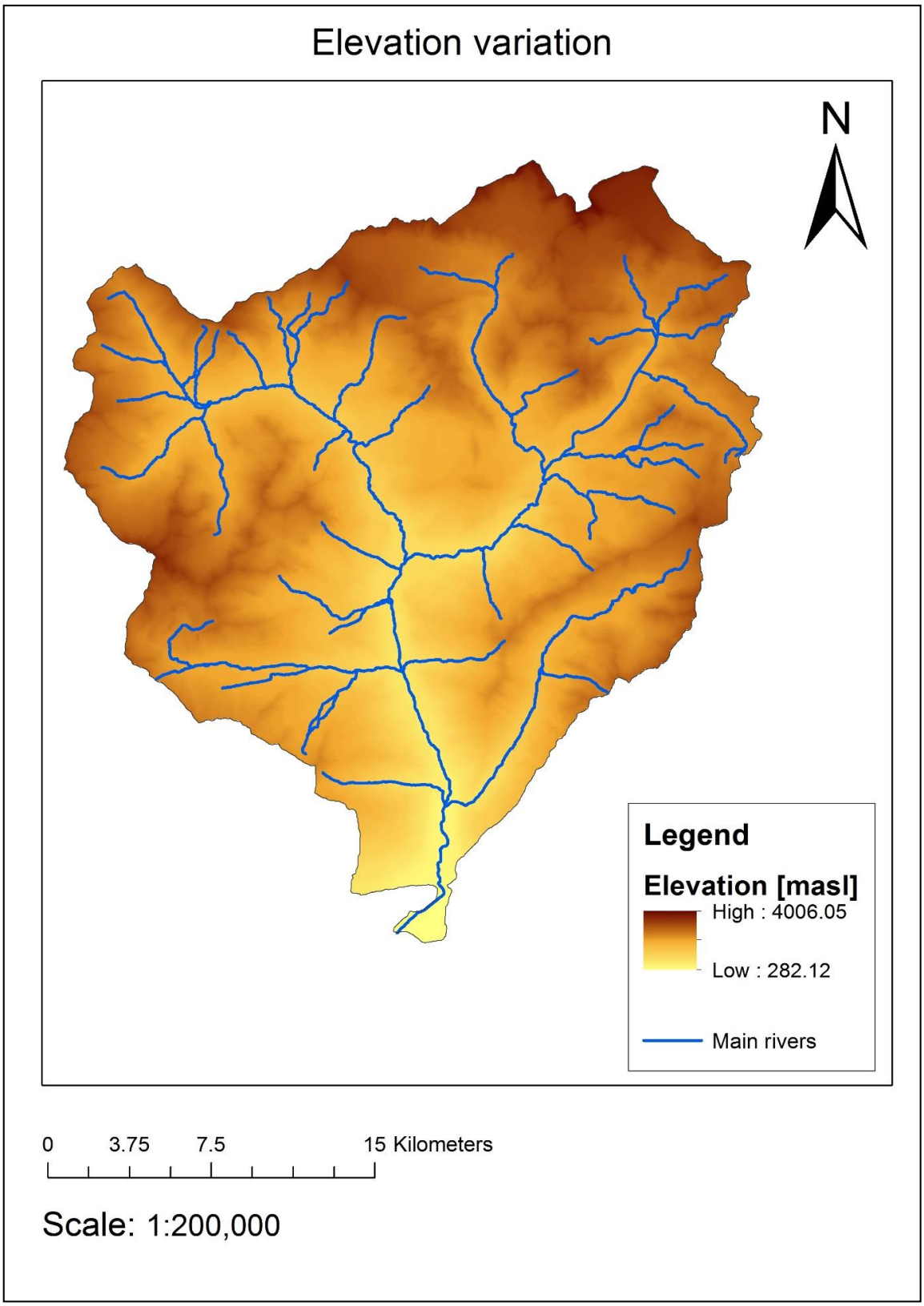

Figure II-2 Elevation variation

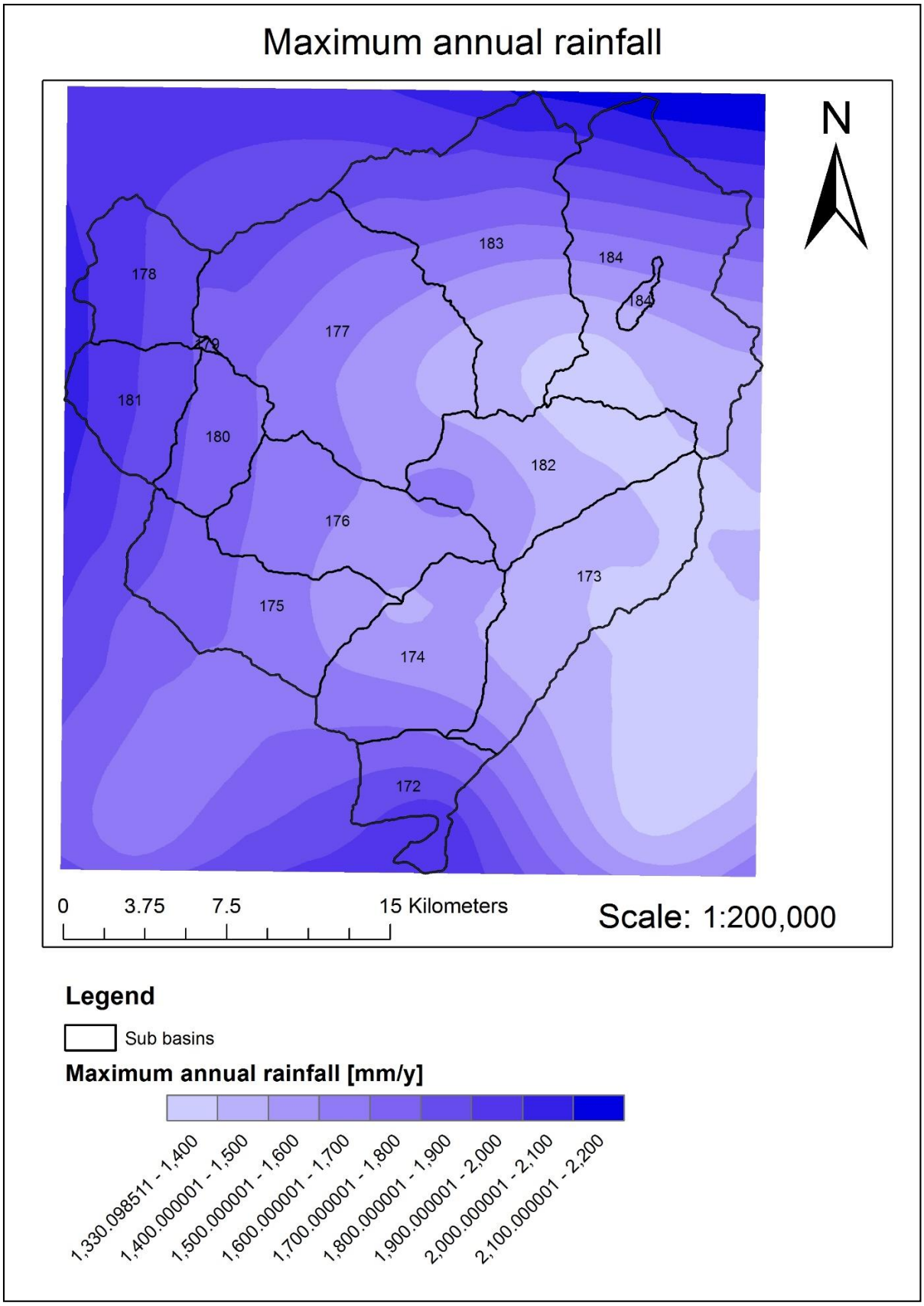

Figure II-3 Maximum annual rainfall

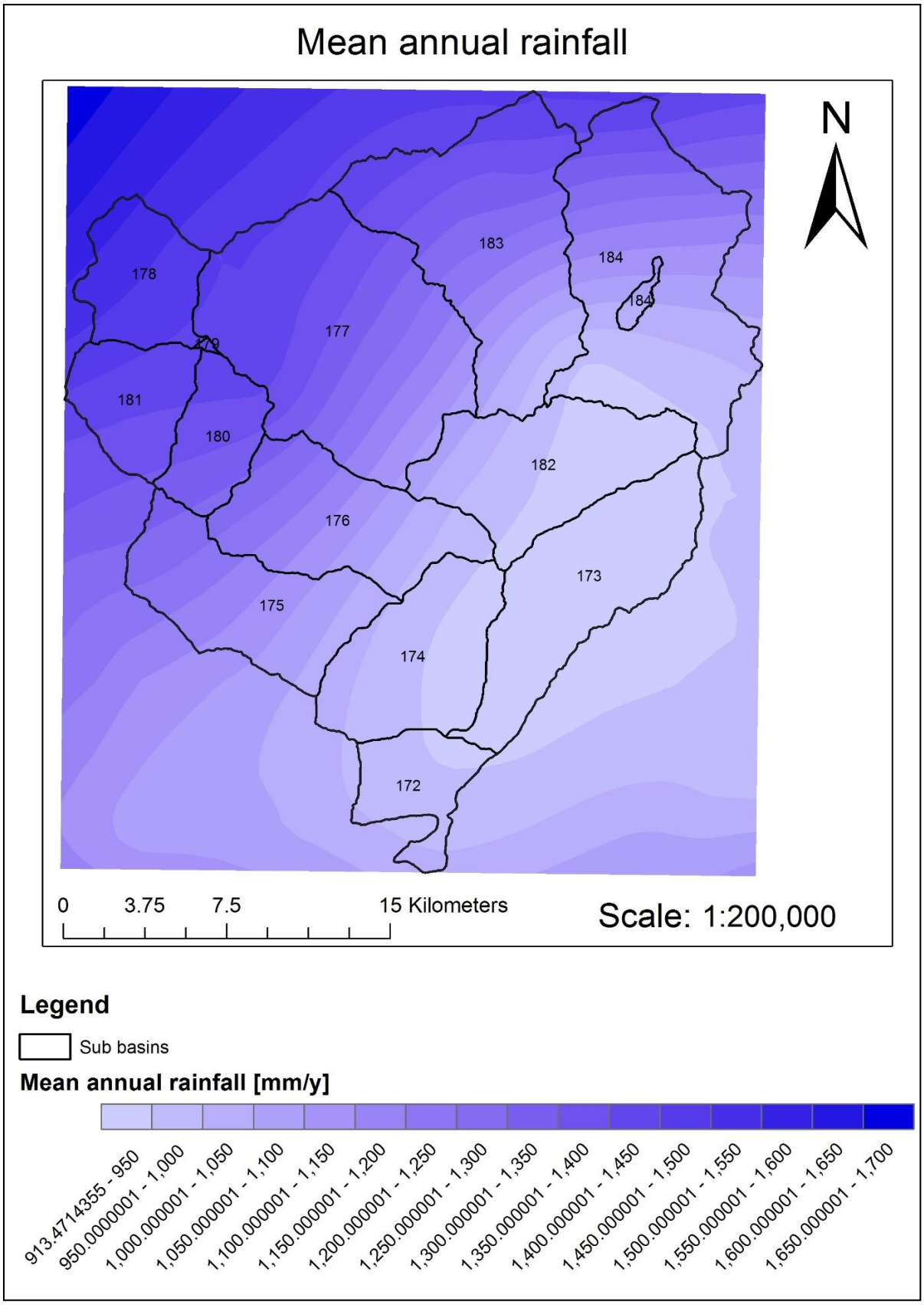

Figure II-4 Mean annual rainfall

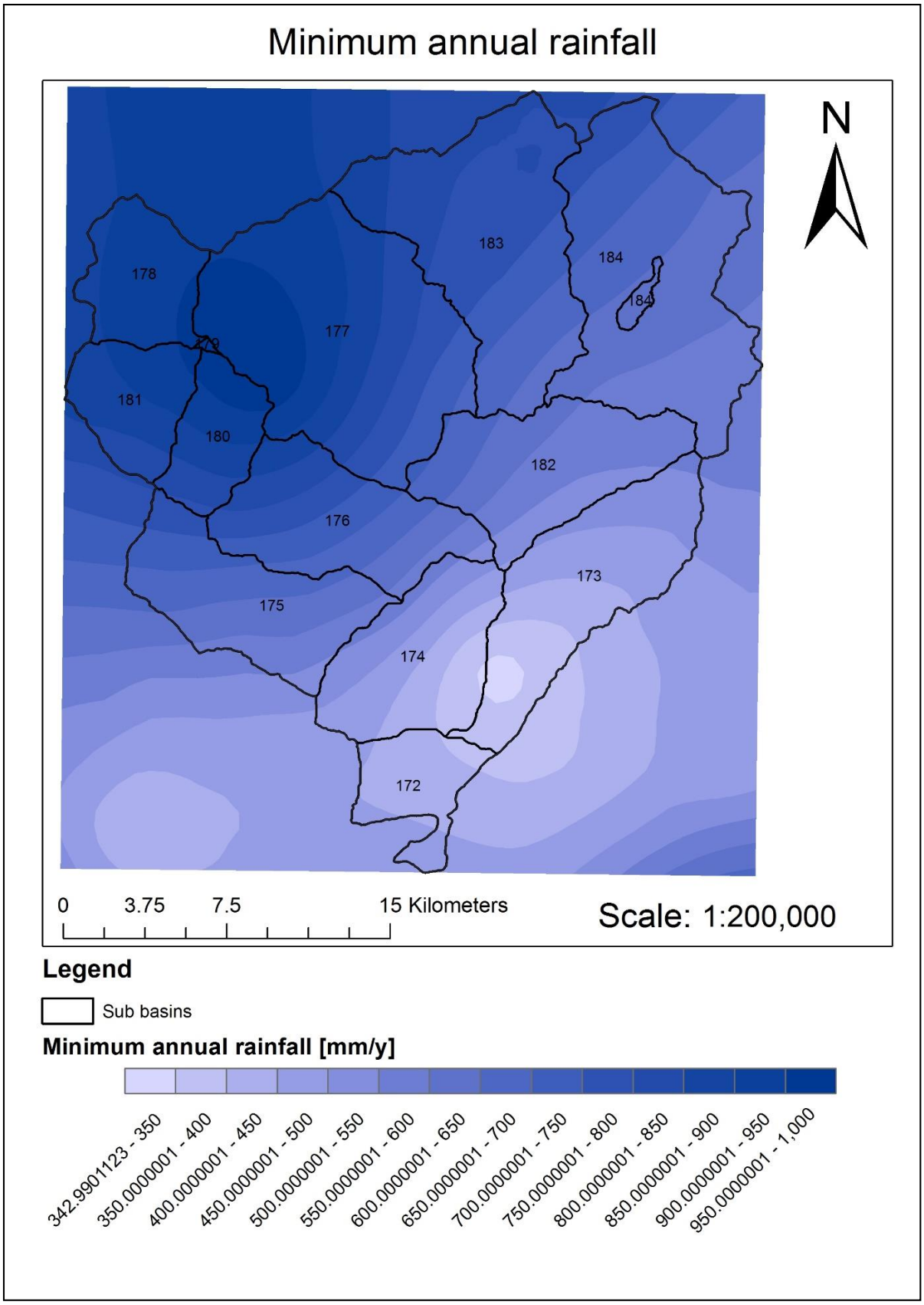

Figure II-5 Minimum annual rainfall

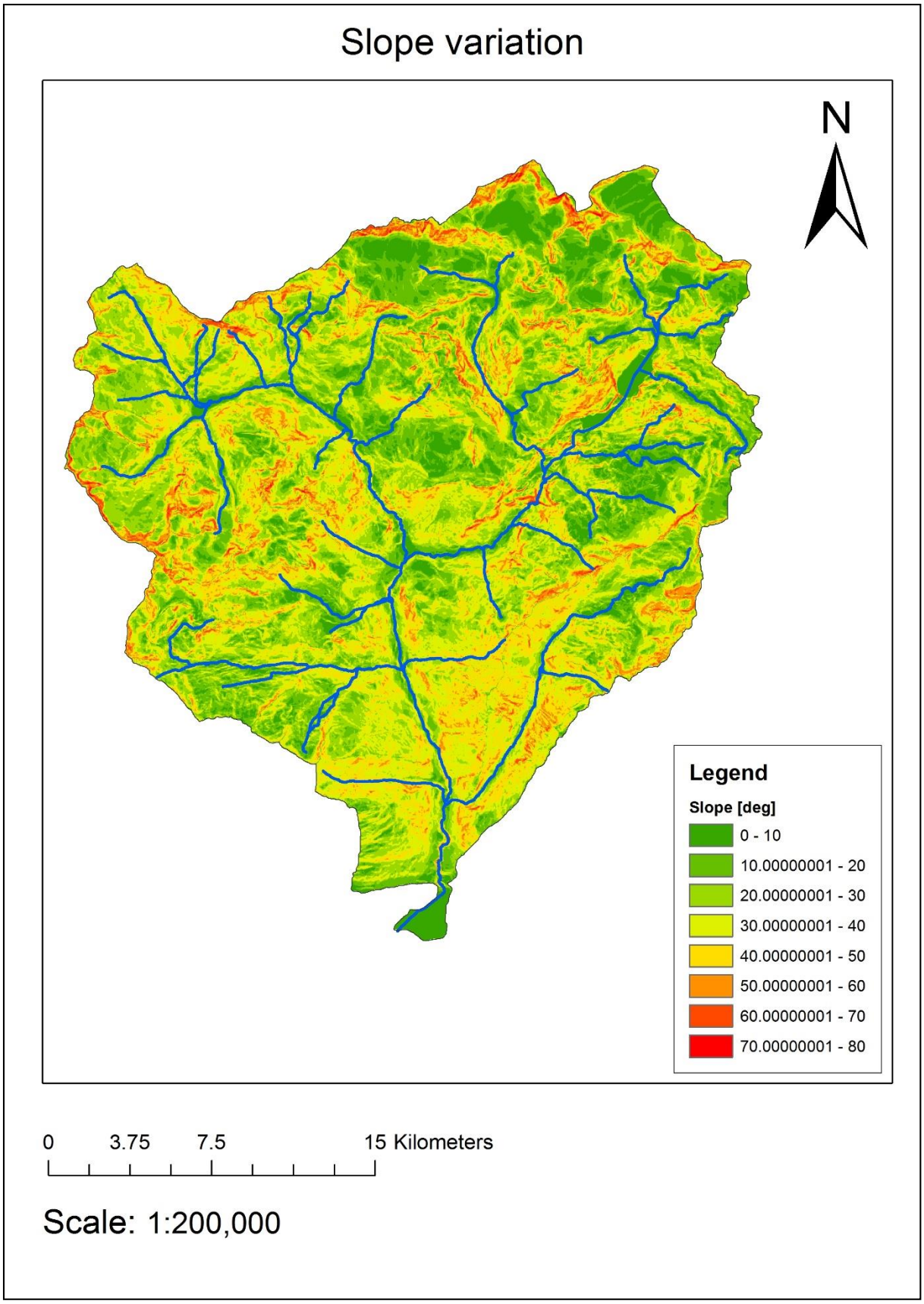

Figure II-6 Slope variation

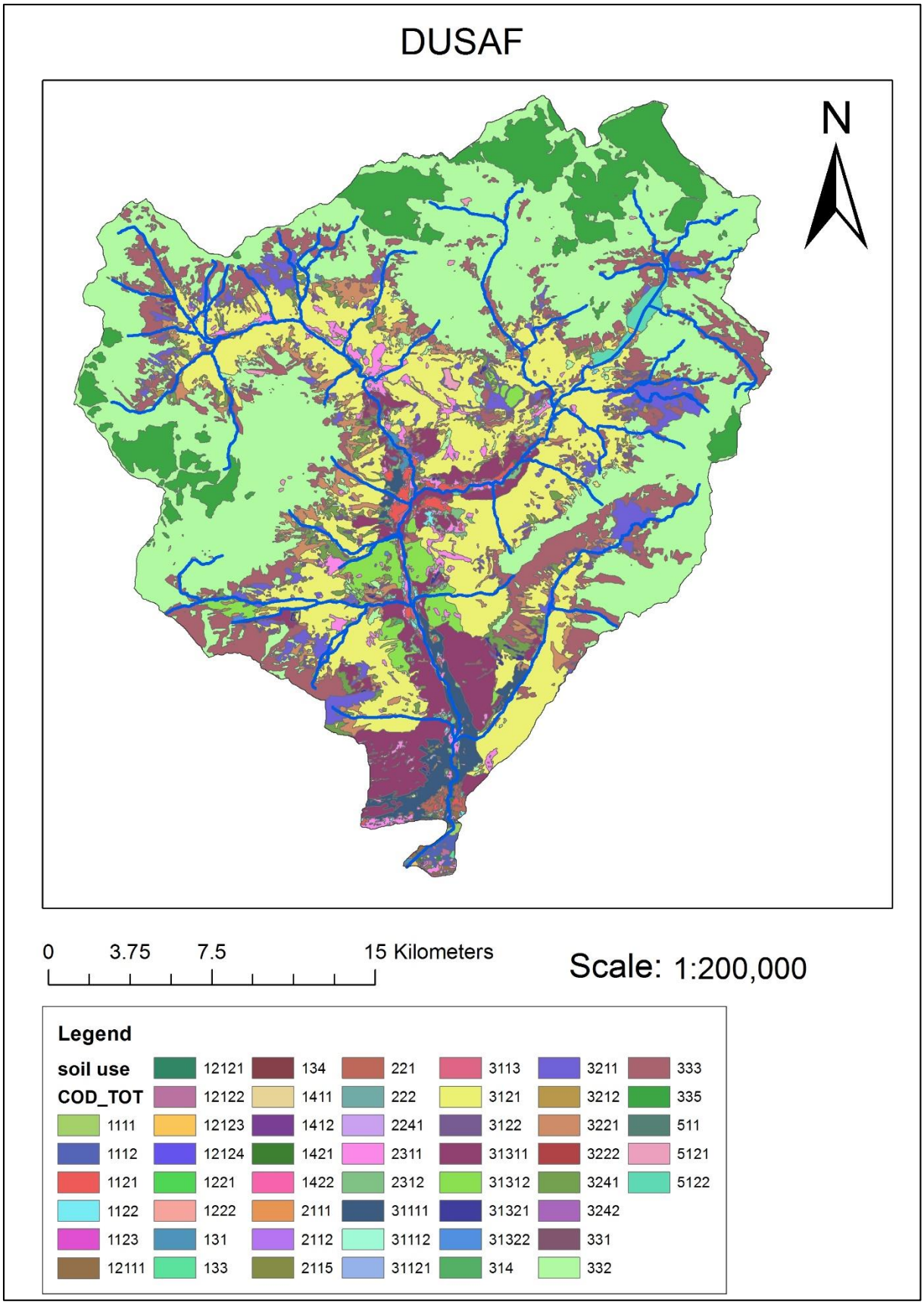

Figure II-7DUSAF map indicating the different land use codes in different colors.

4. Results and discussion

Since three different rainfall datasets have been provided, the relevant computations have been carried out with all three of them. Respective values are presented in the table below. The numbers obtained show high variability depending on the rainfall, which is naturally expected since the rainfall term directly multiplies the others and the volume would grow linearly with rainfall depth per year. However, since the maximum or minimum annual rainfall represent the highest or lowest value recorded in a year, the author considers that these two cases would not be representative of ordinary conditions. Therefore, the result of the mean rainfall data will be regarded as the most acceptable.

Table II-5 Yearly sediment yield according to rainfall variation

Sub-Basin ID	Maximum [mm/y]	Mean [mm/y]	Minimum [mm/y]
172	1828.58	971.82	433.95
173	1445.32	924.58	446.77
174	1572.12	965.63	467.59
175	1683.93	1154.62	649.76
176	1616.79	1140.10	721.02
177	1651.95	1313.89	868.91
178	1904.69	1500.25	922.32
179	1779.22	1433.90	962.82
180	1756.07	1361.93	894.39
181	1904.53	1416.73	885.82
182	1470.96	965.34	593.52
183	1683.47	1249.13	762.12
184	1636.15	1119.89	651.64
ΣG [m^3/year]	926,200	661,400	395,300

Based on this result, two different cases have been chosen to assess the spatial scale variation. 1) Considering individual coefficients of sediment retention, R, for each sub-basin; 2) Considering a global routing coefficient for the entire Mallero basin.

It is evident from Table II-5 that when we consider results with a single routing coefficient for the entire basin, the sediment volume obtained is considerably smaller. This can be explained with the fact that when the area becomes much larger, the zones of accumulation become prevailing over the zones of production (del Curto and Invernizzi, 2011). This effect was also explained by de Vente and Poesen (2005) with the change of the system from erosion limited to transport limited. Or in other words, the effect of sediment sinks becomes predominant over sediment sources resulting in gradual decline of the specific sediment yield for basins with increasing area (> 10 km^2). The larger the area,

the greater the likelihood of sediment deposition on the way, which may result in lower sediment yield at the basin outlet compared to erosion rates measured locally. As already mentioned, the spatial scale effect has been put to evidence in the work of Ballio et al. (2010) when considering sub-basins with smaller areas and therefore more uniform land cover. However, the sub-basin areas here are still large enough to ensure the presence of several types of surface. Thus, it is more reasonable to accept the result obtained with individual routing coefficients for each sub-basin. In fact, this coefficient becomes much smaller in comparison with the rest, computed on the sub-basin scale.

Table II-6 Routing coefficient, R

Basin ID	R (individual)	R (global)
172	0.2139	
173	0.6757	
174	0.5653	
175	0.4852	
176	0.4989	
177	0.5737	
178	0.8225	0.2475
179	0.0962	
180	0.2179	
181	0.3993	
182	0.6964	
183	0.3328	
184	0.6516	

Table II-7 Global vs Local routing coefficient, R

	G [m^3/year]
Individual routing coefficients for each sub-basin	661,400
Global routing coefficient for the entire basin	284,200

Comparison has been made between these results and the application of the method on the Tartano valley by Ballio et al. (2010) (see Table II-8) In relation to the areas in the two cases, it could be expected that having 6.5 times larger area, the sediment yield production would be to some extent proportional at least from the point of view of orders of magnitude. This assumption appears to be respected. In fact, by picking up an individual sub-basin with similar area as in the case of Tartano, it could be observed that the erosion volume obtained is similar to the results obtained for Tartano, which vouches for the validity of the results, computed on the sub-basin scale level, and refutes the one computed on a basin scale level. This case study was chosen due to the fact that its results have been compared against measured values of sedimentation in a reservoir located downstream of the

studied site, the area of the catchment is similar to one of the sub basins in the Mallero case study and the two cases are located not so far from each other which may imply that it is reasonable to expect similar results. Since the area of the basin is not the only controlling factor and the subjectivity of the soil erosion coefficient (which also considerably affects the obtained values, as previously discussed), it could be concluded that the resulting volumes are reasonable and can be representative of reality. Therefore, they will be used in further integrated modelling, described in the next chapters.

Table II-8 Case study comparison with Tartano valley (after (Ballio, et al., 2010))

Case study	Area [km^2]	G [m^3/year]
Mallero, Sub-basin 184	46.3	68,191
Tartano (Ballio et al. 2010)	49	52,931
Tartano (Mazza et al. 2011)	49	18,721– 69,230 (95% confidence interval)
Measured at Campo Dam	-	21,287 – 57,299 38,038 (average over 7 years)

Chapter III. Modelling river bed aggradation

Having defined the role of soil erosion in the flood risk assessment, in this following chapter, the next process in the chain will be laid out – the morphological change of river beds. As a process that is mainly considered as a long term process, it has been often disregarded in the flood risk assessment evaluations. However, as it has been pointed out by Radice et al. (2012), mountain streams provide an environment, favorable for the development of high energy streams which can lead to an increased rate of morphological change, especially when intense precipitation events take place. In such cases, a river bed may aggrade up to several meters within not many hours as the difference in the time scales of a flood wave and a morphological change of the channel would become negligible. Therefore, the two processes have to be treated in a coupled manner in order to produce a complete hazard assessment and possibly a mitigation tool. On the other hand, not only bed aggradation should be considered as a hazard. The undermining effects of river bank erosion or bridge scouring have caused numerous failures of banks and levees, structures and roads etc. Moreover, the sediment transport may also lead to the siltation of reservoirs or to the damage of propellers in hydro-electric plants as well as to the enrichment of agricultural soil by transporting nutritious sediments.

The main focus of this chapter will be the morphological evolution of a river bed as a result of sediment transport. Therefore, a theoretical background will be set out in the following section with the intent of explaining the essential physical principles standing behind this phenomenon. Further, the modelling process that has been carried out will be described along with the reconstruction of the event that blocked the channel of Mallero in 1987 as previously described in Chapter I.

1. Theoretical background

In this sections, the sediment transport phenomenon will be described along with its implications for morphological river bed evolution.

1.1. Sediment transport

Sediment transport is the general term used for the transport of material (e.g. silt, sand, gravel and boulders) in rivers and streams. The term sediment, however, covers a wide range of grain sizes transported by flowing water, ranging from fine clay particles to large boulders. These are usually classified in specific size classes such as “fine sand”, “coarse gravel” etc. (ASCE, 2008). The transported material is called the *sediment load*. Distinction is made between the *bed load* and the *suspended load*. The bed load characterizes the coarser grains transported along the bed intermittently by rolling, sliding or saltating along the bed while suspended load refers to the finer grains maintained in suspension by turbulence (Chanson, 2004). Bed load may take place by simply

translating layers of particles along the channel or by evolution and migration of various bed forms (dunes/antidunes, bars, bends, etc.). On the other hand, suspended load is generally transported within the water flow and at a similar velocity. However, the boundary between suspended sediment and bed-load transport is not precise. The integrated volume of suspended load and bed load is the *total sediment load*.

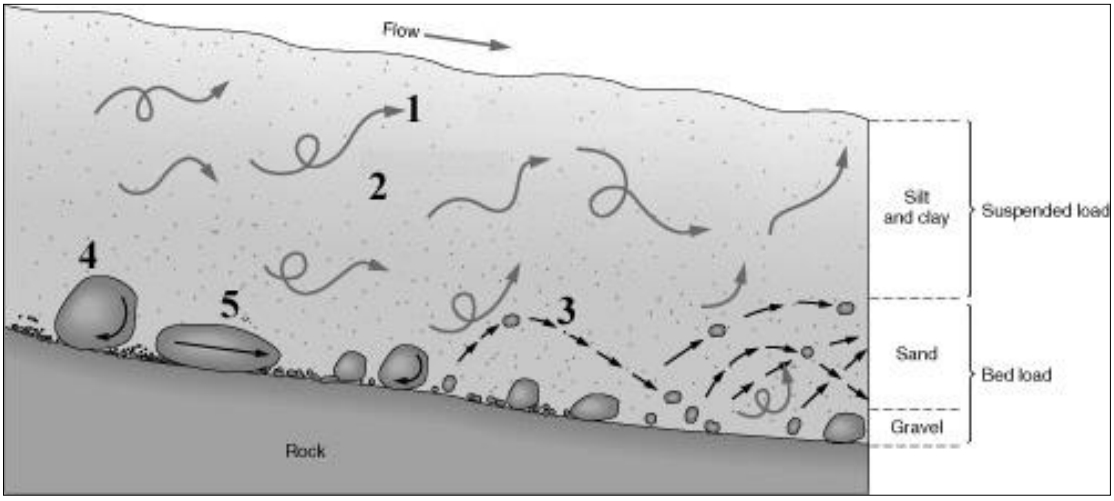

Figure III-1 Modes of sediment transport. 1) Fine particles in suspension; 2) Dissolved load; 3) Sand moving by saltation; 4) Rolling; 5) Sliding.

As a river naturally flows from inland areas toward the ocean, its velocity gradually decreases towards the estuary, where slopes are far from steep. During this process, smaller particles of sediment settle towards the bottom, while the coarser material is found upstream, creating what is known as a sediment gradient. In the slower currents of rivers' lower reaches, only the finest sediments will remain suspended in the water.

Sediment movement is entrained where the stream has enough energy and deposited wherever currents are slower (e.g. transition from steep slope to a mild one) as well as at bends, where sediments create shallow islands in the inside of the curve. Currents are also slowed when they flow over vegetation and algae formations, causing nutrient-bearing sediments to sink to the bottom where they nourish the vegetation.

1.2. Bed formations

The bed form results from the drag force exerted by the bed on the fluid flow as well as the sediment motion induced by the flow onto the sediment grains. In short, the predominant parameters which affect the bed form are the bed slope, the flow depth and velocity, the sediment size and particle settling velocity. At low flow velocities, the bed does not move. With increasing flow velocities, the inception of bed movement is reached and the sediment bed begins to move (incipient motion,

explained further). The basic bed forms which may be encountered are the ripples (usually of heights less than 0.1 m), dunes, flat bed, standing waves and antidunes. At high flow velocities (e.g. mountain streams and torrents), the so-called chutes and step-pools may form. Ripples and dunes move in the downstream direction while antidunes and step-pools are observed with supercritical flows and they migrate in the upstream flow direction.

1.3. Physical properties of sediments

Perhaps the most basic hydraulic property of sediment is the characteristic particle size, d_s. For non-cohesive sediments (sand, gravel) the size can be measured in several ways: (1) Equivalent diameter: the diameter of a sphere having the same volume as the particle, (2) Sieve diameter: the minimum sieve size opening that releases the particle, (3) Sedimentation diameter: the diameter of a solid sphere having the same density and fall velocity, and (4) Surface diameter: the diameter of a sphere having the same surface area. Sieve diameter is the simplest one to perform experimentally.

Another hydraulic property of interest is the particle shape. There are several ways of characterizing this value. Traditionally, the particle shape has been defined in terms either of sphericity (the ratio of surface area of a sphere of equal volume to that of the particle) or of roundness, (the ratio of the average radius of curvature of the edges of the particle to the radius of the largest circle that can be inscribed within the particle cross section).

The specific gravity, *s* (also referred to as $G_s = \frac{\rho_s}{\rho_w}$), of the sediments is an influencing factor when determining its hydraulic characteristics. Specific gravity is defined as the ratio of the solid weight of a particle to the weight of an equal volume of water under standard conditions. Typically, quartz particles such as sands have a specific gravity of around 2.65, but aggregates of smaller materials typically have much lower specific gravities, sometimes approaching 1.

1.3.1. Particle size distribution

Natural sediments are mixtures of many different particle sizes and shapes. The particle size distribution is usually represented by a plot of the weight percentage of a sample, which is smaller than a given size, plotted as a function of the particle size. A cumulative curve fitted to data points is shown in Figure III-2. The characteristic sediment size d_{50} is defined as the size for which 50% by weight of the material is finer. Similarly the characteristic sizes d_{10}, d_{75} and d_{90} are values of grain sizes for which 10%, 75% and 90% of the material weight is finer, respectively. The d_{50} (or d_m) is

known as the median sediment size and is commonly used as the characteristic grain size. A sorting coefficient defined by $(D_{84} / D_{16})^{0.5}$ is also often used to represent the uniformity of the sediment mixture (Wang, et al., 2012).

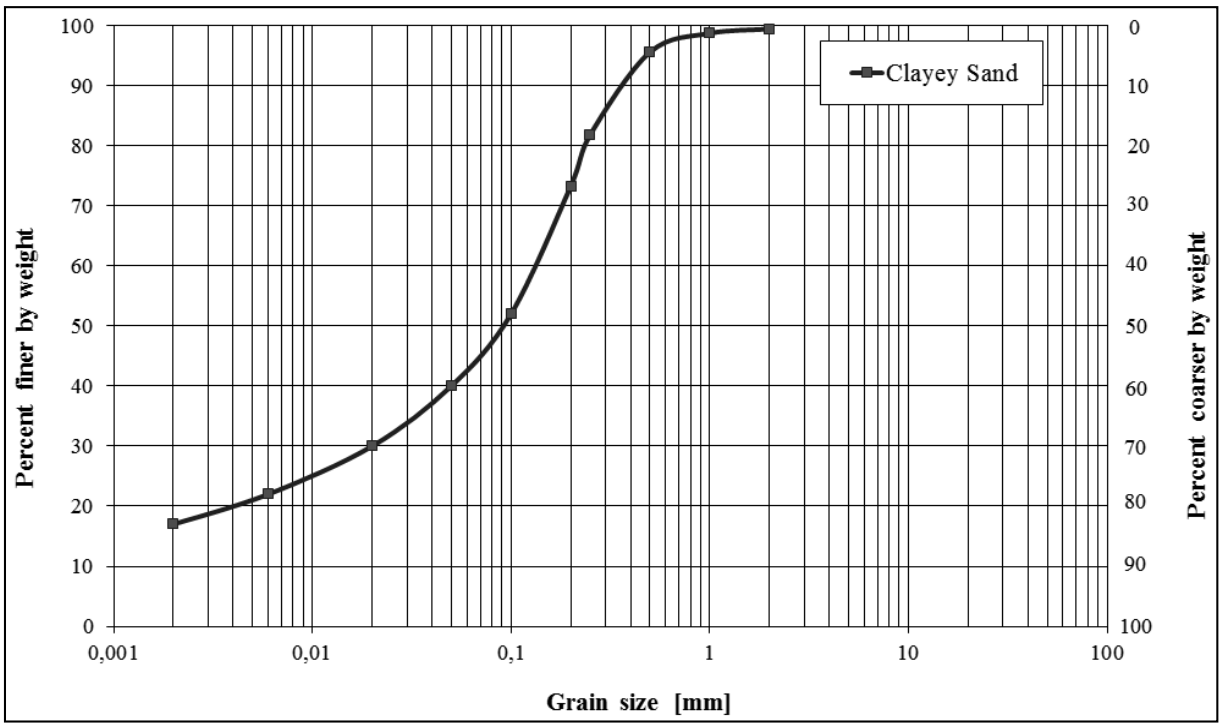

Figure III-2 An example of particle size distribution of clayey sand.

1.3.2. Settling velocity

Imposing equilibrium of forces on a submerged spherical particle we have:

$$\frac{1}{2}\rho_w \omega_0^2 C_D \frac{\pi d_s^2}{4}$$

$$g(\rho_s - \rho_w)\frac{\pi d_s^3}{6}$$

Therefore, the settling velocity can be expressed as:

$$\omega_0 = -\sqrt{\frac{4gd_s}{3C_d}(s-1)} \qquad \text{Eq. (III.1)}$$

where d_s is the particle diameter, C_d is the drag coefficient and s is the specific gravity of the sediment. The negative sign indicates a downward motion (for $s > 1$). Dimensional analysis implies that the drag coefficient is a function of Reynolds number and the particle shape. At low Reynolds numbers (Re < 1), the flow around the particle is laminar. At large Reynolds numbers (Re > 1000), the flow around the spherical particle is turbulent and the drag coefficient is nearly constant. Typical drag coefficient values for spherical particles are presented in Figure III-3.

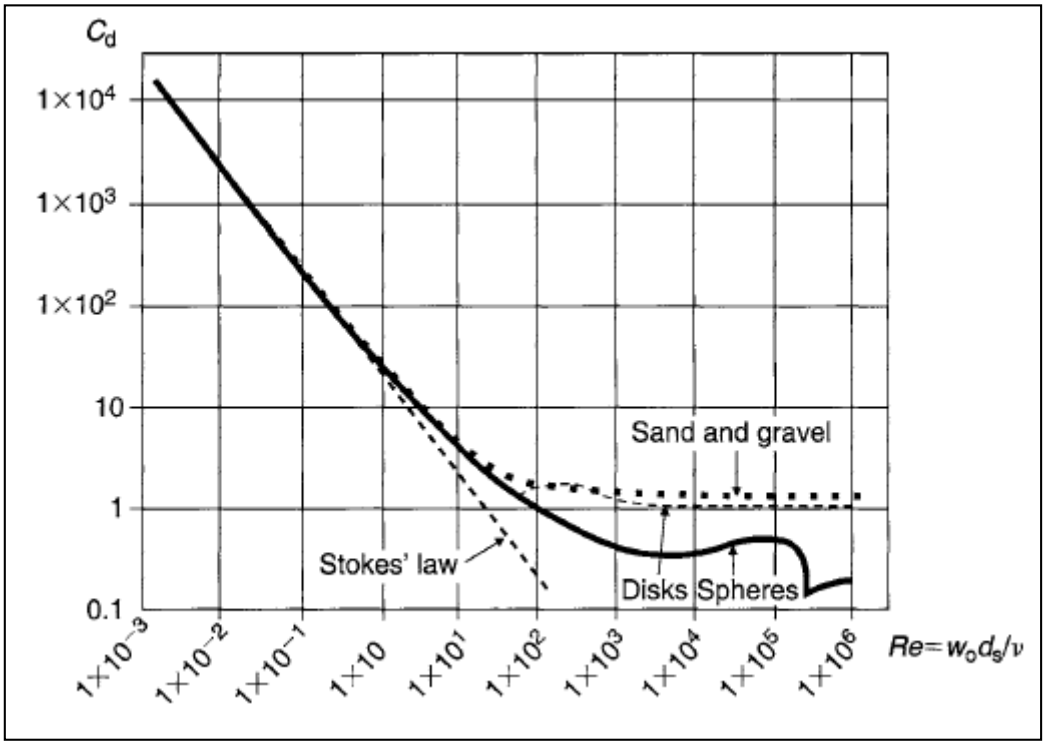

Figure III-3 Drag coefficient of a particle in still fluid (Chanson, 2004)

The settling velocity of a single particle is modified by the presence of surrounding particles. Experiments have shown that thick homogeneous suspensions have a slower fall velocity than that of a single particle. Furthermore, the fall velocity of the suspension decreases with increasing volumetric sediment concentration. This effect, called hindered settling, results from the interaction between the downward fluid motion induced by each particle on the surrounding fluid and the return flow (i.e. upward fluid motion) following the passage of a particle. As a particle settles down, a volume of fluid equal to the particle volume is displaced upwards. In thick sediment suspension, the drag on each particle tends to oppose to the upward fluid displacement.

1.3.3. Angle of repose

Considering the stability of a single particle in a horizontal plane, the threshold condition for motion is achieved when the center of gravity of the particle is vertically above the point of contact. The

critical angle at which motion occurs is called the angle of repose, φ_s. The angle of repose is a function of the particle shape and, on a flat surface, it increases with angularity. Typical examples are shown in (Figure). For sediment particles, the angle of repose ranges usually from 26° to 42°. For sands, φ_s is typically between 26° and 34°.

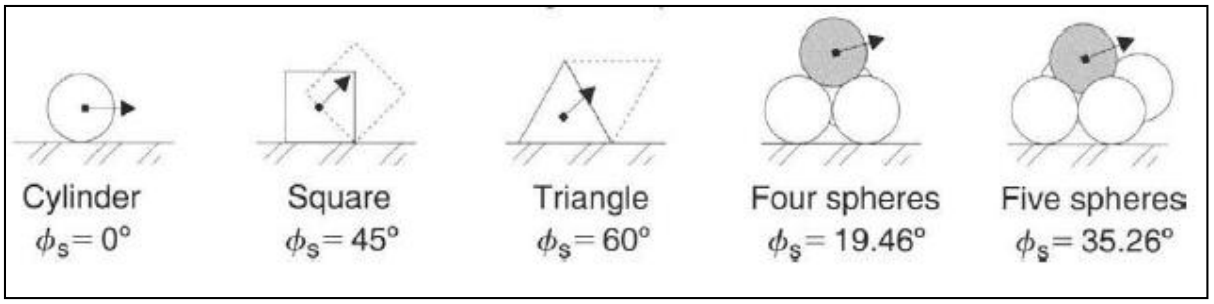

Figure III-4 Examples of angle of repose. (Chanson, 2004)

1.4. Inception of motion

The phenomenon of solid movement is linked to the hydraulic characteristics of the current (velocity distribution, forces on the bottom) which are calculated from the geometry of the channel, the flow and sediment characteristics.

Following a hypothesis of non-cohesive, homogeneous particles and horizontal bed, Shields, starting from the equilibrium of stabilizing and destabilizing forces, developed a theory of incipient motion. In the moment of inception of movement there is an equilibrium between the resistance force and the shear driving force on the particle. Two dimensionless parameters can be defined: the first one defines the mobility:

$$\tau^* = \frac{\tau_0}{\rho(s-1)gd_s} = \frac{u_*^2}{(s-1)gd_s} \qquad \text{Eq. (III.2)}$$

Where $\tau_0 = \rho g R_h \sin\theta$ is the average shear stress on the wetted surface, $u_* = \sqrt{\frac{\tau_0}{\rho}}$ is the shear velocity, s is the specific gravity of the sediment, d_s is its characteristic diameter, $R_h = \frac{A}{P_w}$ is the hydraulic radius of the cross section for which A is its area and P_w is its wetted perimeter; θ is the bed slope.

The second parameter is the Reynolds number which defines the turbulence of the flow:

$$\mathrm{Re}_* = \frac{du_*}{\nu} \qquad \text{Eq. (III.3)}$$

Where ν is the kinematic viscosity of water.

These two parameters are linked by means of laboratory work carried out by Shields and identify the trend which separates the zone of mobility from the zone of immobility of the particles (Figure III-5).

For the points which are situated below the curve ($\tau^* < \tau^*_{cr}$) the current is not able to provoke movement of particles, while the points above the curve represent the conditions of particle movement.

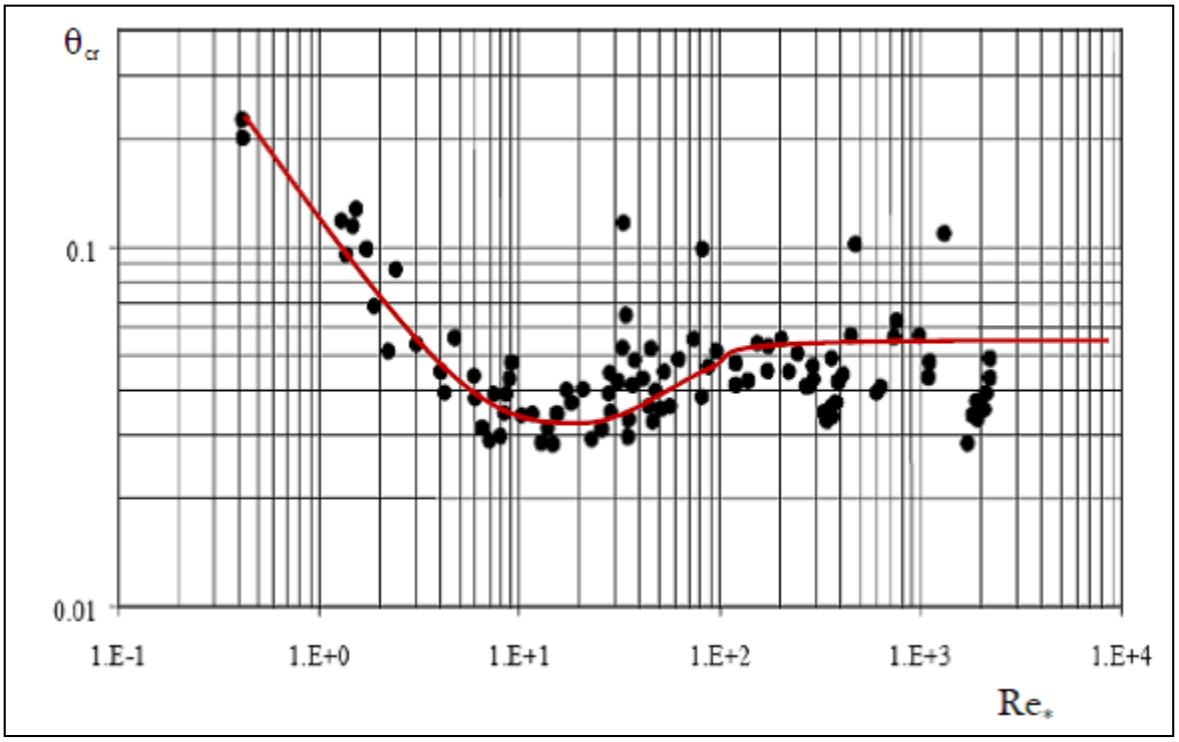

Figure III-5 Shields diagram

The curve itself represents the inception of motion $\tau^* = \tau^*_{cr}$ and can be subdivided in three parts:

- $\mathrm{Re}_* < 2$: The trend is represented by a straight line with a negative slope in the logarithmic scale. The critical shear velocity of the particles does not depend on the diameter but only on the viscosity of the fluid. The flow is generally viscous.
- $2 \le \mathrm{Re}_* \le 200$: An intermediate part where the shape of the trend is curvilinear with a relative minimum. The condition for particle motion depends both on the viscosity of the fluid and the dimensions of the grains.
- $\mathrm{Re}_* \ge 200$: Although the graph is characterized by a high dispersion of the results, the parameter of mobility is assigned a constant value of the line which interpolates them in the

best way $\tau_{cr}^{*} \approx 0.057$. The motion conditions are independent of the viscosity and depend only on the dimensions of the particle. The flow is fully turbulent.

The Shields theory is based on restrictive hypotheses which usually do not represent real conditions. The conditions for inception of motion can be very different than the theoretical ones. A range of different correction coefficients exist, based on experimental results which take into account different features:

- A very steep slope. The destabilizing contribution of the particle weight is taken into account and therefore the inception of motion occurs for a lower critical shear force.
- Effect of relative submergence. When the size of the grains is of the same order of magnitude as the water depth it forms a mixing layer which reduces the mobility of the grains.
- Effect of the inhomogeneity of the material: the particles of smaller size are protected from those of greater size and their mobility is reduced while the larger particles undergo an increase in mobility.
- Effect of armoring – in a channel characterized by a non-uniform particle size distribution, the effort exerted by the water on the different sediments is related to their diameter. In particular, the larger the diameter, the greater the likelihood that these sediments remain motionless. Conversely, the smaller the sediments are, the easier they are transported downstream. Thus the term armoring indicates the fact that the bottom forms a layer of coarser sediments protecting the underlying finer layer from erosion
- Effect of a transverse bank slope- there is a force component in the plane tangential to the bank.

In order to determine the conditions for incipient motion of a mountain stream, usually the critical slope can be defined. This critical slope is calculated under the hypotheses that the flow is turbulent and uniform in the cross sections, which is wide enough to allow the approximation of wetted perimeter with the width of the section.

1.5. Effective bed roughness

The flow in an open channel is usually resisted by numerous sources of friction (Figure III-6). In this sense, the estimation of bed roughness should consider all sources such as grain size roughness, bed form, vegetation cover, channel regularity, obstructions etc. Then the friction coefficient will be some

kind of combination of the different factors such as rough mean $n_{eq} = \frac{1}{N}\sum_i n_i$ or average weighted over the wetted perimeter $n_{eq} = \sum_i p_{wi} n_i$. Many different formulations have been proposed (e.g. Yen, 2002) depending on different conceptual assumptions.

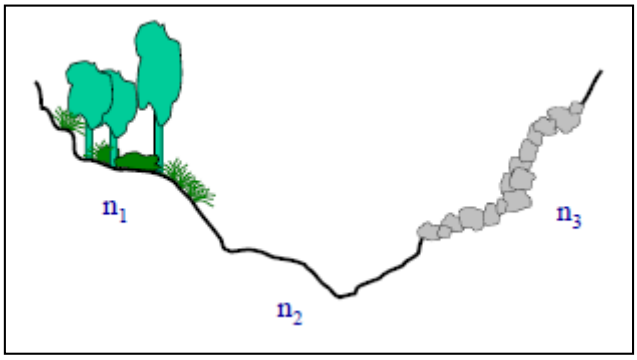

Figure III-6 A composite channel with different friction values (Radice, A. Lecture notes, 2013)

The United States Geological Survey (USGS) organization has provided verified roughness characteristics of natural channels since the evaluating of such a coefficient without a quantitative procedure is extremely subjective. A range of channels with different appearance, geometry, and roughness characteristics have been linked to specific Manning's n-values by calibration. Therefore, a suitable value can be chosen and used with a certain degree of credibility.

http://wwwrcamnl.wr.usgs.gov/sws/fieldmethods/Indirects/nvalues/index.htm

However, according to Chanson (2004) the bed-load transport should be related to the effective shear stress, resulting from skin friction only and not to the effects of bed forms. Therefore, for natural rivers, the Shields parameter and bed-load layer characteristics should be calculated using exclusively the skin friction shear stress. Thus the Shields parameter will have the form:

$$\tau^* = \frac{\tau_0'}{\rho(s-1)gd_s} \qquad \text{Eq. (III.4)}$$

Where, τ_0' is the skin friction and can be derived from the Manning equation as:

$$\tau_0' = \rho g R_h S_f \qquad \text{Eq. (III.5)}$$

Where

$$S_f = n_{skin}^2 V^2 R_h^{-4/3} \qquad \text{Eq. (III.6)}$$

Where, in turn, the part of the roughness due to bed grains can be expressed by the Manning-Strickler relation:

$$n = 0.0132 d_s^{1/6} \qquad \text{Eq. (III.7)}$$

For which d_s [mm] is the characteristic bed material grain size. Eq. (III.7) gives the proportionality between the median size of the sediment particles and the Manning roughness coefficient.

1.6. Transport capacity

The bed load formulae generally relate the transport capacity of a cross section with the difference between calculated Shields parameter and the critical one $(\tau^* - \tau_c^*)$ and sediment properties like the median diameter and the specific gravity. In the following, the formulae for estimation of the transport capacity used in this work will be briefly presented.

1.6.1. Meyer Peter and Müller (1948)

$$\frac{Q_s}{B\sqrt{g(s-1)d_s^3}} = 8(\tau^* - \tau_c^*)^{\frac{3}{2}} \qquad \text{Eq. (III.8)}$$

Where Q_s is the bed load capacity, B is channel width, τ_{cr}^* is critical Shields parameter (the author proposed the value of 0.047) and τ^* is the calculated Shields number. According to Fäh et al (2012) the formula of Meyer-Peter and Müller is applicable in particular for coarse sand and gravel with grain diameters above 1 mm. This formula was not specifically calibrated for steep slopes. However, its use should be acceptable for slope values lower than 5%. (Radice et al., 2012).

1.6.2. Meyer Peter and Müller for multiple sediment sizes

The formula for single size is extended by using a correction factor for the inception of motion ε_g then the Shields number for each grain size g is given by $\tau_{c,g}^* = \varepsilon_g 0.0047$. The factor ε_g is estimated by the following equation proposed by Ashida et al. (1971).

$$\varepsilon_g = \begin{cases} \left[\dfrac{\log(19)}{\log\left(\dfrac{19 d_g}{d_m}\right)} \right]^2 & \text{for } \dfrac{d_g}{d_m} \geq 0.4 \\ \dfrac{d_m}{d_g} & \text{for } \dfrac{d_g}{d_m} < 0.4 \end{cases} \qquad \text{Eq. (III.9)}$$

It is clear that this type of equations for multi sizes considers the sorting effect where the smallest grain size is the faster in transporting, then the coarse sediment remain forming the so called armoring layer, preventing the erosion of finer sediment.

1.6.3. Smart and Jaggi

It represents an extension of the MPM for channels with very steep slopes $(3\% < i_f < 20\%)$.

$$\frac{Q_s}{B\sqrt{g(s-1)d_s^3}} = 4\left(\frac{d_{90}}{d_{30}}\right)^{0.2} i_f^{0.6}\tau^{*0.5}(\tau^* - \tau_c^*)\frac{u}{u_*} \qquad \text{Eq. (III.10)}$$

Where $\left(\frac{d_{90}}{d_{30}}\right)^{0.2}$ is the parameter which takes into account the non-uniformity of the material and can be set to a constant value of 1.05. The use of $\tau_{cr}^* = 0.05$ is advised.

1.7. Morphological evolution

The field of morphodynamics consists of the class of problems for which the flow over a bed interacts strongly with the shape of the bed, both of which evolve in time. The flow field over the bed determines a pattern of variation of sediment transport rate. This variation changes the bed by erosion or deposition of sediment.

Felix Exner was the first researcher to state a morphodynamic problem in quantitative terms. The term “morphodynamics” itself evolved many decades afterward.

Considering a control volume of length *Δx* and width *B*, mass conservation requires that the rate of change of sediment mass in the bed is equal to the mass sediment inflow rate minus the mass sediment outflow rate. Or in mathematical terms:

$$\frac{\partial}{\partial t}\left[\rho_s(1-p_0)\eta\right]\Delta xB = \rho_s\left[Q_s\big|_x - Q_s\big|_{x+\Delta x}\right]B \qquad \text{Eq. (III.11)}$$

$$(1-p_0)\frac{\partial \eta}{\partial t} = -\frac{\partial Q_s}{\partial x} \qquad \text{Eq. (III.12)}$$

Where Q_s is the sediment transport volume, p_0 is the bed porosity, ρ_s is the material density, and therefore $\rho_s Q_s$ represents the mass of sediment per unit width; $\partial\eta$ is the change in bed level.

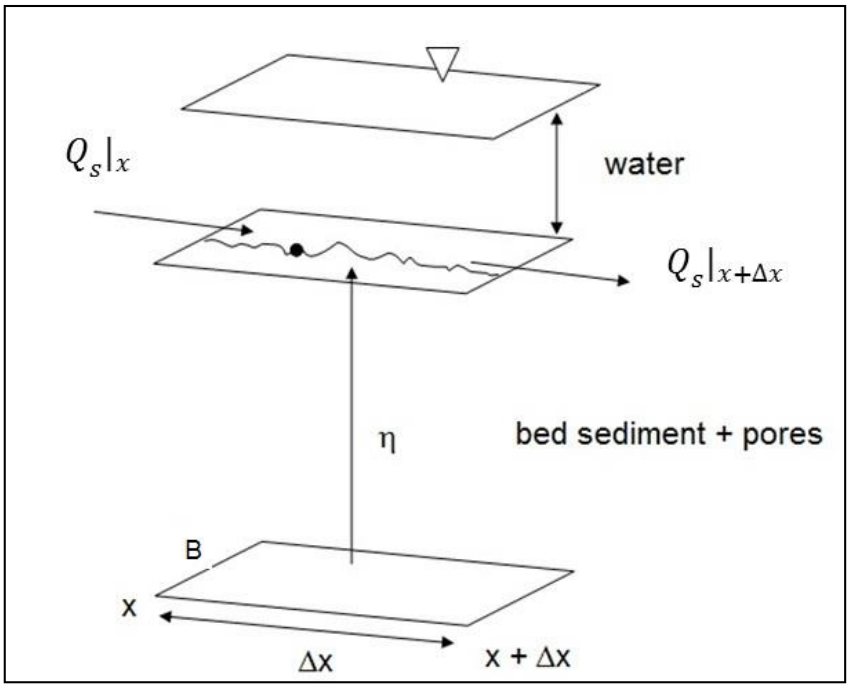

Figure III-7 Representation of the Exner equation (Parker, 2004)

1.7.1. One dimensional governing equations

In order to describe a morphological change in river bed, the coupling effect of water wave modelling (Saint-Venant equations) and bed elevation change (Exner equation) is needed as well as a suitable closing equation for the calculation of sediment transport capacity in a river section (e.g. see Section 1.6.). In order to describe all these processes, the following governing equations are used for one-dimensional flow:

1) The Saint-Venant equations
   a) Conservation of mass:

$$\frac{\partial A}{\partial t}+\frac{\partial Q}{\partial x}=0 \qquad \text{Eq. (III.13)}$$

   b) Conservation of momentum:

$$\frac{\partial V}{\partial t}+V\frac{\partial V}{\partial x}+g\frac{\partial h}{\partial x}=g(S_0-S_f) \qquad \text{Eq. (III.14)}$$

2) Exner equation:

$$\frac{\partial Q_s}{\partial x}=-(1-p_0)\frac{\partial \eta}{\partial t}B \qquad \text{Eq. (III.15)}$$

3) Solid discharge:

$$Q_s=f(Q,h,d_s,\rho_s.....) \qquad \text{Eq. (III.16)}$$

1.8. Multiple grain size distribution

A river that is supplied with a wide range of grain sizes has the opportunity to sort them. Although the grain-size distribution found in river beds is never uniform, the range of sizes tends to be particularly broad in the case of rivers with beds that consist of mixtures of gravel and sand. The river can sort its material in the streamwise, lateral, and vertical directions, resulting in each case in a characteristic morphology (ASCE, 2008). Sorting phenomena range from very small scale to very large scale. In many river channels, the bed is vertically stratified, with a coarse armor layer on the surface. This layer limits the supply of fine material from the subsurface to the bed load at high flow. The phenomena is known as *armoring*. Sorting can be observed near bends and bar formations as well as upstream of reservoirs. Considering a larger scale, sorting appears as the tendency for characteristic grain size to become finer over tens or hundreds of kilometers in the downstream direction. This effect is evident in the table of characteristic sediment sizes of Mallero presented in Chapter I. Grain size sorting plays an important role in the 'digestion' of sudden sediment inputs, such as debris flows or landslides, with sediment sizes much larger or smaller than the ambient bed material. On the other hand, an extensive investigation is necessary to collect data for sediment size distribution along a river reach and often single sized models are adopted as a first approximation.

1.9. Numerical schemes

The complete unsteady water flow equations along with the sediment continuity equation are a system of partial differential equations. Closed form solutions for them are available only for idealized cases, so these equations are solved by means of numerical techniques (the finite difference method (FD), the finite volume method (FV) or the finite element method (FE)).

In FD methods: the partial derivations of equations are approximated using Taylor series. This method is particularly appropriate for an equidistant Cartesian mesh. In FV methods: the partial derivations of equations are not directly approximated like in FD methods. Instead, the equations are integrated over a volume, which is defined by nodes of grids on the mesh. The volume integral terms will be replaced by surface integrals using the Gauss formula. These surface integrals define the convective and diffusive fluxes through the surfaces. Due to the integration over the volume, the method is fully conservative. This is an important property of FV methods. It is known that in order to simulate discontinuous transition phenomena such as flood propagation, one must use conservative numerical methods. In FE method: the problem domain is ideally subdivided into a collection of small regions, of finite dimensions, called finite elements. The elements have either a triangular or a quadrilateral form and can be rectilinear or curved. After subdivision of the domain, the solution of discrete problem is assumed to have a prescribed form. This representation of the solution is strongly linked to the geometric division of sub domains and characterized by the prescribed nodal

values of the mesh. These prescribed nodal values must be determined in such way that the partial differential equations are satisfied.

1.10. Uncertainties

Uncertainties in modelling hydro-morphological processes arise from our attempt to describe natural phenomena that are intrinsically complex, act in a coupled way among each other, and are affected by numerous variable parameters along a single channel under consideration. For example, the choice of a friction coefficient is more of an educated guess than a definition and experience in the field plays a major role in the choice of such a parameter. Further, results are strongly affected by the formulation of certain quantities such as the bed load, for which there are numerous empirical formulas, conceived under different laboratory conditions and even though trends are usually similar, the quantities obtained show extensive variations. The way in which an aggradation/erosion is distributed in a channel is also a source of uncertainty considering that this may occur uniformly or in a localized manner over a cross section.

2. Modelling with Basement.

In order to apply the theory described above for the case of Mallero, the numerical solver Basement was used to run the computations. An extensive comparative study carried out by Elsayed (2013) showed that Basement is handling much better among other software (HEC-RAS, ISIS) when morphology is concerned. For this reason it is a preferred choice in this work.

2.1. Software conceptual scheme

Basement is a software created with the purpose to evaluate morphological evolution in a water stream, developed by the Hydraulic Department of the Swiss Federal Institute of Technology ETH Zürich (Fäh et al., 2010). The figure below give a graphical representation of the interconnection between the different components of the numerical simulation tool.

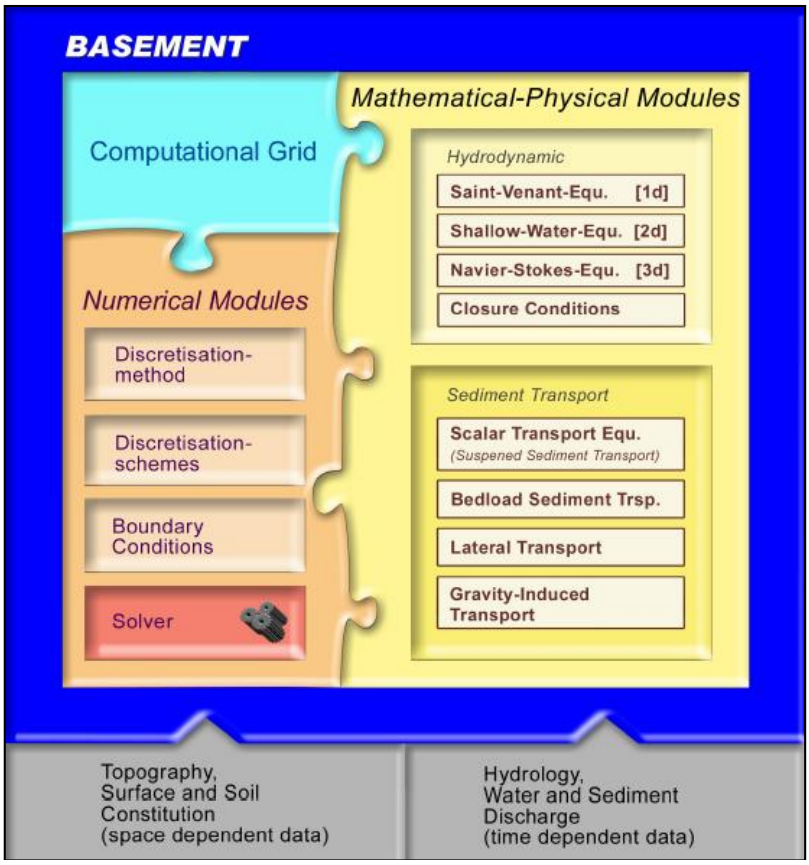

Figure III-8 Conceptual scheme of Basement

The subdivision can be described as follows:

1) Mathematical-physical modules consisting of the governing flow equations: for the hydrodynamic part, with respect to one-dimensional simulation, the Saint-Venant equations are used to obtain results for the water level and mean velocity in the direction of the stream. Sediment transport and behavior of the riverbed are computed using empirical formulae.
2) A computational grid representing the discrete form of the topography, consisting of control volumes, which are in turn, formed by three components: (i) nodes, or mass free points in relation to a coordinate system; (ii) edges defined by two nodes and define the place of information flux between two elements in Finite Volume Methods; (iii) elements, which are defined by several nodes and define the place of the physical variables. (Figure III-9)
3) Numerical models with their methods for solving the equations (e.g. implicit/explicit schemes, see section III.1.9.).

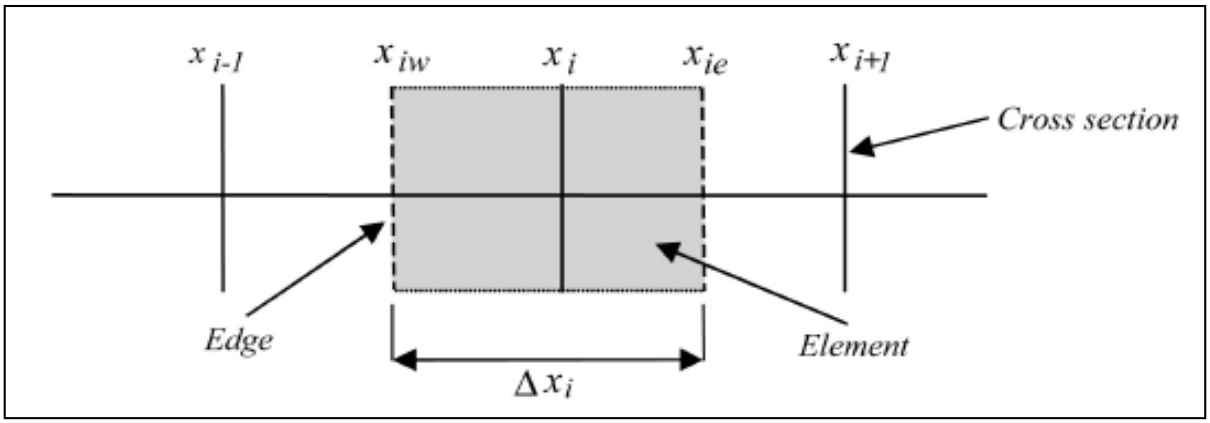

Figure III-9 Spatial discretization used in 1D simulation in Basement.

2.2. Computational scheme

Basement solves the system of partial differential equations, comprised of the Saint-Venant equations for conservation of mass and momentum and the Exner equation for conservation of solid mass. As discussed above, such equations can be solved by different discretization schemes: finite differences, finite elements, method of characteristic lines, finite volumes. In Basement, the latter is incorporated, where the equations are integrated by volumes, defined by meshes of nodes and computational grids, representing the continuum in a discrete form and allow the simulation of phenomena such as the propagation of a water wave. The time discretization is based on the explicit Euler scheme, where the updated values are calculated considering only values from the precedent time step. On the other hand, the spatial discretization is carried out by the finite volume method, where the differential equations are integrated over the single elements. It is assumed that values, which are known at the cross section location, are constant within the element. Considering the scheme depicted above, it can be stated that:

$$\int_{x_{iL}}^{x_{iR}} f(x)dx \approx f(x_i)(x_{iR} - x_{iL}) = f_i \Delta x_i \qquad \text{Eq. (III.17)}$$

Where x_{iR} and x_{iR} are the positions of the edges at the right and the left side of the ith element, as illustrated in Figure III-9. In this way, the governing equations can be integrated as follows:

$$\int_{x_{iL}}^{x_{iR}} \left(\frac{\partial A}{\partial t} + \frac{\partial Q}{\partial x} - q_l \right) dx = 0 \qquad \text{Eq. (III.18)}$$

$$\int_{x_{iL}}^{x_{iR}} \frac{\partial A_i}{\partial t} dx \approx \frac{\partial A_i}{\partial t} \Delta x_i \approx \frac{A_i^{t+1} - A_i^t}{\Delta t} \Delta x_i \qquad \text{Eq. (III.19)}$$

$$\int_{x_{iL}}^{x_{iR}} \frac{\partial Q_i}{\partial x} dx \approx Q(x_{iR}) - Q(x_{iL}) = \Phi_{c,iR} - \Phi_{c,iL} \quad \text{Eq. (III.20)}$$

$$\int_{x_{iL}}^{x_{iR}} q_l dx \approx q_{iR}(x_{iR} - x_i) - q_{iL}(x_i - x_{iL}) \quad \text{Eq. (III.21)}$$

$\Phi_{c,iR}$ and $\Phi_{c,iL}$ are the continuity fluxes and q_{iR} and q_{iL} the lateral sources in the corresponding river segments. For the explicit time discretization, the new values of A will be:

$$A_i^{t+1} = A_i^t - \frac{\Delta t}{\Delta x_i}(\Phi_{c,iR} - \Phi_{c,iL}) - \frac{\Delta t}{\Delta x_i}(q_{iR}(x_i - x_{iR}) + q_{iL}(x_{iL} - x_i)) \quad \text{Eq. (III.22)}$$

Integrating the momentum equation is carried out in a similar way, namely starting from

$$\int_{x_{iL}}^{x_{iR}} \left(\frac{\partial Q}{\partial t} + \frac{\partial}{\partial x}\left(\beta \frac{Q^2}{A_{red}} \right) + \sum soruces \right) dx = 0 \quad \text{Eq. (III.23)}$$

The expression of the flow in the successive time instant can be obtained as:

$$Q_i^{t+1} = Q_i^t - \frac{\Delta t}{\Delta x}\left(\Phi_{m,iR} - \Phi_{m,iL}\right) + \sum sources \quad \text{Eq. (III.24)}$$

Where $\Phi_{c,iR}$ and $\Phi_{c,iL}$ are the momentum fluxes.

The last equation of the system is the Exner equation for solid transport, it is solved as follows:

$$\int_{x_{iL}}^{x_{iR}} \left((1-p_0)\frac{\partial A}{\partial t} + \left(\sum_{k=1}^{ng} \frac{\partial Q_s}{\partial x} + S_g - Sl_g \right) \right) dx = 0 \quad \text{Eq. (III.25)}$$

$$\int_{x_{iL}}^{x_{iR}} \frac{\sum_{k=1}^{ng} Q_{s,i}}{\partial x} dx = \sum_{k=1}^{ng} Q_s(x_{iR}) - \sum_{k=1}^{ng} Q_s(x_{iL}) = \Phi_{s,iR} - \Phi_{s,iL} \quad \text{Eq. (III.26)}$$

$$\int_{x_{iL}}^{x_{iR}} \sum_{k=1}^{ng} (S_g - Sl_g) dx = \sum_{k=1}^{ng} S_g - \sum_{k=1}^{ng} Sl_g \quad \text{Eq. (III.27)}$$

Where $\Phi_{c,iR}$ and $\Phi_{c,iL}$ are the bed sediment transport fluxes.

A two phase system (water and solids), in which the sediment mixture can be represented by an arbitrary number of different grain size classes, is then formulated. The continuous physical domain has to be horizontally and vertically divided into control volumes to numerically solve the governing equations for the unknown variables. The figure below represents a single control volume with the vertical fragmentation of three principal segments of the control volume: the upper layer for the

momentum and suspended sediment transport, the active layer for the bed load sediment transport as well as bed material sorting and sub layers for sediment supply and deposition.

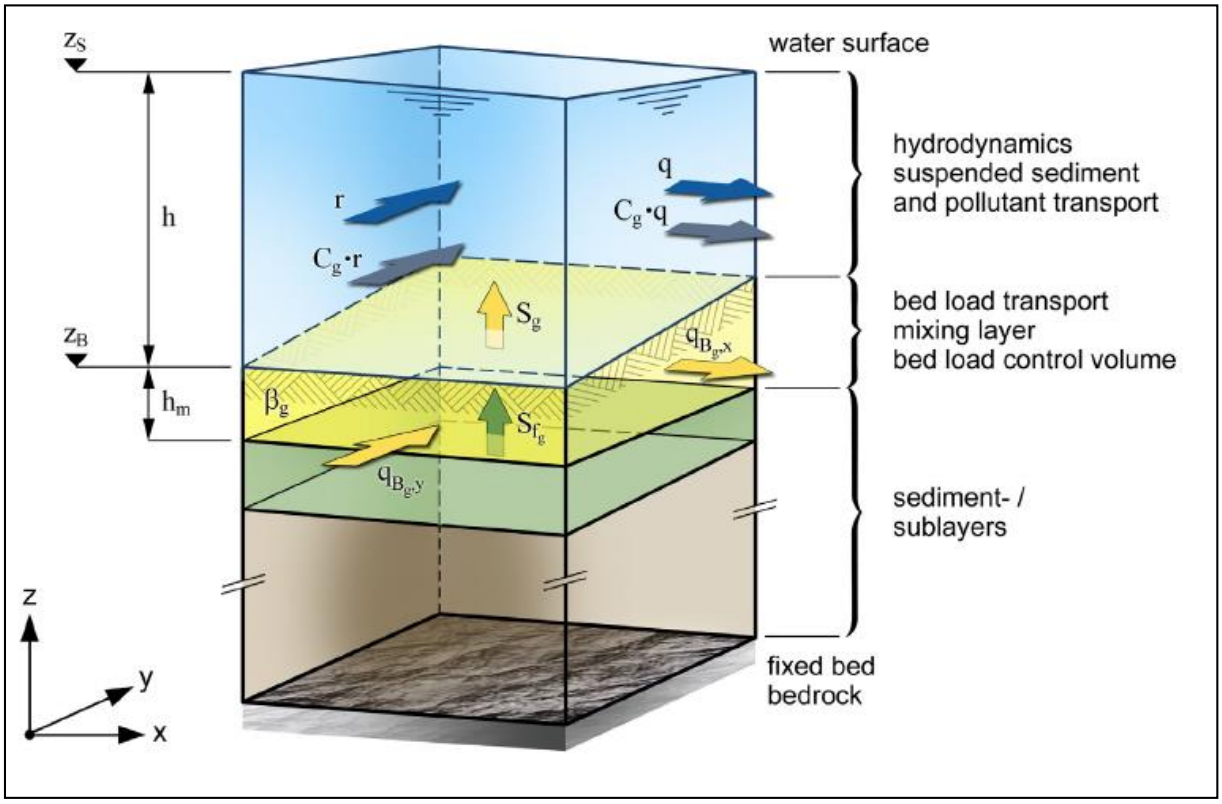

Figure III-10 Vertical discretization of a computational cell describing the general 2-dimensional case

The primary unknown variables of the upper layer are the water depth, *h* and the specific discharge in x and y directions. In the active layer, $q_{B_{g,x}}$ and $q_{B_{g,y}}$ describe the specific bed load fluxes. A change of bed elevation, z_B can be obtained by a combination of balance equations for water and sediment and corresponding exchange terms (source terms) between the vertical layers. In this work, a 1-dimensional flow is considered and therefore bed load flux is computed only in one direction.

The way in which the code modifies the sections in case of erosion or deposition is an arbitrary choice made by the developers of the software. It is largely affected by the choice of "bottom" and "active layer" when defining the geometry of the problem. This is a key moment in the following analysis, since the understanding of the bed level changes due to bed load made possible the creation of a more precise geometry.

3. Case study – Mallero 1987

As already discussed, hazard assessment of a stream cannot ignore the modelling of the change of bed elevation due to transport of solids by the current. Such necessity is particularly important for mountain streams where usually there is a high availability of sediment and the current intensity is

elevated due to the significant slope ranges. The flood event of 1987 described in Chapter I threatened the town of Sondrio even though its intensity was not particularly high – less than a 100 years return period. This provoked the onset of many studies aimed at understanding the hydrogeological hazard and in particular the dynamics of solid transport in mountain streams. In addition, after such an event measured data have become available relative to the geometry, hydraulics and hydrology in the Mallero water basin. Therefore, this flood event has been used as a case study to create and validate models that simulate solid transport in mountain streams. Also in this work, an attempt has been made to simulate as accurately as possible the circumstances that led to a significant flood threat.

3.1. Geometry definition

Several models of Mallero have been developed with the purpose of analyzing hydro-geological risk. A starting point was the systematization of the original cross-section geometry, one of which is illustrated below. Previous models used trapezoidal shaped sections (Figure III-11) as an approximation to the real ones. More recently, in the work of Elsayed (2013), bank elevations were given unrealistic values (e.g. 5000 m) with the purpose of reaching a complete profile for the total duration of an event in stable conditions. The reason for this was the difficulty of numerical codes to overcome the complexity of such irregular cross sections, typical for mountain regions. In this sense, one of the tasks of this work has been the refinement the geometry used for modelling in order to obtain a more realistic, higher quality model. Therefore, starting from the originally surveyed geometry of the channel, an attempt was made to obtain a complete, numerically stable model, avoiding the simplifications, previously introduced.

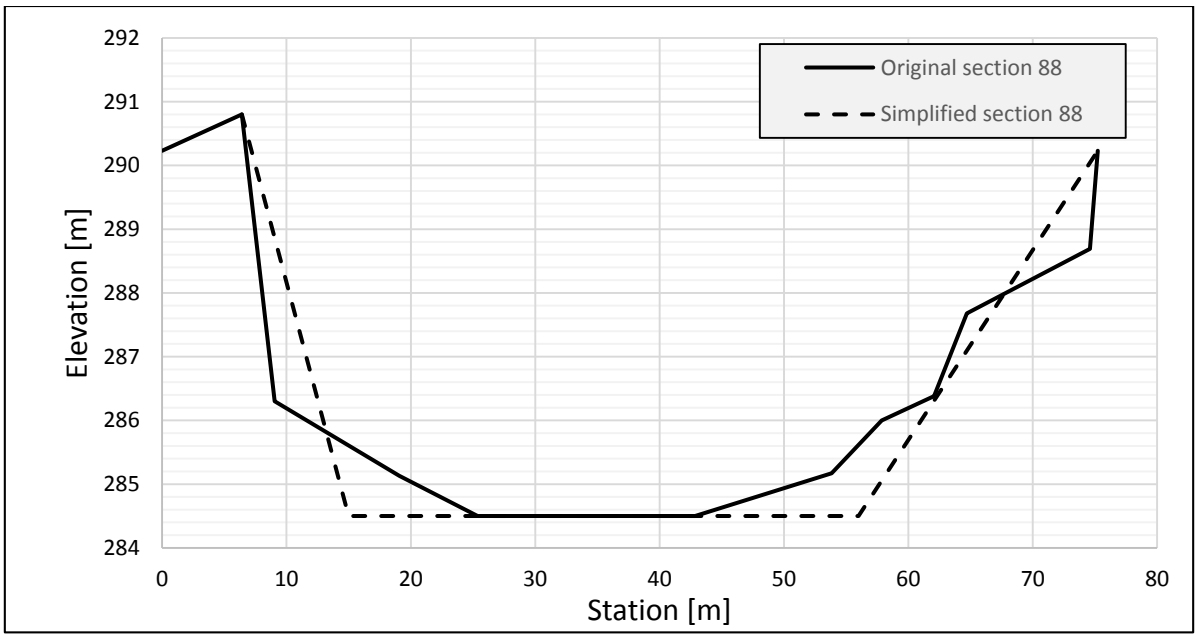

Figure III-11 Cross section 88 and its simplified version.

As a first step, a re-organization of the data on the geometry of the river was carried out, paying attention to section shape and bank elevations. A total of 9.5 km starting from the confluence with Adda river were collected from the originally surveyed by (Ismes & Cae, 1988b) together with 2 km of artificially created cross sections that are attached to the downstream end in order to avoid the effect of downstream boundary conditions on the model. Further, this set of data had to be input in a format suitable for analysis in Basement. A geometry file was therefore created in the following format.

```
}
CROSS_SECTION {
        name              = CS40
        distance_coord    = 4.991
        main_channel_range  = (0.00,54.60)
        friction_coefficients = (30)
        friction_ranges     = ((0.00,54.60))
        node_coords         = (( 0.00,429.78 ), ( 23.60,386.82 ), ( 32.90,385.12 ), ( 54.6,423.39 ))
        bottom_range        = (23.6,32.9)
        SOIL_DEF {
                index = 1
                range = (0.00,54.60)
        }
```

The software requires several parameters in addition to the nodal coordinates of a cross section and the longitudinal distance. These are: main channel range, friction coefficient in terms of Manning or Strickler value, a definition of a bottom portion, and a definition of a soil index, with previously assigned sediment mixture, along with its range in the cross section as it may also be variable. In this way a definition of different soil mixtures and friction coefficients can be assigned along the channel.

The “bottom” of a cross section is the portion where erosion and deposition are supposed to take place. As already mentioned, the “bottom” definition is of a crucial importance for the model, especially when considering large quantities of sediment input as in this particular case. The main issue arises from the way in which sediment deposition/erosion is distributed in the cross section. From (Figure III-12), it is clear that when no points are present between the bank and bottom defining points, a distributed change in bed elevation occurs. On the other hand, provided a cross section point is lying between the end point of a bottom portion and the bank point, aggradation/degradation occurs until the moveable part of the bed (*bottom*) is connected immediately with the intermediate point as illustrated on (Figure III-13) and in this way the new bottom is defined. This effect may be no so evident when the bed load is of small quantities. In this work, however, the effect of extreme aggradation is to be studied and a massive sediment input is used. Then, the complex geometry of some cross sections along the Mallero river makes the choice of bottom section extremely important for the proper distribution of morphological changes.

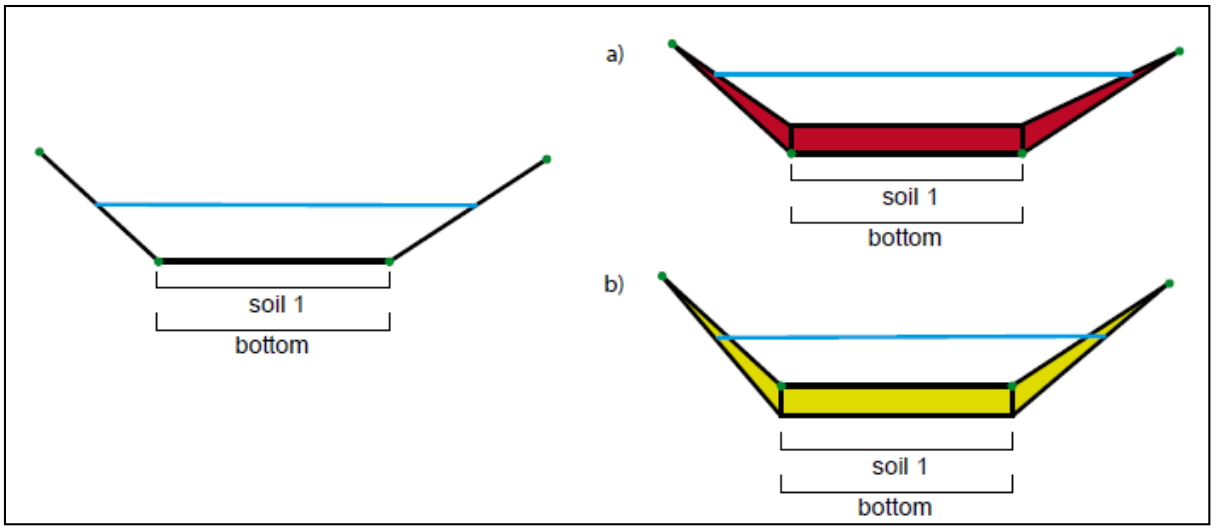

Figure III-12 a) Deposition and b) erosion due to bed load without cross section points on embankments.

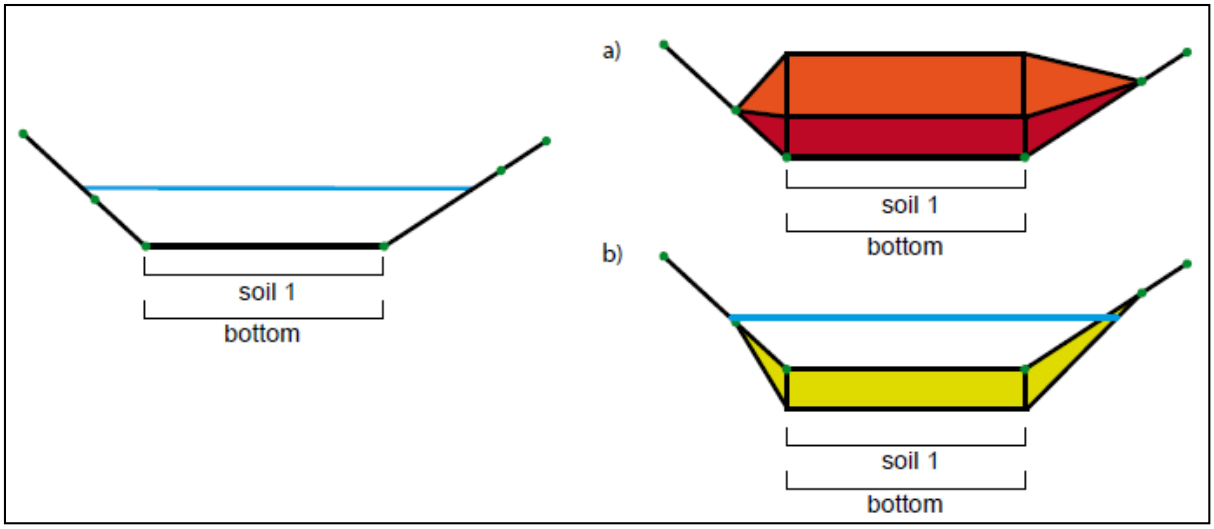

Figure III-13 a) Deposition and b) erosion due to bed load with cross section points on embankments.

After having attempted to run a model with the originally surveyed geometry (Figure III-14 top), the software crashed with a message indicating that aggradation at a certain section has reached the bank elevation and further computation could not continue. The problem occurred mainly in the downstream portion of the channel, where the town of Sondrio is situated (2 km upstream of the confluence with Adda as illustrated). As expected, the deposition of sediment is significant exactly there due to the decreased steepness of the slope. In addition, the bank elevations are considerably lower in comparison with the remaining part of the river upstream from Sondrio. This is obviously the reason why previous models have used elevated banks. In search for a more realistic approach, the developers of the numerical software have been contacted with a request for an advice on the possible source of the problem and its elimination. Their answer emphasized on the enormous amount of sediment discharge input and the careful choice of a bottom when creating the geometry.

The amount of sediment discharge however, is representative of the event of 1987. Since the goal is to model exactly this very high sediment discharge and its effect on the downstream end of the river the proper assignment of bottom ranges remained as a crucial modelling choice. An effect of bottom range choice is illustrated on Figure III-14. Circled in red is an aggradation pattern as a consequence of the presence of a cross section point on the embankment. Numerous attempts to modify bottoms showed some minor improvements in the overall behavior of the model. However, changing the bottom range in one section affected the aggradation in others and resulted in another software crash. Therefore, the problem did not really converge to a solution – software crash was merely translated from a cross-section to another one. It was thus decided that the combination of an intricate mountain geometry, the large amount of sediment discharge input and the manner in which aggradation is distributed over a cross section (Figure III-12, Figure III-13) together result in an extremely complex problem. On that account, some kind of simplification would be inevitable. Making use of the remarks made by the software developers and the understanding of how aggradation is modelled by the numerical code, it was decided that the geometry could be modified in a such a way that it could accommodate the increase in bed elevation in a smoother, distributed manner (Figure III-12) while trying to keep the original shape as much as possible. Therefore, any points situated between the bottom range and the points that define an embankment would be modified or removed, keeping the geometry barely changed and allowing for the smooth aggradation/degradation as shown on Figure III-14 below. After a few adjustments, a complete model was obtained on the basis of which a calibration of the 1987 event will be further carried out.

Naturally, after a crash message appeared during the computation, the results relevant to the time instant of the crash were inspected in order to try to understand the behavior of the software and possibly to overcome the difficulties causing its malfunction. It was observed that in some cases when a crash occurs with indication of an exceeded bank elevation by the deposited sediment, the results output show otherwise – there is in fact no significant change in bed level.

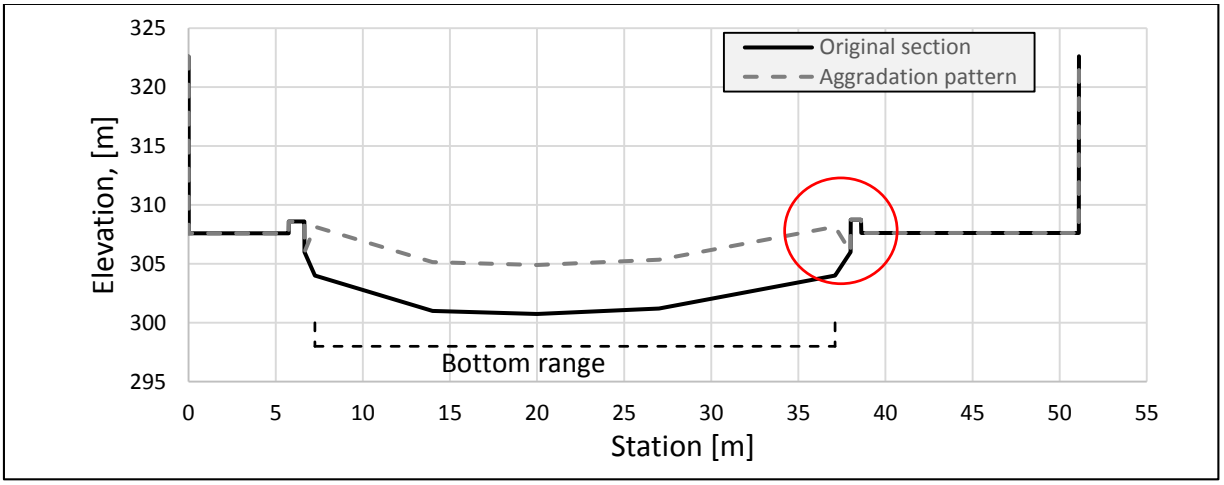

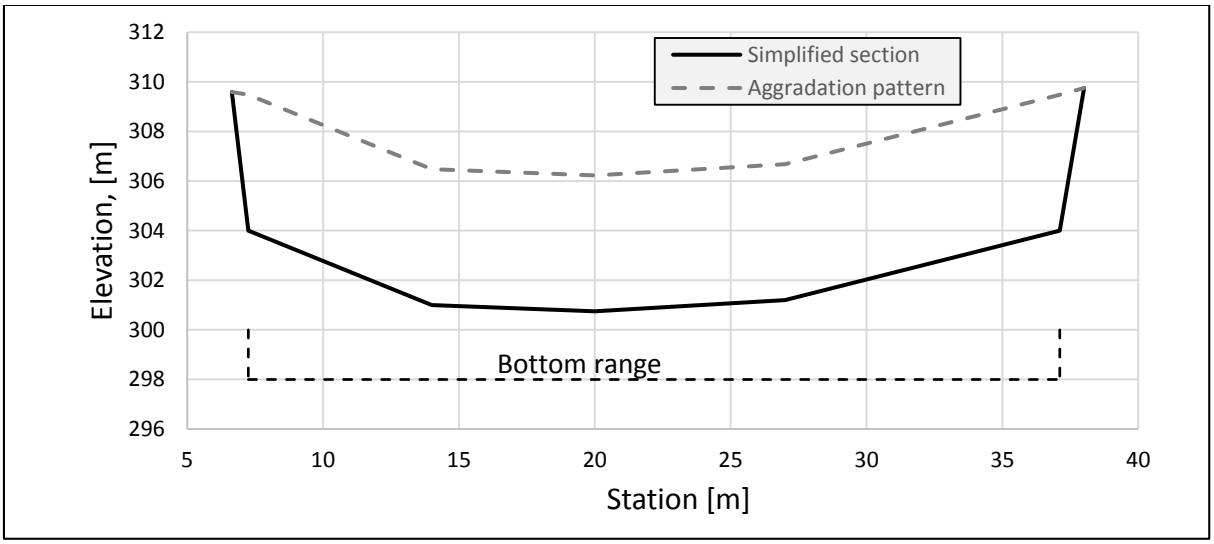

Figure III-14 Cross section CS73and its aggradation pattern. Top – original; bottom – simplified.

It was then noted that this peculiarity is common for sections in which two or more of the points that define them are considerably close one to another, separated by a small distance such as 1 cm. This issue was solved by simply modifying the coordinates of such points or by completely removing them.

3.2. Modelling issues

Apart from the geometry definition, several choices affecting the model need to be mentioned.

3.2.1. Boundary and initial conditions

An initial condition is necessary for the hydraulic model. It has been obtained by running the software with a fixed bed and an inflow of water for a duration that will ensure the steady condition of a constant flow in the total length of the channel. The obtained condition is then used as an input for the morphological model.

As an upstream boundary condition, a flow hydrograph is required. As a downstream boundary condition, a normal depth with a slope value is necessary for the model.

In terms of the bed load computation, as an upstream boundary, a sediment discharge was selected in order to simulate sediment feed upstream of the last section. The downstream boundary selected (IODown) guarantees that all sediment entering the last computational cell will leave the cell over the downstream boundary, namely simulating a further discharge. Since this boundary condition requires that the elevation of the bed in the downstream section remain unchanged, which is obviously not realistic, an artificial (dummy) reach is attached after the last section for 2 km as also used in previous models in order to minimize the adverse effect of the boundary condition on the validity of the model upstream.

3.2.2. Artificial banks

During the modelling process, the influence of a number of different parameters on the model was explored. Results with different sediment mixtures, boundary conditions, physical parameters, numerical schemes, bed load formulas etc. were executed in order to choose the most appropriate ones. This led to the creation of sometimes unstable models and over aggradation. Therefore, the banks of some sections were artificially elevated (as in the work of e.g. Elsayed, 2013) so that the software does not crash and the process remains undisturbed. Naturally, results were compared to the real bank elevations and when reaching a satisfactory result, it was again computed the original geometry so that it is ensured the model works properly in both cases.

3.2.3. Length of the model

As already mentioned, 9.5 km of the river geometry was recreated for analysis. However, after the successful model run, it was noticed that near the abrupt change in the slope, there is an enormous amount of aggradation (Figure III-15). This may be expected due to the sudden change, where the energy of the flow is possibly dissipated into a hydraulic jump and therefore sediments are likely to settle. However, it does not seem quite natural and in addition this creates a problem for the software with bed aggradation levels overpassing the real banks. On the other hand, considering the integrated modelling that is to follow, computation of erosion material that would be used as input is done on a sub basin level. This makes it easier to choose which point would be the point of interaction between the two models. It was therefore decided that in order to avoid the overcomplicating condition imposed by this geometrical feature, a shorter length of the river of 4.8 km upstream of the confluence with Adda river can be used and the sediment yield calculated accordingly. The point of interaction would then be immediately after the abrupt change of slope, circled in red on the figure below.

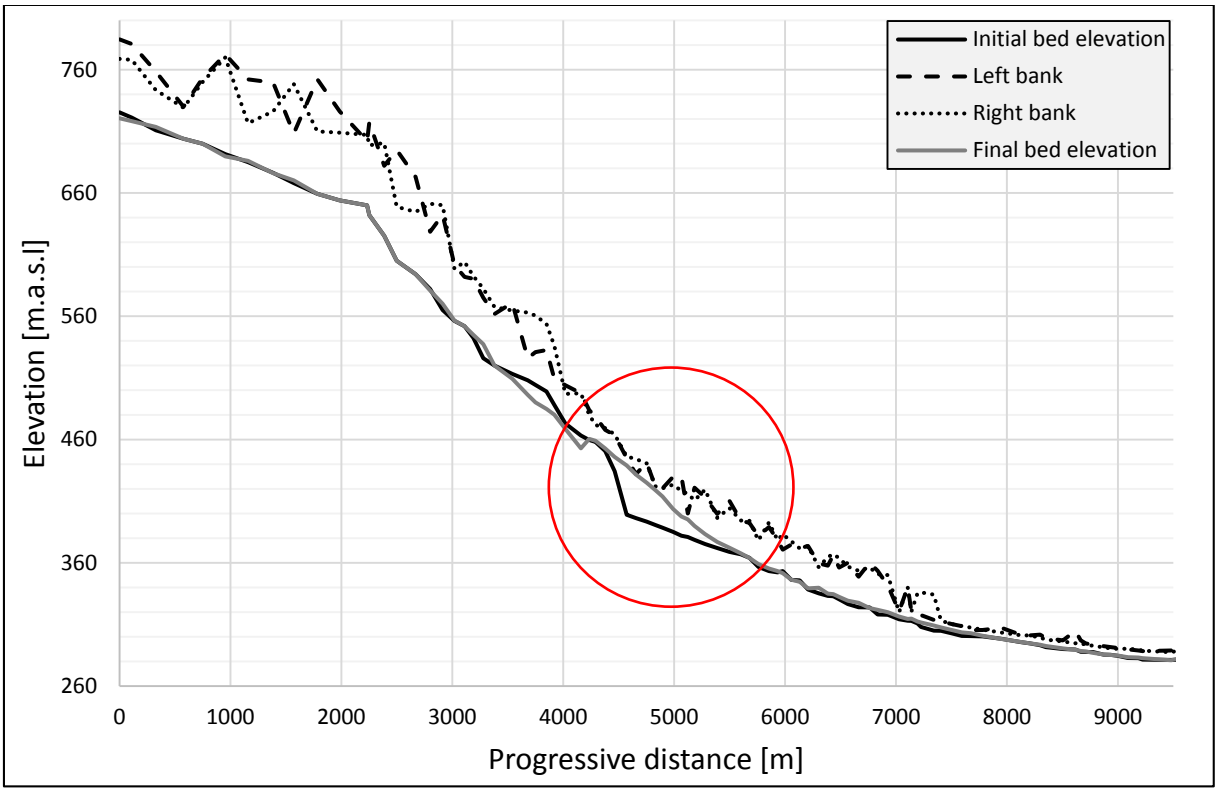

Figure III-15 Mallero 9.5 km, abrupt change circled.

3.2.4. Sediment size

As a first approximation, a single sediment size of d_s = 5 cm was used for the computation, both for sediment discharge and soil layer, until a stable model was reached. Afterwards, different sediment mixtures were defined, consulting the sediment size distribution in Mallero.

3.2.5. Porosity calibration

A discussion has been led in relation to the correct input units of porosity, required by Basement. Two possibilities have been outlined – whether to input it as a fraction (e.g. 0.35) or as a percentage (e.g. 35 %). The ambiguity arises from the fact that computation is carried out regardless of which one is used and no warning or error message appears to indicate that, for example, the input value is not acceptable. In this respect, a test was set up to define the correct input value. A rectangular channel of length L = 1000 m, constant width, B = 20 m and slope S_0 = 2 ‰ was used, for which a constant sediment input equal to three times the transport capacity of a section ensured a corresponding bed aggradation. The volume of deposited sediment between the first two sections was noted. With respect to time, two time steps were considered since, the transport capacity would change when the cross section changes its geometry. The model was executed twice – with values of p_0 = 0.4 and p_0 = 40 respectively. On the other hand, similar computation was carried out manually,

using an Excel spreadsheet and the same geometrical and physical parameters. By means of a discretized form of the Exner equation between two sections, a corresponding volume of sediments was computed. Here however, the units of porosity are well known due to dimensional consistency. A comparison between the resulting deposited volume and the previously computed ones with Basement, confirmed that the correct porosity units are indeed in percentage. Calculations provided in Appendix B.

3.2.6. Basement output

One shortcoming of the software is the form of the general output of the results. While it may be convenient to plot a few profiles, when dealing with, e.g. calibration of a model, a number of parameters are to be plotted versus time or space and the process becomes rather cumbersome if an additional software is not used (e.g. Tecplot). For this reason, a Matlab code was created in order to sort the output in a more user friendly manner. When executed, the code imports directly the output file of Basement and arranges all the parameters (e.g. bed elevation, bank elevation, water surface elevation etc.) in matrices where the first column is filled with all the corresponding time steps and the first row with all spatial steps respectively. In this format, an Excel file is created where each matrix is recorded in a different spreadsheet with its corresponding name. Of course, the data can also be exploited in Matlab, but this is left to the preference of the operator. The only needed input for the code is the number of cross sections that are analyzed. Code provided in Appendix C.

3.3. Calibration to the 1987 event

Following the above considerations, a recreation of the 1987 event will be carried out in order to serve as a basis for an integrated modelling. The purpose of the calibration is to represent a real event, using a numerical software, thus confirming the validity of the numerical results. Therefore, any following model would behave in a way verified by the calibration. For the purpose a set of data has been provided:

- A water discharge hydrograph recreated with the rainfall-runoff Nash model after the event.
- A sediment discharge created as a proportional to the square of the water flow, created on the basis of post event evaluation of the mobilized sediments load.
- A post event measurement of bed elevation for the in-town part of the channel.
- A set of 94 cross sections (36 of which are created as a dummy reach) accounting for 4.8 km of the river from the confluence with Adda.
- Characteristic grain size distribution along the channel surveyed by ITALTEKNA et al. (1990).

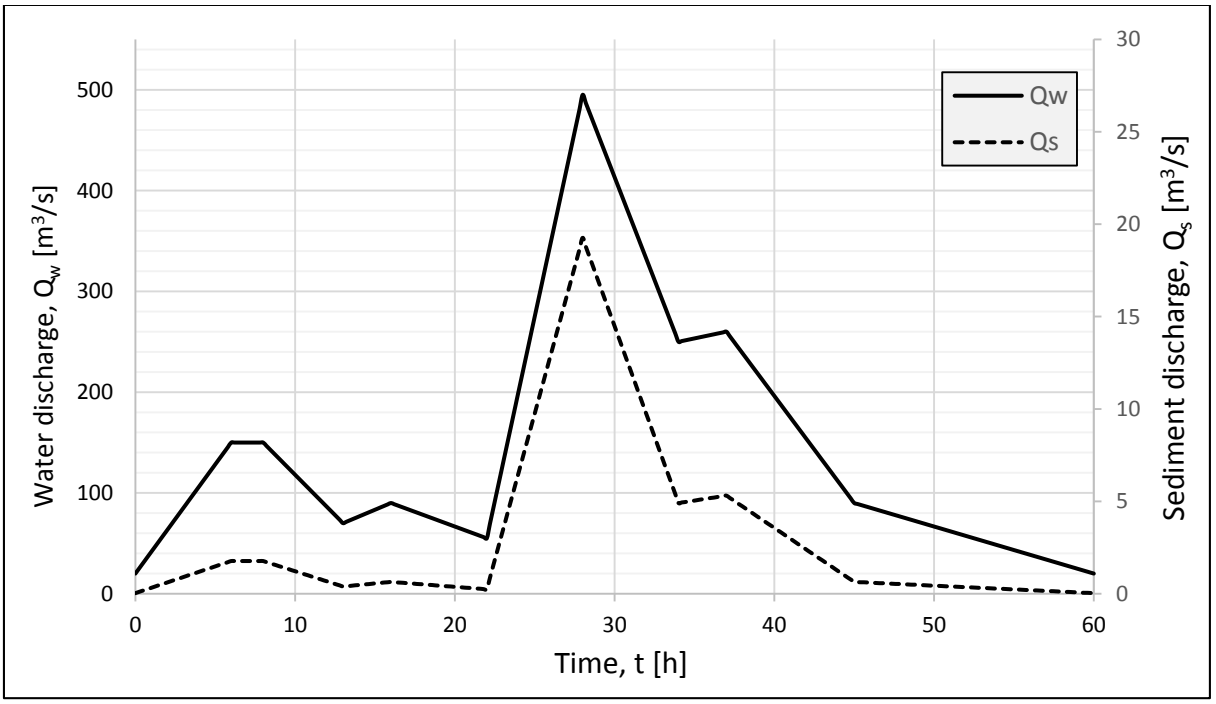

Figure III-16 Water and sediment discharge in time according to post '87 event evaluation.

A starting point for the analysis of this real case is the geometry adjustment previously explained as well as scientific work carried out on the same case (e.g. Filippetti & Zoppi, (2012); Radice & Rosatti, (2012); Elsayed (2013)). As already mentioned, it has been decided that a shorter part of the channel will be analyzed – the last five kilometers before the confluence with Adda. This portion includes around 2 km of in-town channel, for which the post event measurements have been carried out. The slopes are of the order 3-4 % in the upstream part while towards the valley, they decrease to 2.5 %. The urban channel has a mean slope of 1.2 % with minimum values of 0.1-0.2 % towards the downstream end. In this part the cross sections are of a quite regular shape, while upstream of Sondrio, the shape becomes rather irregular, typical for mountainous rivers. The sections used here are the modified ones obtained in the previous section of this work.

3.3.1. Initial and boundary conditions

As an upstream boundary condition, the reconstructed hydrograph is used. It has a duration of 60 hours and a peak of 500 m^3/s. In terms of sediment transport, a sediment discharge accounting for 697,000 m^3 of sediments has been assigned as a boundary condition in accordance with post event evaluations (≈700,000 m^3). Since the flow in the upstream part of the channel is mostly supercritical (Fr > 1), a second boundary condition is needed – the slope at the boundary which is easily determined to be 3.1%. Downstream, normal depth is set as a boundary condition for the water flow and a boundary, which does not allow the change of bed (all sediments leave the over the boundary)

for the sediment transport respectively. Initial condition is guaranteed by a constant flow of 20 m^3/s in the whole length of the channel, in correspondence with the first value of the flow hydrograph.

Some parameters that affect the bed load computation, as discussed in the theoretical background, are chosen as follows: porosity $p_0 = 35\%$; material density $\rho_s = 2650\,kg/m^3$; angle of repose $\phi_s = 30^o$; critical Shields parameter $\tau_{cr}^* = 0.045$.

3.3.2. Grain size distribution and soil assignment

After the single grain size model has been used to adapt the cross section geometry, this simplification can be removed and a more realistic representation of the granulometric distribution can be created. A starting point is previous work, where different cases have been analyzed. Referred to as Case 1, four characteristic grain size classes have been chosen for the analysis. As a Case 2, measured data has been exploited and another, generally coarser distribution has been chosen from the field measured data, presented below.

Table III-1 Sediment size distribution

d_{50} measured [cm]	Distance from Adda [km]	d_{50} rearranged [cm]	d_{50} mean [cm]	d_{50} measured [cm]	Distance from Adda [km]	d_{50} rearranged [cm]	d_{50} mean [cm]
16.70	23.60	164.00		11.50	8.70	11.90	
16.60	23.00	118.00		8.40	8.10	11.80	
34.80	22.60	104.00		12.70	8.00	11.50	
51.20	21.80	96.80		11.90	7.70	9.77	
35.70	21.00	77.30		57.80	7.30	8.50	
32.00	20.40	72.20	82.62	27.40	7.10	8.49	9.17
6.27	19.30	66.90		64.60	6.40	8.40	
7.92	19.20	64.60		72.20	5.70	7.98	
11.80	17.50	57.80		77.30	4.80	7.92	
36.00	17.00	51.20		118.00	3.00	7.30	
164.00	16.60	36.00		9.77	2.80	7.27	
104.00	16.10	35.70		4.13	2.40	7.23	
96.80	14.10	34.80		5.40	2.10	6.91	
8.50	13.90	32.00		7.27	1.90	6.54	
7.30	13.30	31.30		2.11	1.60	6.27	
7.98	12.90	27.40		6.54	1.10	5.84	
31.30	12.60	21.20	23.51	4.12	1.00	5.56	5.35
66.90	12.00	16.70		6.91	0.80	5.40	
21.20	10.80	16.60		5.56	0.70	4.78	
16.20	10.00	16.20		5.84	0.50	4.13	
14.00	9.50	14.00		7.23	0.10	4.12	
8.49	9.20	12.70		4.78	0.00	2.11	

The data has been arranged from smallest to largest and divided in 4 classes. For each, the average value has been computed and used as input for the software. The scope of these measurements is far beyond the analyzed part of the channel. However, the sediment input will likely be the result of material entrained exactly from upstream.

Further, mixtures have been created by allocating a percentage to each size, where the terms of every mixture should add up to 100%. Two different mixtures have been created representing the dominance of coarse sediments upstream and finer sediments downstream as a result of the sorting effect, characteristic for natural channels. This is also evident from the measured values showing the lower values in the downstream part. The input sediment yield is also assigned a mixture. The different mixtures have been altered numerous times under various assumptions about the granulometry and bed fixity. Results have been progressively inspected and compared with post-event measurements in order to obtain the best fit possible. Values for the final characteristic sizes and mixtures that presented the best results is reported in the table below.

Table III-2 Sediment sizes and corresponding mixtures used in the model.

Case 1

d_s	(1	5	8	50)cm
Coarse	(0	50	40	10)%
Finer	(50	50	0	0)%
Feeding	(10	40	30	20)%

Case 2

d_s	(5	9	20	80)cm
Coarse	(0	50	40	10)%
Finer	(50	50	0	0)%
Feeding	(10	40	30	20)%

The proposed mixtures are used in the creation of soil layers which are in turn assigned to each cross section as its property and therefore define the channel bed characteristics. A fixed layer was also created with the intention of its assignment in the in-town channel section, where the bed is paved and thus non-erodible. This however, did not appear to have any effect on the final profile of the river bed – it can be then concluded that deposition is the dominant process taking place downstream, while erosion is not observed. The choice of sediment size and mixtures is an important calibration parameter. The use of increasing number of sediment sizes affects the computation since the sorting effect is stronger. In addition, finer sediments for which incipient motion occurs for lower values of Shields parameter, are more easily transported. Therefore, alteration in the characteristic sizes may leads to profiles of different elevations in different parts of the channel.

3.3.3. Friction coefficients

As a first approximation, a value of Strickler friction coefficient, $k_{Strickler} = \frac{1}{n_{Manning}} = 30\,m^{1/3}/s$ has been assigned to all the cross sections. Since this is a parameter controlling both water surface elevation and sediment transport, its effect on the model plays an important role for the calibration. The upstream part is mainly a natural channel, characterized by irregular geometry, vegetation cover, bed forms, all of which increase the resistance to the flow and therefore the equivalent friction. The downstream is a regular channel, with a relatively smooth surface and sparse bushes can be observed occasionally. However, Chanson (2004) pointed out that bed-load transport should be related to the skin friction shear stress only, as described in section 1.5. On the other hand, the Manning-Strickler relation to sediment size, states that $n_{Manning} = 0.0132 d_s^{1/6}$. For this reason, a transition of the friction coefficient has been implemented corresponding to the two cases of sediment size distribution, previously defined. Namely, for Case 1, $k_S = 25\,m^{1/3}/s$ upstream and varies progressively to $k_S = 40\,m^{1/3}/s$ downstream, while for Case 2, the range is $k_S = 25 \div 52\,m^{1/3}/s$ respectively. These variations present generally better results than the constant value assumed at the beginning and since they are corresponding to the grain size distribution, the ranges are considered acceptable for the simulation.

Case	
1	$k_S = 25 \div 40\,m^{1/3}/s$
2	$k_S = 25 \div 52\,m^{1/3}/s$

3.4. Results and discussion

Figure III-17 represents the starting point of the calibration: a model with a single grain size, $d_s = 5cm$ over the whole length of the stream and a constant friction coefficient $k_S = 30\,m^{1/3}/s$. It is evident that this case does not represent the measured data in a good way. Although in the downstream end of the town the fit is quite reasonable, the bed aggradation is largely overestimated upstream with bed elevation overpassing the banks along around 500m of the channel length. The use of artificially elevated banks was needed in order to obtain results without a software crash. Then, for visualization, the real bank elevations have been plotted. The simulation overestimated the bed elevation by 3 m on average with respect to the post event measurements. This also results in a water surface elevation to be outside the boundaries of the channel as shown by the maximum water surface elevation. This may not represent reality since an outflow was not observed but it may have occurred if intervention measures had not been undertaken during the event. Therefore, an

improvement of this result has been sought. In this respect, calibrations of governing parameters have been carried out, namely friction coefficient and sediment mixtures. The results of the two reference cases are presented in the following figures.

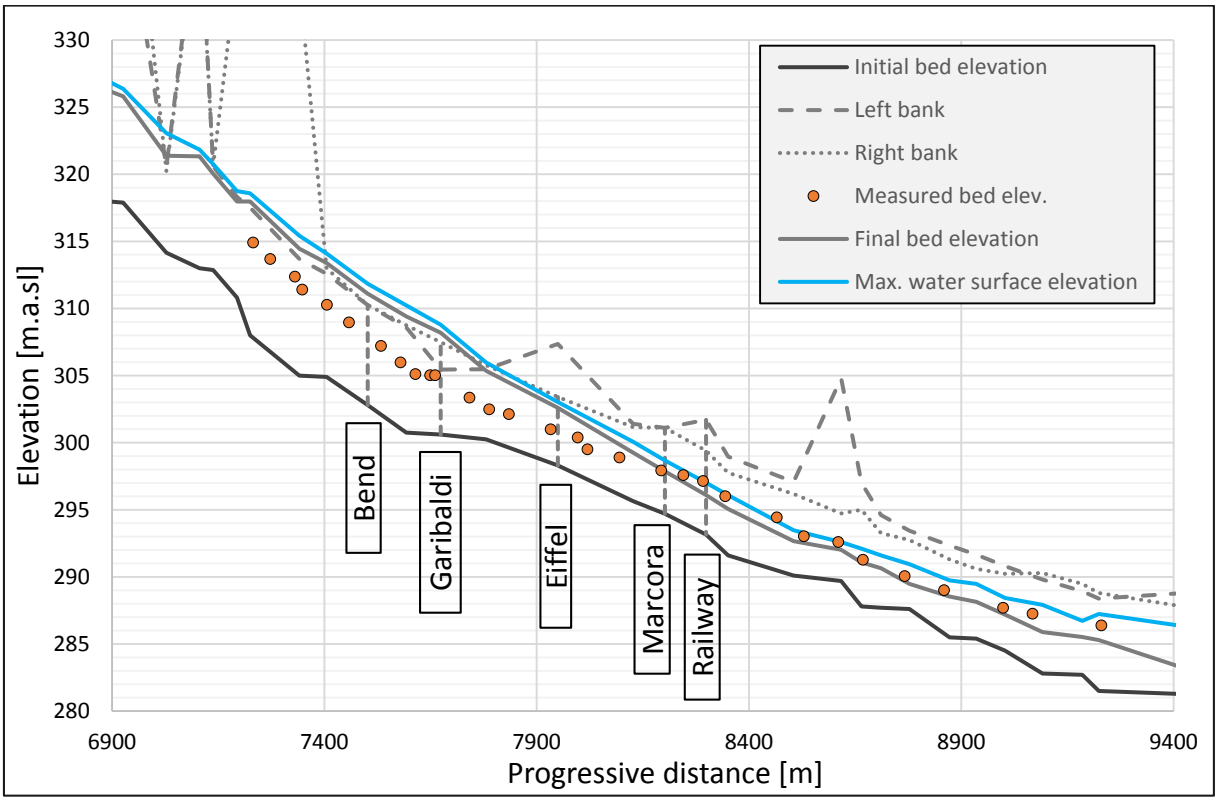

Figure III-17 Single sediment size, single friction coefficient.

3.4.1. Case 1

On Figure III-18, the complete length of the profile has been presented. A high deposition near the upstream boundary is evident, as a result of the sediment discharge. High deposition is further observed downstream, as expected, at around 7600 m from the upstream end where the slope changes from an average of 3.5% to 1.2%. Bed elevation around this change is crucial, with aggradation measured during the event reaching the level of the bank, while further downstream there is some freeboard still available. This is however, more clearly visible on the second plot Figure III-19 which is focused on the in-town area. Several characteristic sections have been plotted, namely, the acute bend and the four bridges that cross the river. As it was the case during the ’87 event, sediment deposition near the Garibaldi bridge is the highest. In the simulation, however, the bed elevation is still overestimated and the results show that sediment is around 1 m over the left bank. On the other hand, in comparison with the simpler model, the same section has a bed level at the final time instant of almost 3 m above the left bank. In terms of water elevation, an outflow is still observed in this case. Despite the overestimation, the data here is better represented in the

upstream end of the town, where the crucial sections are, namely near the bend and the change of slope, both of which are conditions that favor sediment settlement.

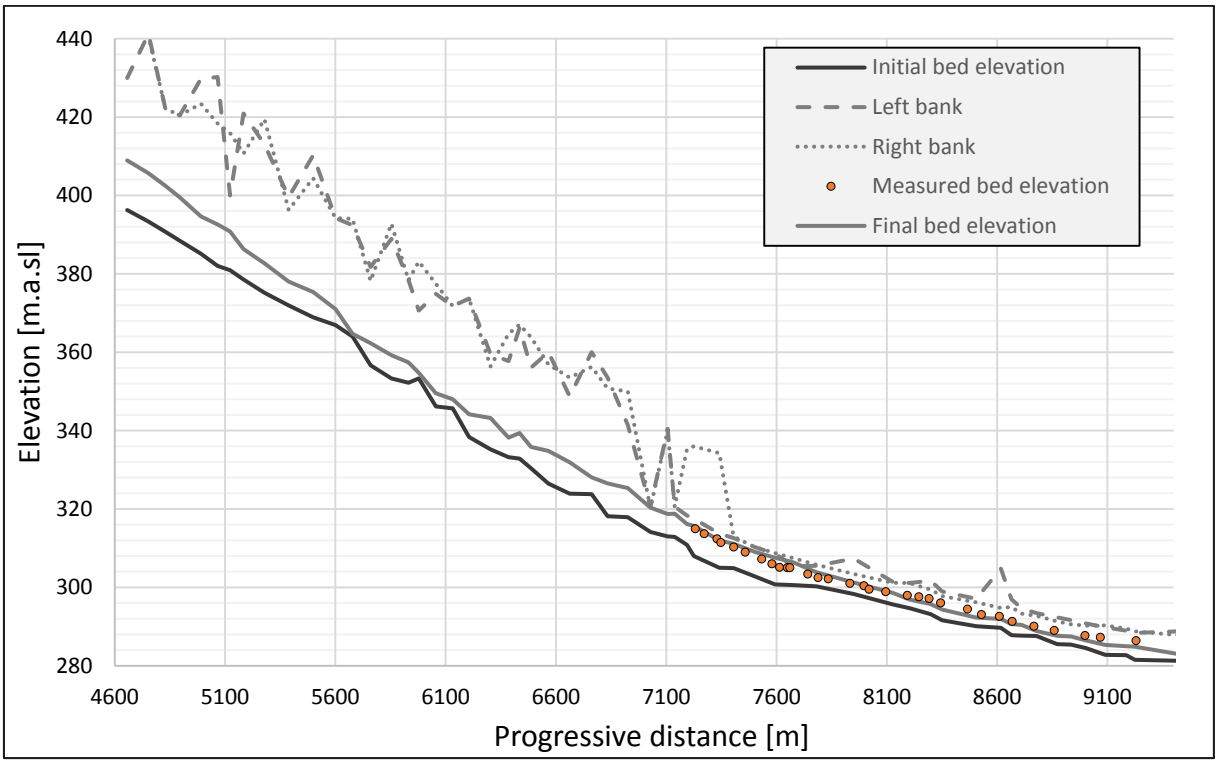

Figure III-18 Case 1

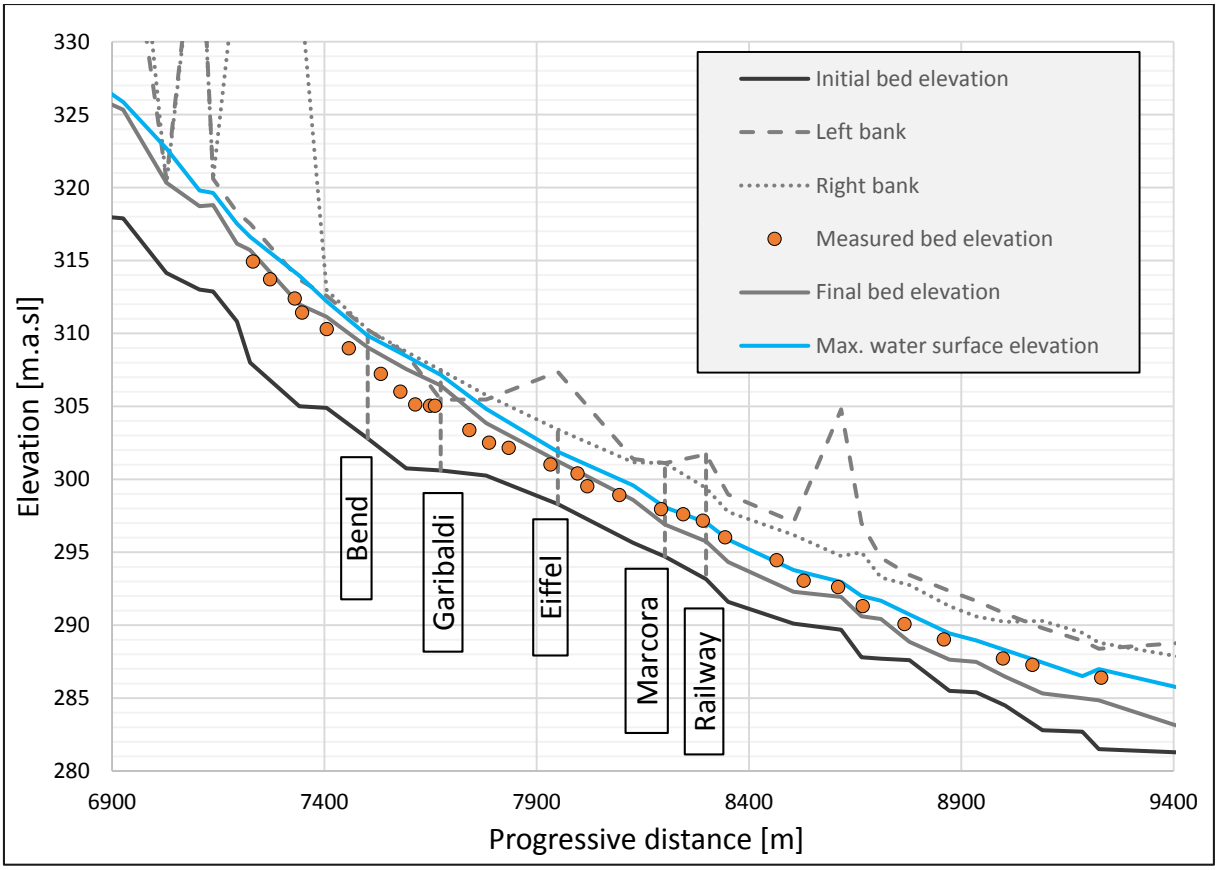

Figure III-19 Case 1 in-town

3.4.2. Case 2

Here, as mentioned above, a consultation with measured sediment distribution along the Mallero led to the inception of a different model – one including larger sediment sizes. The full size plot (Figure III-20) shows similar results as in the first case. Deposition near the boundary appears to be larger as a result of the reduced mobility of the larger sediment load. Here, also the effect of the upstream boundary condition has been tested. The dash-dotted line represents a model in which the upstream sediment yield has been removed. It is clearly evident that the in-town part of the stream is not affected by the sediment discharge. Therefore, the deposition there occurs as a result of erosion upstream. Indeed, this effect has been confirmed (e.g. Radice et al., 2013) and it can be pointed out that the time duration of the present case is not sufficient for the sediment discharge to affect the downstream end of the river. In fact, Radice and Rosatti (2012) presented a numerical quantification of the minimum duration of the event for which the upstream sediment yield could significantly influence the profile of aggradation in Sondrio, such duration being more than 80 hours.

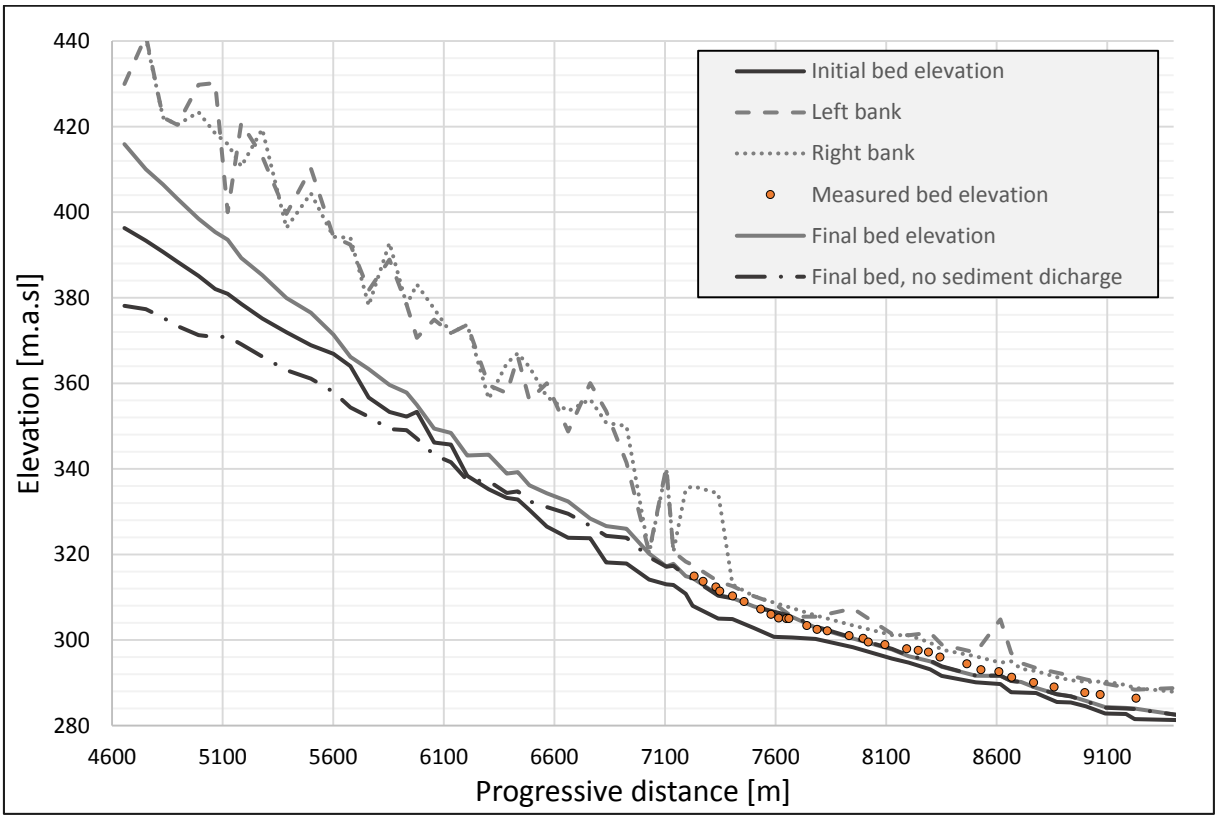

Figure III-20 Case 2 complete

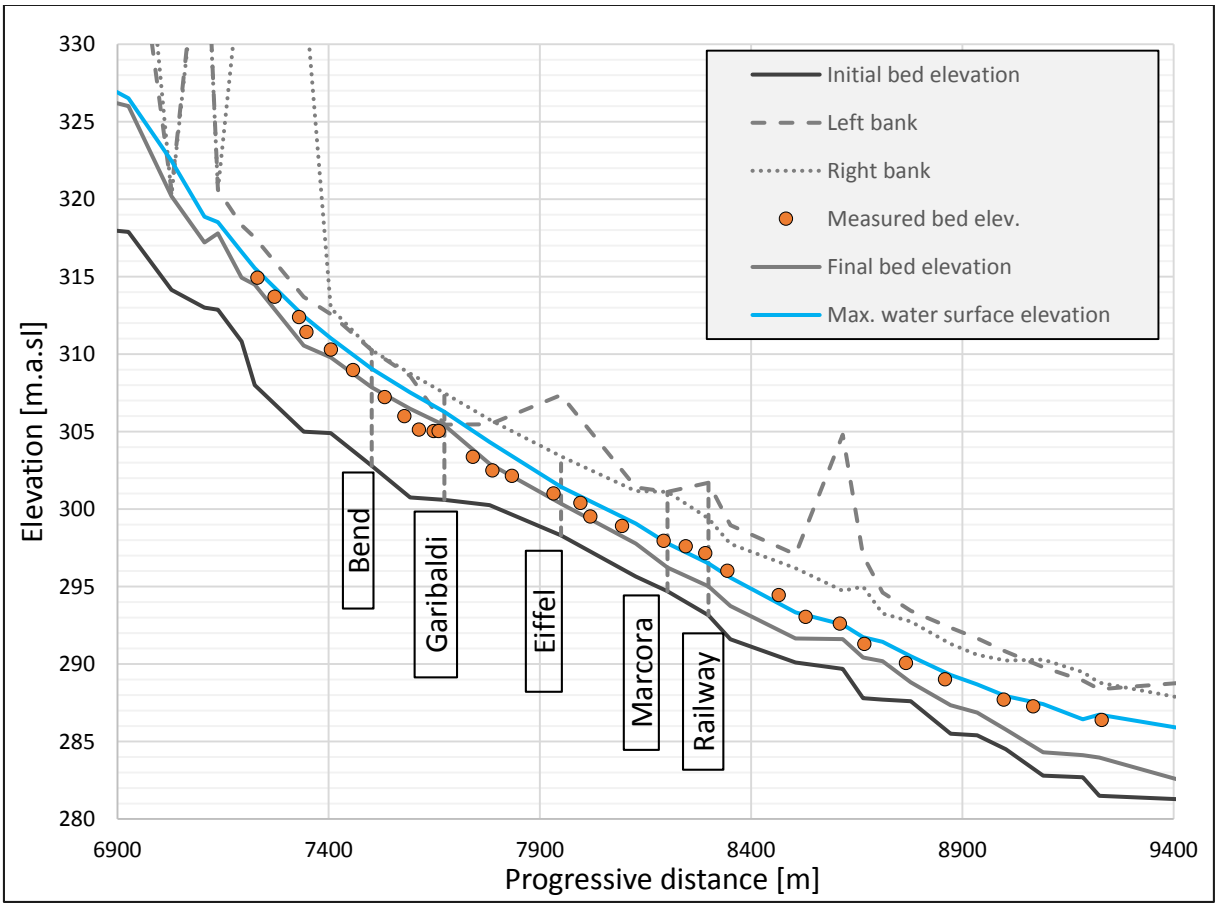

Figure III-21 Case 2 in-town.

Figure III-21 is again focused on the downstream end of the channel. In this case, it is evident that the profile is considerably lower, and aggradation is within the banks of the channel. This makes possible the use of the real cross section geometry, which is a step further in the modelling of Mallero river. Measured bed elevation is represented in a good way by the simulation mainly in the upstream end. Although, in the downstream, the change of bed level is underestimated, it can be observed that the trend of the line follows the aggradation pattern of the surveyed data. In addition, the critical section is at the Garibaldi bridge where the channel is completely full with only 4 cm of freeboard. Maximum water surface elevation shows a similar trend, however, with considerably lower values as opposed to the first two models. The time evolution of the bed and water surface elevation shows a limited variability of the maximum water elevation. This is due to the combination of the rise of the bed and the progression of the wave, which can be interpreted from the Figure III-22 below. It depicts the bed and water elevation at the Garibaldi bridge which is a key location both for the analysis and the ’87 event. At the peak of the wave, the aggradation in this section is less than half of that at the end of the event. However, water surface is slightly over the minimum bank elevation (thus, the outflow visible in the profile plot). This level remains constant for a short period due to the increase in bed level and a corresponding decrease of the water flow. At a certain instant, bed increase takes

dominance over the effect of the decreasing water discharge and water level is slightly increased. Until the end of the event, it slowly decreases while the progressive aggradation results in almost constant water level.

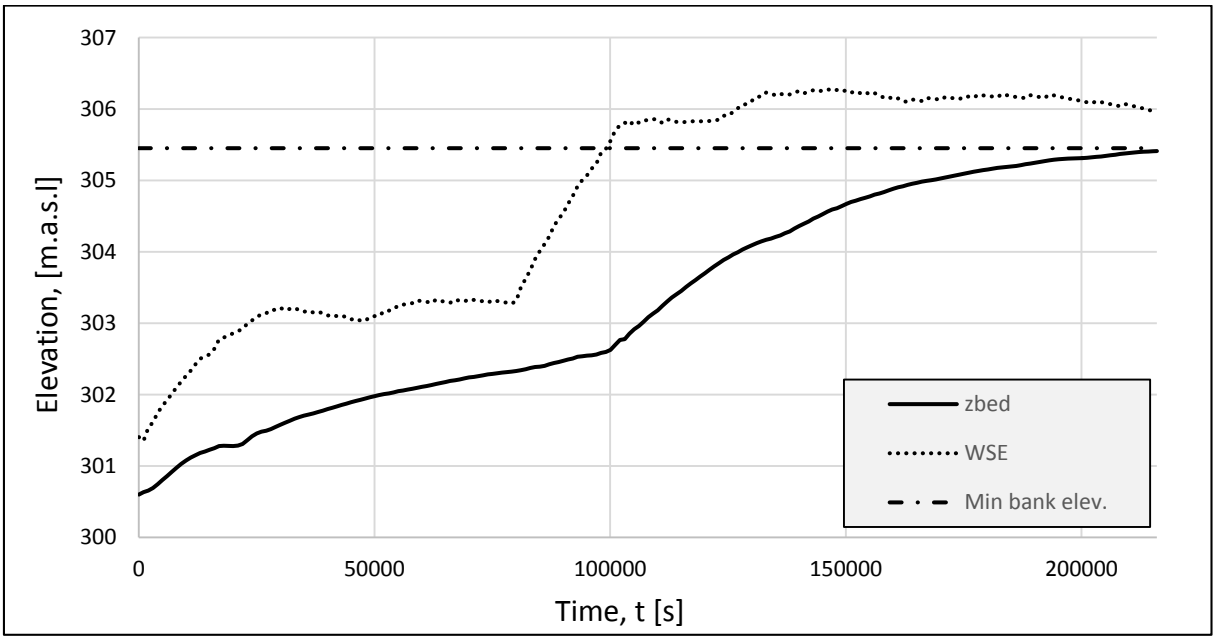

Figure III-22 Temporal evolution of the elevation of river bed a water surface at the Garibaldi bridge.

The effect of sediment size and friction coefficient increase on the model is clearly evident. An efficient way to further calibrate the model can be achieved using a plot of the percentage of each sediment class in the soil layer along the channel. An example is presented here for Case 2.

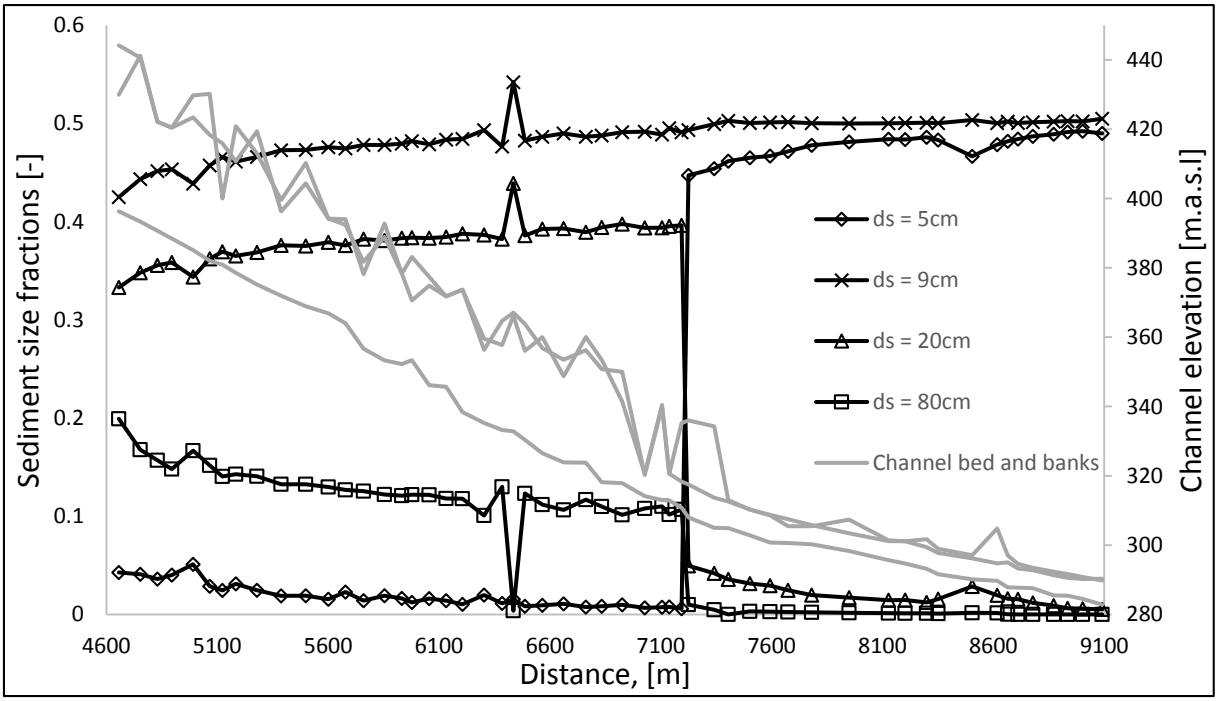

Figure III-23 Variation of sediment classes along the channel.

Figure III-23 represents the sediment classes at the end of the computation and therefore the final distribution of sediments in the channel. It can be evaluated that the finer sediment sizes occupy, on average, 98% of the sediment load in the cross sections downstream of CS69 (7225 m), which is essentially the in-town reach. Thus, controlling the availability of finer sediment at the expense of the coarse one, the aggradation in Sondrio could be manipulated. Of course, such manipulation should consider realistic sediment sizes according to the case.

In conclusion, the obtained results show an expected behavior of lower sediment deposition downstream with increasing sediment size and corresponding skin friction. Considering that Case 2 has been created using a surveyed sediment distribution data, it can be reasonable to assume that the results represent reality to a sensible extent. The calibration to post event bed level measurements has shown a slight underestimation at the downstream end of Sondrio. However, the most critical sections (i.e. near Garibaldi bridge) have been reasonably represented. In addition, maximum water surface shows limited variability as expect. A minor outflow can be observed, however, as it has been the case also in 1987, the limit between flood and no flood is extremely subtle. In this respect the obtained results are considered satisfactory. In addition, it has been made evident that quantification of the hydraulic hazard during a flood event for the town of Sondrio would be impossible without considering the morphologic evolution of the river bed that greatly affects the water surface elevation.

Considering the results obtained by the calibration process, a simulation of a flood scenario is to be created in the following chapter. As a datum for scenario development, reference Case 2 will be used since the model outcome is closest to both bed elevation measured after the event and water surface elevation. In summary, the main features that represent are starting point for the following work are:

Table III-3Summary of model features

Model length	Last 4.8 km before the confluence with Adda
Geometry	Simplified as described in section 3.1.
Granulometry	d_s (5 9 20 80)cm *Coarse* (0 50 40 10)% *Finer* (50 50 0 0)% *Feeding* (10 40 30 20)%
Friction coefficient	$k_s = 25 m^{1/3}/s$ Upstream $\rightarrow$ $52 m^{1/3}/s$ Downstream

Chapter IV. Integrated modelling

This chapter will describe the integration process that will complete the model developed in this thesis. As already discussed, the need to model sediment yield and river bed aggradation as interacting processes is fundamental for the proper estimation of an event induced river bed aggradation and a possible flood. However, the two models differ in their spatial and temporal scales and therefore their interaction is also a matter of modelling choices. The outcome of this work will be the production of a scenario leading to a flood in the town of Sondrio along with an estimate of flood discharge. The results will be discussed focusing on the feasibility of a joint modelling in the light of limitations imposed by the different nature of the models.

1. Interaction between the processes. (Conceptual framework)

Probably the main issue that arises during the development of this integrated model is the scale inconsistency between the corresponding natural phenomena and their respective models. Although a variety of spatial and temporal scales exists in sediment supply and transport, their modelling requires a particular definition in terms of computational resolution. For a morphological evolution estimation, the necessary spatial resolution is much finer than basin scale as it is typically an on-site (defined in II.1.3.) process. On the other hand, sediment yield and, in particular, widespread phenomena such as soil erosion is modelled in a much more spatially distributed context. With respect to temporal distribution, integral volumes for the basin are typically estimated due to extensive data requirements that are virtually impossible to obtain for basins covering hundreds of square kilometers. On the other hand, morphological changes are an unsteady process and their modelling requires a time varying sediment discharge as a boundary condition. This scale difference originates from the inherent complexity of natural phenomena and its relevant modelling approaches. For this reason, Radice et al. (2012) proposed a conceptual separation within the basin referred to as “break-point”. The introduction of such a point will impose for the spatial and temporal aspects respectively the following:

- Sediment yield will be modelled on the basin scale, for the portion of the basin upstream of the break-point. Downstream of this point, cross-section resolution will be used for the morphological evolution evaluation.
- The bulk sediment volume obtained will be artificially distributed in a time varying discharge in order to correspond to the temporal resolution of the morphological model and serve as a boundary condition.

An illustration of the “break-point” chosen for this integrated model is presented in the figure below.

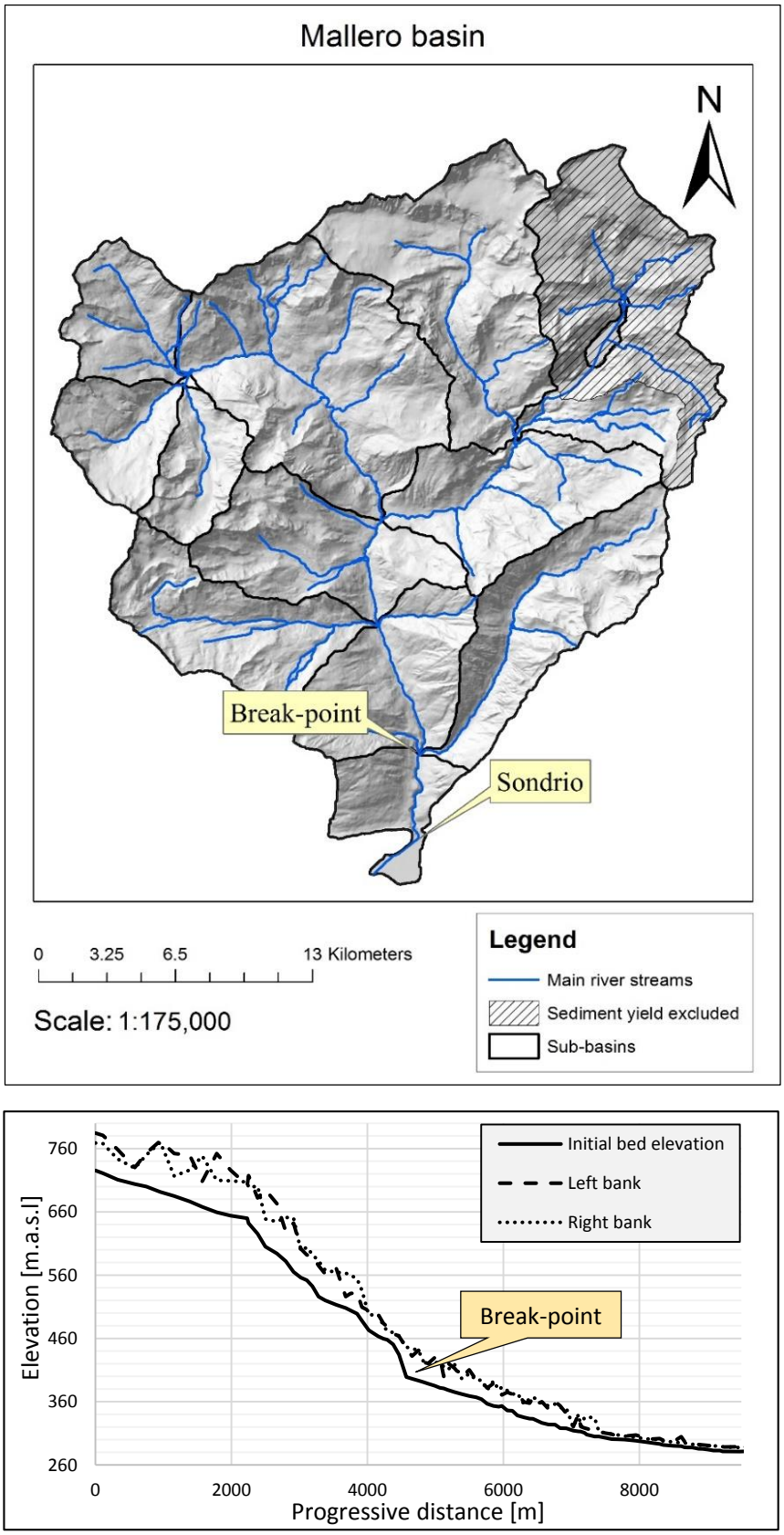

Figure IV-1 Top – map of Mallero basin, indicating “break-point” location. Bottom – longitudinal profile of Mallero river with “break-point” location.

2. Scenario definition

Following the objective stated at the beginning of this paper, a flood scenario would be the final outcome of the work carried out. Therefore, the relevant scenario and its creation will be described here.

The choice of a scenario is based on its intensity, which is in turn, related to the corresponding return period. As a reference, the 1987 Valtellina flood had a return period of 60 years. Both the historical records and the calibrated model presented in Chapter III agree that flood did not occur with the circumstances present at that time. Therefore, an intriguing question would be: *what would be the discharge if there had been an outflow?* For this reason, this particular case will make use of a time varying water discharge related to a return period of 100 years.

In terms of sediment yield, an attempt will be made to use the Gavrilovic model, previously described in Chapter II, to calculate a volume of eroded material from the slopes in Valmalenco. The sediment discharge is, in fact a necessary boundary condition for the morphologic model. Although the Gavrilovic model is not designed for a short term event, it has been chosen among other models as a more appropriate for the Alpine region, on the basis of the site where it has been conceived and tested as well as its application to different case studies present in literature (e.g. Brambilla et al. (2011)) which vouch for its validity. Thus, the model has been adapted to take into account seasonal properties of the basin as well as the rainfall depth related to a single event.

The obtained sediment volume as well as the geometry of Mallero will be used to create a model describing the morphological evolution of the river with particular interest in the portion of its course that passes through the town of Sondrio.

Finally, the resulting outflow will be modelled by means of a quasi-steady approximation in order to obtain a time varying discharge.

The development of the following steps will be based on the framework previously described.

2.1. Hydrologic modelling

The need for hydrological analysis arises from the necessity for rainfall depth data that will be later used as input for the sediment yield model. Typically, when a rainfall-runoff model is created, the water discharge is estimated for the same return period as the respective DDF curves. In this case, the discharge data is available and what is missing is the rainfall depth. In this sense, the rainfall depth calculation will make use of parameters, relevant for a return period of 100 years and duration of 1-5 days, both parameters in correspondence with the flow hydrograph. The corresponding data

has been retrieved from ARPA Lombardia. The rainfall depth has been therefore estimated by means of the expression of the DDF curve relevant for a return period of 100 years:

$$h_T(D) = a_1 w_T D^n \qquad \text{Eq. (IV.1)}$$

Where

- $h_T\,[mm]$ is the rainfall depth
- $D[h]$ is the event duration
- $a_1\,[mm/h^n]$ is the scale invariance coefficient
- $w_T\,[-]$ is the rainfall quantile, depending on the return period, T
- $n[-]$ is the exponent through which the variability of the phenomenon is transferred from the reference temporal scale to other temporal scales

These parameters have been estimated by ARPA for reference pluviometric stations and extrapolated for the territory of Lombardia region. Maps illustrating the variability of the parameters are presented below. For the region of interest to this model, the following values have been adopted:

$$a_1 = 18\,mm/h^n$$
$$w_T = 2.1$$
$$n = 0.44$$

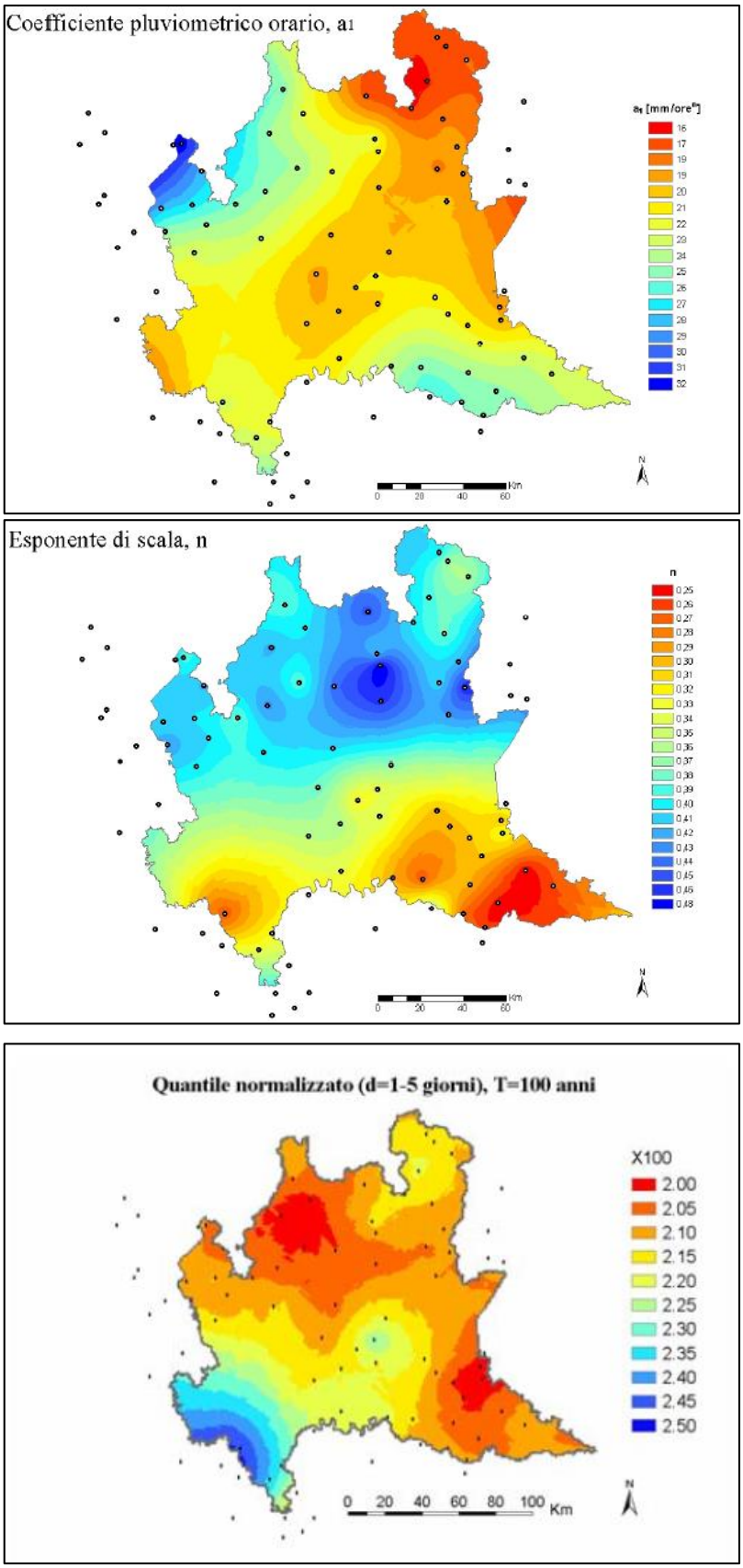

Figure IV-2 Spatial variation of Top – a_1; Middle – n; Bottom - w_T. (source: LSPP Lombardia)

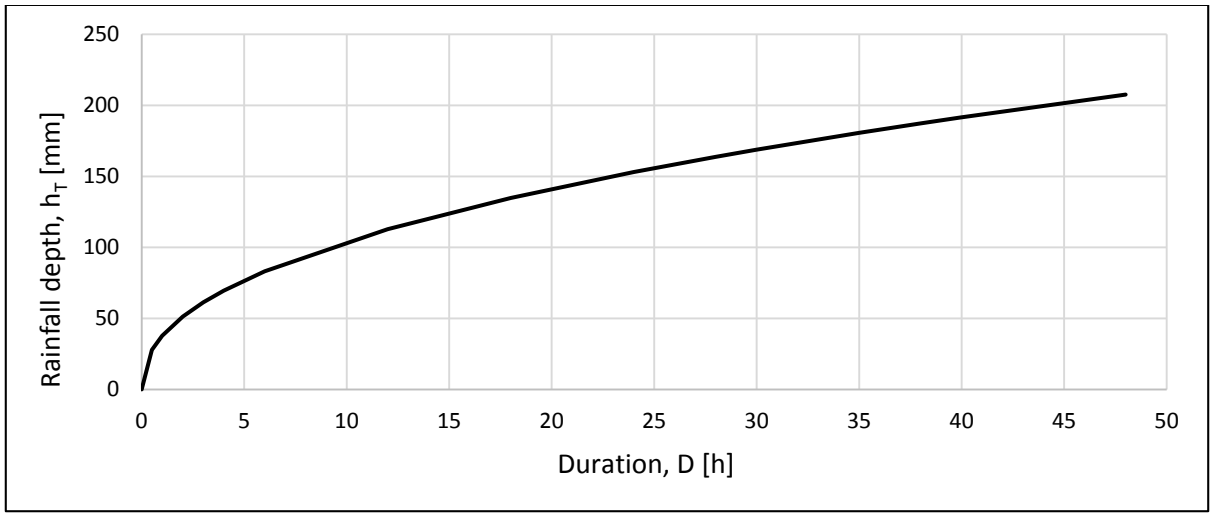

Figure IV-3 Depth-Duration-Frequency curve for a return period of 100 years.

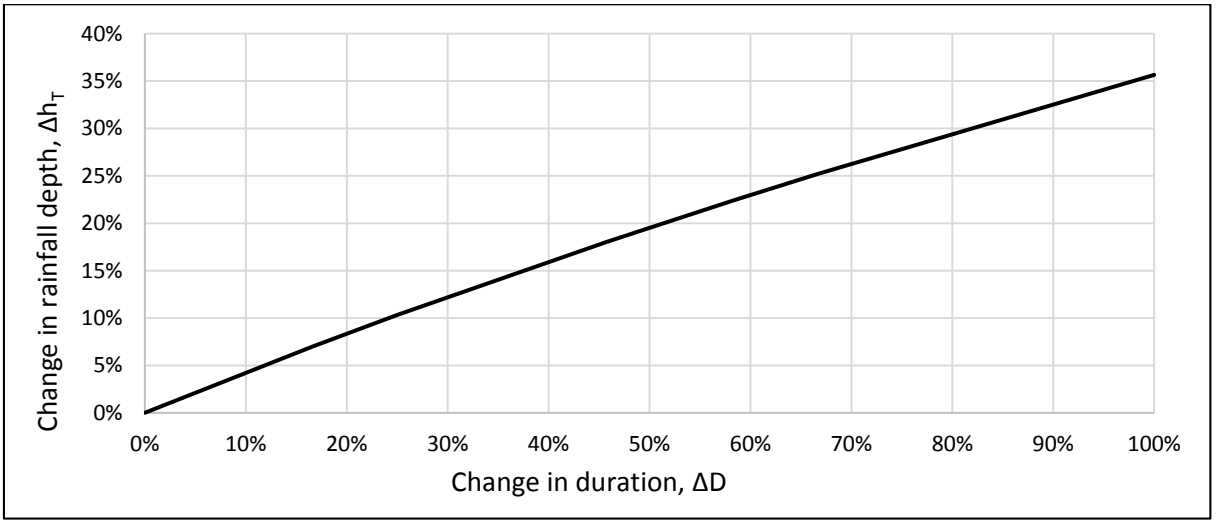

Figure IV-4 Sensitivity of the DDF curve to change in duration. Base value, D_0 = 30 h.

The duration of the rainfall event has been chosen to be equal to 30 hours. This value is obviously in the range $1d < D < 5d$ and therefore corresponds to the estimated parameters. A check on the sensitivity of the duration shows that doubling the rainfall duration will affect the result by around 35% (Figure IV-4). On the basis of this model, rainfall depth for the event has been calculated to be:

$$h_T \approx 170\,mm$$

It is assumed that the rainfall depth is space uniform over the area of the basin.

2.2. Sediment supply

Assuming that a widespread phenomenon would contribute to the sediment yield production significantly, erosion has been modelled by means of the Gavrilovic formula. Although the process has been described in detail in Chapter II the adjustment of some of its parameters was necessary in order to adapt it to the particular scenario here.

Instead of yearly mean rainfall, a value of rainfall depth relevant for the time duration of the event was used. In addition, in order to take into account the seasonal influence, the mean temperature values have been calculated for each season, as it is characteristic of the climate in the area that apart from the two rainy periods of May and November, high intensity thunderstorms are typical for the hot summer season (Guzzetti et al. 1992). Furthermore, the coefficient of land cover has been modified in order to represent the state of vegetation since canopy during the summer allows for increased interception and protects the soil from being eroded while during the winter vegetation is sparse. For the spring and autumn seasons, it has been decided to keep the coefficient equivalent to the one representing average annual conditions. In this respect, the sensitivity of the model to these parameters has been analyzed. A plot of variation of sediment yield with respect to variation of the coefficient of land cover, Ξ, the mean temperature, t ^{o}C, and the rainfall depth, H [mm] is presented on the figure below.

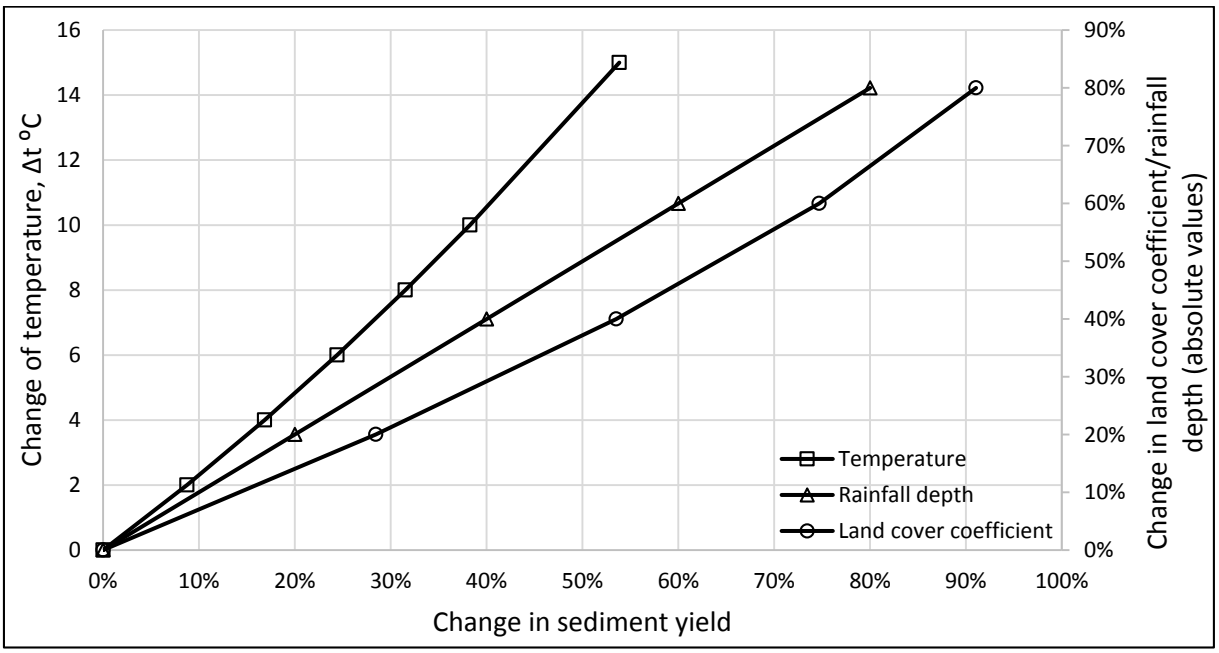

Figure IV-5 Sensitivity of Gavrilovic method to the parameters relevant to the integrated modelling. Base values for land cover coefficient equivalent to the ones used in Chapter II (Appendix A). Base values for temperature representative of summer (Appendix A).

Table IV-1 shows the sediment volumes calculated according to seasonal variation in temperature and land cover coefficient with respect to the average annual values, previously used. As the value

corresponding to summer is the highest, it has been chosen for the scenario definition. In particular, for the summer model it has been chosen to decrease the coefficient of land cover by 20% for all sub-basins as an attempt to incorporate the protective effect of abundant vegetation. The temperature has been computed as a mean value of the average daily values for the summer months – June, July and August. This showed an increase of 10.5 ^{o}C on average with respect to the yearly values, previously used in Chapter II. In terms of rainfall, the value obtained from the hydrological analysis has been adopted. Further, as it is visible from the graph, the change in sediment volume varies linearly with rainfall depth. Although in the present case, the rainfall depth remains constant, much higher values have been used for the analysis carried out in Chapter II and the influence of this change on the model is acknowledged here. Therefore, by scaling down the Gavrilovic formula for an intense event, volume will generally decrease due to the decreased rainfall depth and the decrease in land cover coefficient. On the other hand, this effect will be partially counter balanced by the increase in temperature values, relevant for the summer season. With this set up, the model yields a total volume

Table IV-1 Seasonal sediment yield volumes

	Annual (Chapter II)	Spring	Summer	Autumn	Winter
Δt [^{o}C]	-	-0.09	+10.5	+3.82	-4
ΔΞ [-]	-	-	-20%	-	+20%
h [mm]	-	170	170	170	170
G [m^3]	≈661,400	≈150,000	≈200,000	≈175,000	≈110,300

It is interesting to note that the sum of the four “event-induced” erosion volumes is quite close to the mean annual estimated in Chapter II which may be an additional support to the assumption that high intensity events could provoke the transport of large portions of the sediment yield in a short duration.

2.3. Morphologic evolution of the river bed

The morphological evolution of Mallero related to the particular scenario has been modelled using the same procedure as described in Chapter III. For the purpose, the geometry, friction coefficients and sediment grain size distribution of the previously calibrated model have been adopted here. A water discharge representative of 100 years return period has been used as provided by (ITALKENA et al. 1990). A time-varying sediment discharge is necessary for the morphological model. However, the outcome of sediment yield computation is a bulk volume. For this reason, this volume has been

artificially distributed in time as proportional to the square of the water discharge. The results is a curve following a shape similar to the water discharge variation in time and reaching a peak of 2.9 m^3/s (Figure IV-6).

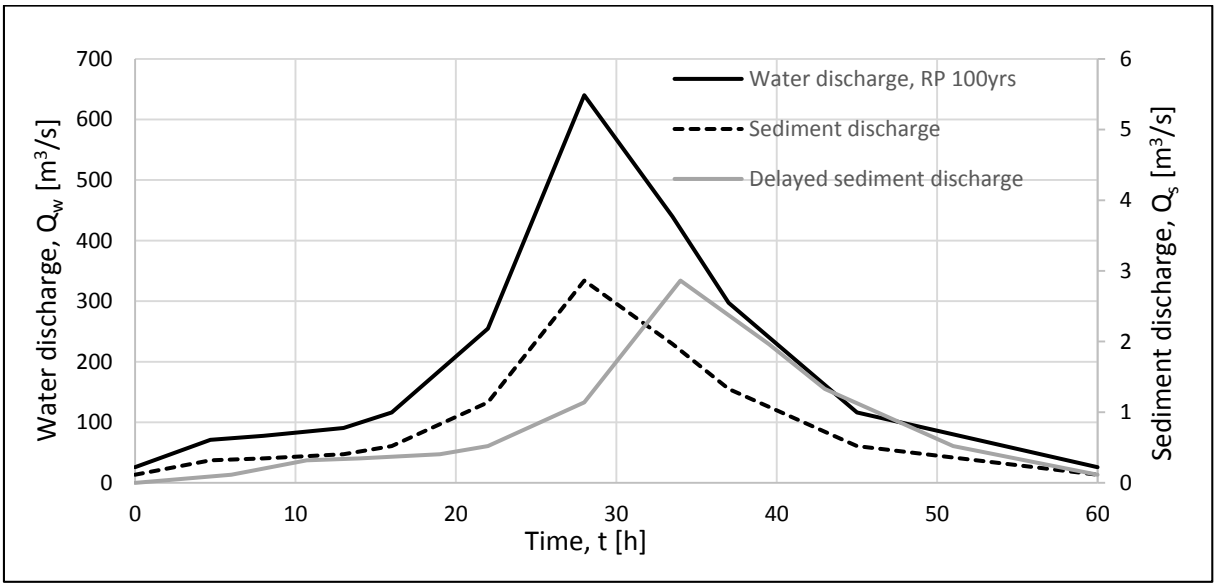

Figure IV-6 Water and sediment discharge

2.3.1. Sensitivity to sediment supply

The model has been tested to its sensitivity to the amount of sediment supply. For the purpose, the computations have been carried out once with the total amount of sediment supply (200,000 m^3) and one with sediment supply increased by 50%. In terms of river bed elevation, the results were similar to what has already been discussed in Chapter III, section 3.4.2. Namely, the downstream end of the river, relevant to the town of Sondrio has not been affected by the increased sediment volume. On the contrary, propagating upstream, the effect becomes more and more sensible approaching the boundary (Figure IV-7).

2.3.2. Time delay of sediment supply

In the presented model, the water and sediment discharges evolve in a similar way and their peaks coincide. However, it may be expected that the sediment discharge would have its peak in a delayed time instant, arriving with the tail of the flood wave. For this reason, a check has been carried out in order to investigate the effect of possible delay of the sediment yield distribution in time. For the purpose, the rising limb of the sediment discharge has been aligned with the peak of water discharge as illustrated on (Figure IV-6). This investigation however, showed no sensitivity of the model to the time delay. The bed aggradation pattern is almost equivalent to the one previously computed (Figure IV-7) which is consistent with the findings of Radice et al. (2012) for a similar sensitivity analysis. Therefore, such a delay will not be further considered for this model.

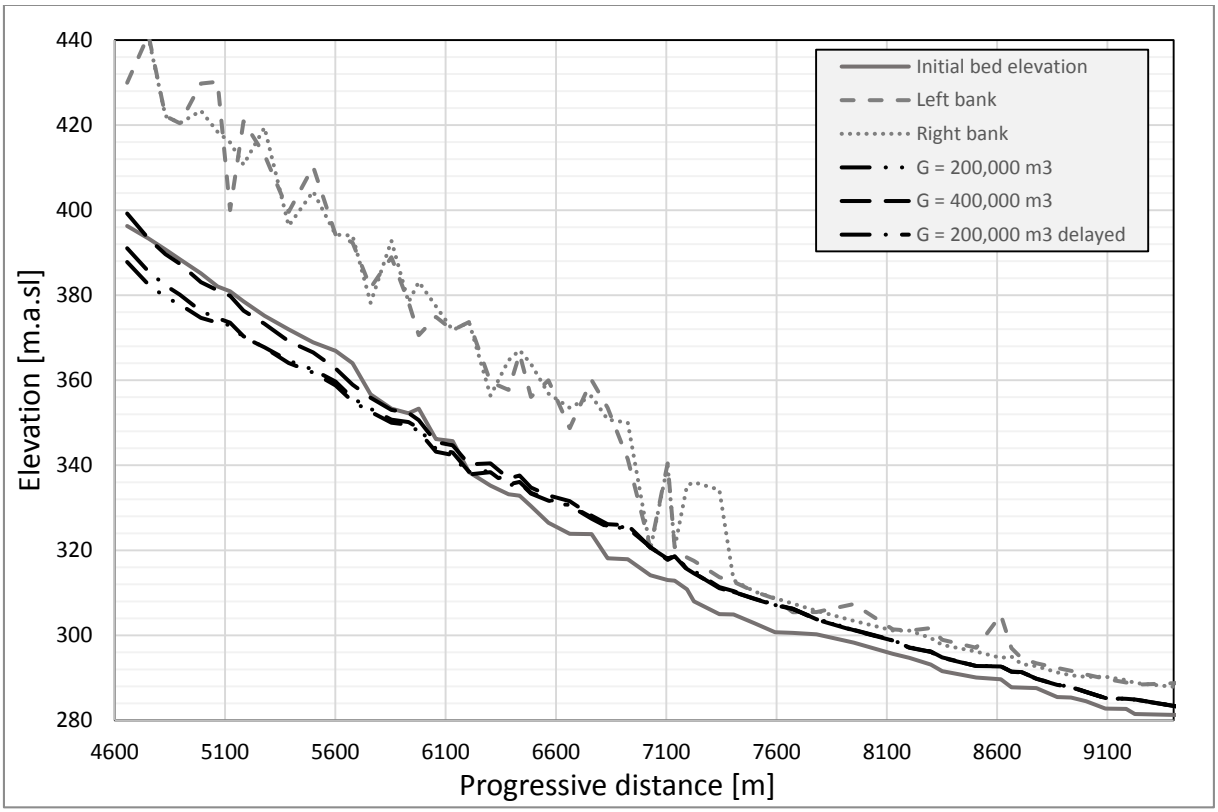

Figure IV-7 Sensitivity of the model to delay of sediment discharge and amount of sediment supply.

2.4. Outflow

Since Basement is not capable of estimating a flow discharge over a river bank, computation of the relevant outflow in the town of Sondrio has been performed by means of the HEC-RAS software developed by the Hydrologic Engineering Center of the US Army Corps of Engineers (http://www.hec.usace.army.mil). The morphological evolution of the river, however, was not incorporated in the HEC-RAS model and computations have been carried out with a static bed. Yet, both the water discharge and morphological evolution are time-varying processes and the relevant outflow would be a result of their combined progression. Therefore, a lack of compatibility has been introduced between the two models. However, in terms of water discharge, an unsteady wave can be modelled as a sequence of several steady ones. This approximation has been made use of in order to cope with the former issue. Thus, the following approach has been adopted:

- First attempts to run the model led to the use of artificially elevated banks at specific sections due to crashes of the software. The obtained bed and water surface elevations are however compared to the real bank elevations.
- The hydro-morphological model computed with Basement has been inspected in order to locate cross-section(s) for which outflow occurs. As it happens, outflow is located over the left bank at the cross-section relevant to Garibaldi bridge.

- An inspection of the time evolution of the event at the relevant cross-section indicates how both bed and water surface elevation change. It has been noted that river bed level at this section increases above the real bank elevation after a specific time instant. As it is believed that it is more likely that the sediment will start to escape the channel and not to pile up, the bed elevation used for the outflow model will be considered to reach at most the elevation of the lower bank.
- A comparison of the bed elevation evolution with the time variation of water discharge further indicates the time instant of peak of outflow. Considering that the curves of water discharge and bed aggradation increase/decrease with similar rate after the peak of the discharge, it can be expected that the peak of outflow would be at the point of intersection between them as indicated on Figure IV-8 below.
- In order to compute the outflow from this section, several additional time instants have been chosen in-between the time instants of initial outflow, peak outflow and the end of the event. In this way, the shape of the outflow hydrograph would be more accurately represented. The relevant river bed and water surface elevations as well as the time instants are presented on Figure IV-8 below.

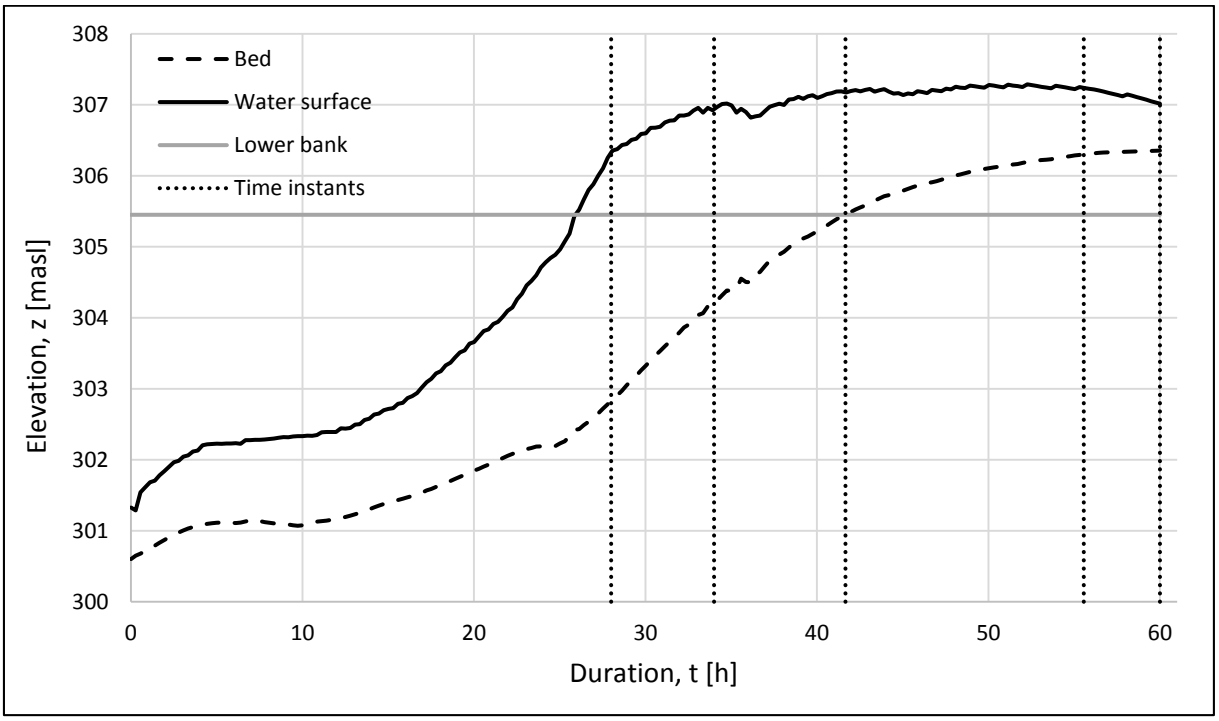

Figure IV-8 River bed and water surface elevation time evolution at Garibaldi bridge. Time instants used for outflow computation.

- For each of the chosen time instants, the relevant geometry has been retrieved from Basement output data and used as input for the HEC-RAS model. The value of discharge at the specific time instant and cross section has been consulted and used as an unsteady

boundary condition with a constant value. The output of this model is a constant discharge at the considered cross-section for the total duration of the event. The value of this constant is, therefore, the outflow discharge at the specific time instant for which the relevant geometry has been used. Due to the modelling differences between the two programs, there has been a disagreement between the water surface elevations at equivalent time instants. For this reason, the HEC-RAS model was further calibrated by changing the friction coefficient of the river bed so as to represent the same conditions obtained by Basement. Repeating this procedure for several points in time describes the outflow curve from the time of initial outflow until the end of the event. In order to make the process more clear a flow chart is presented on (Figure IV-10).

It is worth pointing out that following this approach, an erroneous bed aggradation will be computed after the initial outflow at the relevant cross-section (Garibaldi bridge) due to the decreased water discharge in the channel. Therefore, the bed elevation will be, to some extent, overestimated for the following time instants. However, this issue will not be addressed in the present work.

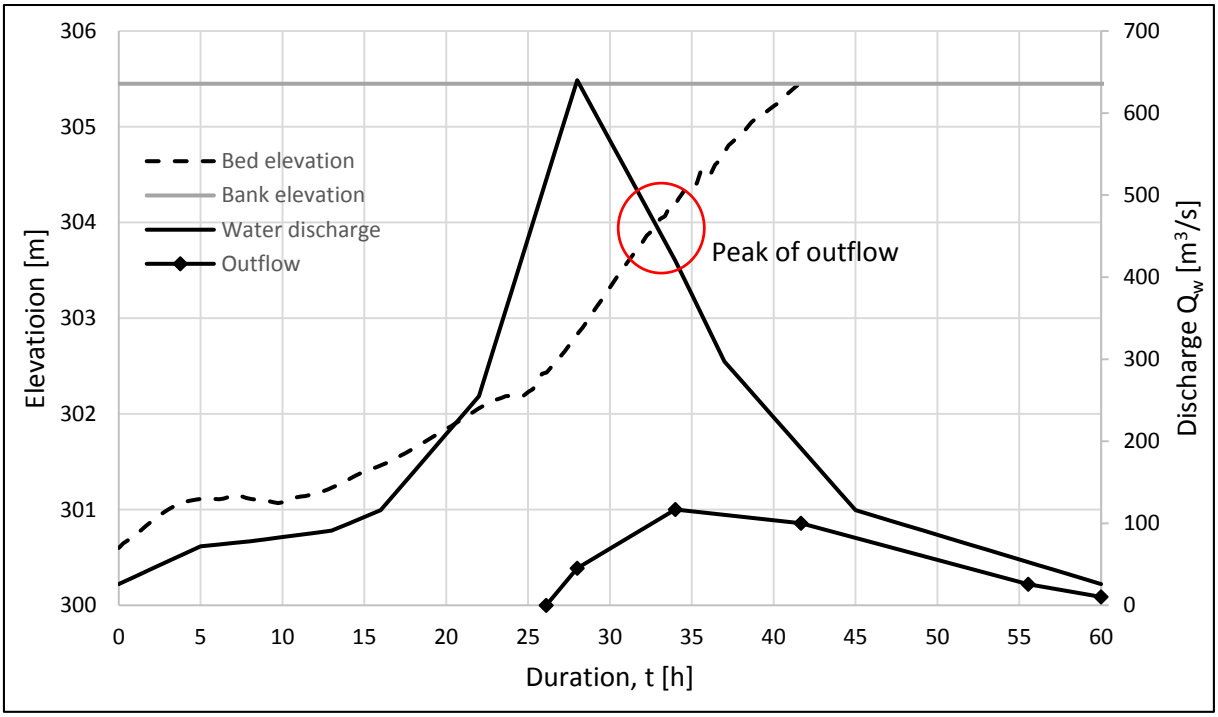

Figure IV-9 Time evolution of water discharge, river bed elevation and outflow at Garibaldi bridge.

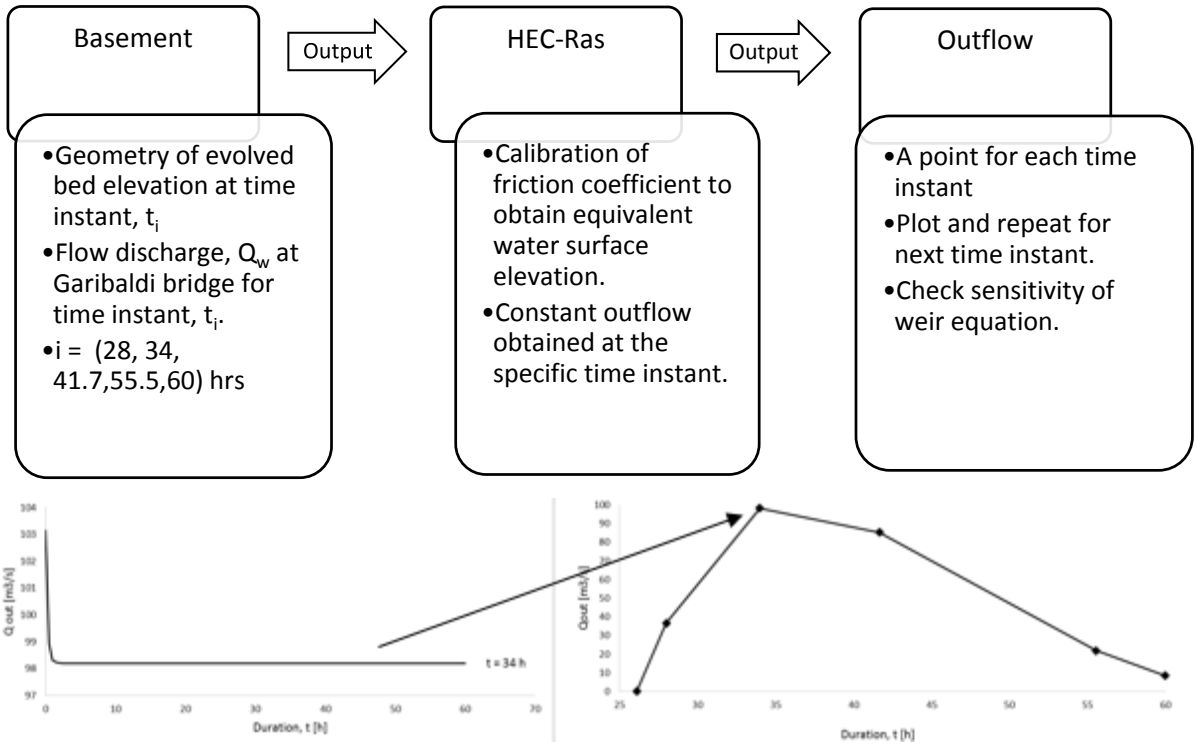

Figure IV-10 Flow chart describing the outflow computation procedure.

The computation of outflow in HEC-RAS is carried out by introducing a lateral weir between the sections where outflow is expected. The flow over the weir is then computed by the software by means of the standard weir equation:

$$Q_{out} = C_d H L^{3/2} \qquad \text{Eq. (IV.2)}$$

Where C_d is a weir flow coefficient, L is the length of the weir and H is the energy head above the weir. Therefore, the weir coefficient introduces a source of variability of the results since its choice is arbitrary. The HEC-RAS user manual recommends the coefficient to be chosen in the range $1.45 < C_d < 1.7$. In order to explore the effect of the choice of the coefficient on the results, the outflow has been computed for the two limit cases of weir coefficient.

Table IV-2 Outflow computation values

t [h]	$Q_{t,\ Garibaldi}$ [m^3/s]	Outflow discharge, Q_{out} [m^3/s]		Water volume, ΔW [m^3]	
		C_d 1.45	C_d 1.7	C_d 1.45	C_d 1.7
26.1	-	0	0		
28.0	640	45.33	50.84	154122	172856
34.0	426	116.77	127.88	1750680	1930176
41.7	194	100.06	108.55	2992254	3262734
55.6	53	25.7	27.94	3144000	3412250
60.0	27	10.3	11.3	288000	313920
			ΣW [m^3]	8,329,056	9,091,936

The outflow curves obtained from this quasi-static modelling approach is presented on Figure IV-11below. It can be observed that outflow begins at around 26 hours after the event has started and peaks 8 hours later with values of $Q_{peak} = 116.8 m^3 / s$ for $C_d = 1.45$ and $Q_{peak} = 127.9 m^3 / s$ for $C_d = 1.7$ respectively. An integration of the outflow curves with respect to time yields a total volume of outflow water between 8.3 and 9 million cubic meters.

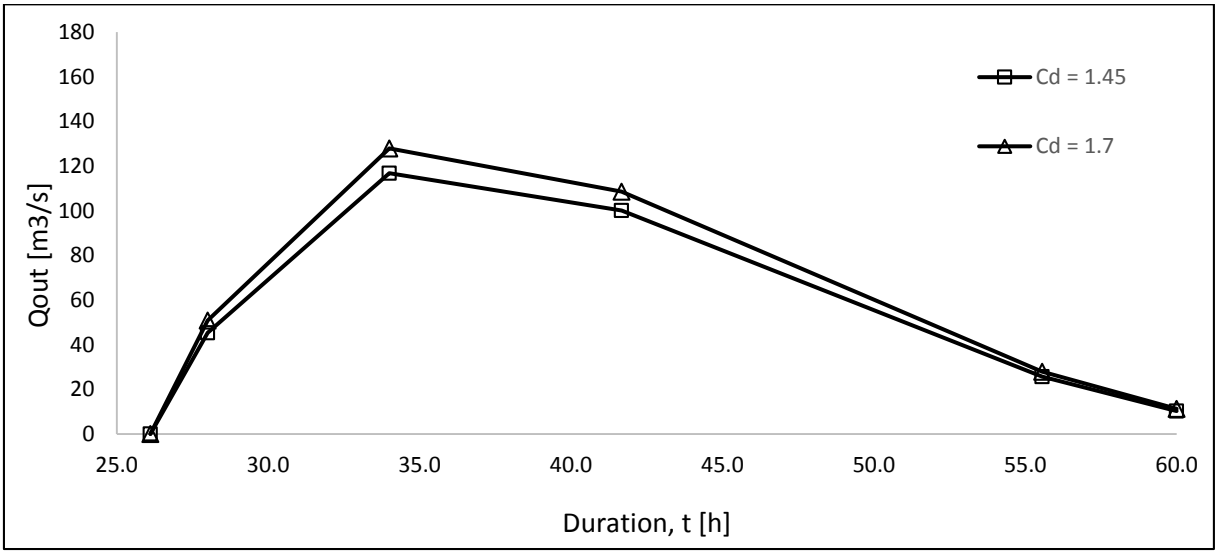

Figure IV-11 Outflow hydrograph.

3. Discussion of the results

In this chapter, an attempt was made to create a flood scenario as a result of the combined effect of an increased water discharge related to an intense rainfall event and the resulting morphological evolution of a river bed. A key concept of the model is the separation in space between the processes of sediment supply and sediment transport through a “break-point”. In terms of temporal consistency of the models, the obtained sediment volume has been artificially assigned a time development proportional to the relevant water discharge. During the process, however, several arbitrary modelling choices have been made. Naturally, they are a source of uncertainty for the model and their validity will be discussed.

In hydrologic modelling, a typical DDF curve has been used for the estimation of rainfall depth. Its parameters have been chosen so as to correspond to an event with intensity having a return period of 100 years. However, no indications for the duration of the event are available. For this reason a duration of 30 hours was assumed in order to obtain a relevant rainfall depth. Although a change in the duration of the event will not affect significantly the resulting rainfall depth, the latter is a key

parameter for the following sediment yield estimation as its variation is directly proportional to the volume obtained. In this sense, the duration of the rainfall event needs a proper evaluation.

The sediment yield model used here introduces the highest level of uncertainty in the process chain. Although the suitability of the Gavrilovic model has been validated for a number of case studies in mountainous regions, its formulation is intended for the estimation of a yearly erosion volume. In the present case, an attempt has been made to rescale it to an intense event level. This included, an implementation of the rainfall depth previously computed, a change in temperature values so as to be representative of summer, and a variation in land cover coefficient in order to capture the effect of increased protective vegetative cover, again related to the season. While the temperature values are estimated on the basis of recorded data, the other two parameters remain to a large extent arbitrary. The uncertainty relevant to rainfall depth estimation is prone to propagate in the sediment yield model with even a higher level of significance. Furthermore, the choice of a land cover coefficient which is based completely on an educated guess, introduces another major source of variability of the result. In fact, an application of a probabilistic method for the estimation of the coefficients used in Gavrilovic formula showed that the volume obtained can belong to a rather broad interval (Mazza et al. 2011). On the other hand, it is believed that short-duration events with significant return periods can lead to concentrated in time sediment yields (Ballio et al. 2010). The volume obtained with the rescaled Gavrilovic model (≈200,000 m^3) is about 1/3 of the volume calculated for the entire year (≈660,000 m^3). In this sense the result of the rescaling process is considered reasonable despite the uncertainty originating from the arbitrariness related to some of its parameters. Yet, a general flaw of the sediment supply model is that no information if provided about the temporal dynamics of the sediment production and the grain size distribution of the material. This poses a limitation for the following model of morphologic evolution of the river bed, since the above pieces of information are necessary as boundary conditions and, in the absence of any indication, certain assumptions need to be applied. In the present case, the time variation of the sediment discharge was considered to be proportional to the square of the water discharge variation. Although it may be expected that the two do not follow exactly the same pattern, the model showed no sensitivity to a time delay of the sediment supply. In terms of granulometry, the sediment size distribution used in Chapter III was adopted also here.

As it showed satisfactory results in the calibration process, it is considered reasonable and no further changes were carried out here. As mentioned earlier, the geometry used for this model was adjusted in order to accommodate the immense deposition of sediment at some sections. For this reason bank elevations were increased where needed and this led to a bed elevation extending over the real banks of the river. However, for the purpose of computing outflow discharge, it was assumed that

the bed elevation can increase up to the elevation of the real river bank. This can be considered then as another source of arbitrariness of the model. Yet, the distribution of deposited sediment volume in a certain cross section of the channel is a process that surely will not follow a predefined geometrical pattern. Conversely, the computational code distributes it by following the same pattern as the bed which was a choice made by the developers of the software. Therefore, assumptions about the material distributions fall in the margins of reality and are considered valid for the purpose of this scenario definition.

Finally, the computation of outflow has been carried out by means of a quasi-steady approach, namely, modelling an unsteady flood wave as a succession of several steady ones. The calculation of outflow discharge at several time instants describes the outflow curve pretty accurately allowing for the calculation of integrated volume of water flowing out of the river bed. The peak discharge and relevant outflow water volume show a rather low variability depending on the choice of weir coefficient, necessary for the implementation of the standard weir equation.

Conclusions

The study of solid transport is rather important, particularly in mountain areas, for the risk evaluation in terms of prevention, land use planning and protection of human life. In the context of flood hazard, the aim of this work has been modelling the morphologic evolution expected for a river bed as a consequence of a short-duration, intense events and related sediment supply. Using a basin in the Italian Alps for a case-study, an attempt was made to create a complete process chain based on integrated modelling of sediment transport on valley slopes and within the main water course of the basin. This thesis adopts as a starting point the work previously carried out at Politecnico di Milano on the study of solid transport in mountain streams. The goal of the present work was to create a comprehensive integration of sediment supply and the corresponding morphologic river bed evolution as a consequence of short-duration intense events considering both geological and hydraulic tools. A key aspect of the model was to find a reasonable way to connect the two processes and to produce a flood scenario for the town of Sondrio with an outflow hydrograph as a final outcome of the model.

In order to link the case study with the natural phenomena that pose the hazard in Valmalenco, this work started with a description of its features in terms of both geological and hydraulic aspects. In order to put into evidence the importance of the issue to the particular site, the notorious flood event that struck the entire Valtellina region in the summer of 1987 was described. As the latter involved the transport of considerable amount of sediment downstream, it provoked the onset of numerous investigations on the hazardous effect of morphological evolution of river beds, including this one. Some research on the topic, previously conducted at the Politecnico di Milano, was presented in order to summarize the current knowledge, including theoretical and methodological contributions to the topic as well as substantive findings.

Following the natural sequence of the processes, the geological contribution was analyzed first. Considering that the Mallero basin is characterized by numerous sources of solid mass into the streams (e.g. fault formations, debris flows, shallow and deep seated landslides, erosion) modelling the particular contribution of each one would be far too time and resource consuming for the scope of this work. On the other hand, examining the dimensions of the entire basin, it was assumed that localized sources would have a rather negligible effect on the total sediment production in comparison to a widespread phenomenon such as the erosion process. In addition, a possible landslide collapse would present an entirely different type of hydro-geological risk for the valley – a formation of an earth dam that could break and release an enormous water discharge downstream with negligible significance of the sediment yield. In this respect, the erosion phenomena was

outlined as responsible for the transfer of solid mass from the slopes in Valmalenco to the stream network. Therefore, the process was modelled by means of the Gavrilovic approach for calculating a yearly sediment yield. The calculation involved the determination of geometrical and empirical coefficients as well as the incorporation of numerical data, such as mean temperature and rainfall depth values. The computations were carried out both on the basis of sub-basin and entire basin levels, showing a strong variability between the results for the two cases, with the latter being considerably smaller than the former. This result was however considered invalid due to the large size of the Mallero basin that allows for the predominance of the zones of sediment accumulation over the zones of production. Therefore, the sub-basin division of the region was considered more reliable and this was supported by a comparison of the results obtained for a single sub-basin to a different analysis carried out on a site with similar dimensions. The latter was in fact validated by measurements at a reservoir downstream of the chosen region.

Following the phenomenological chain, the morphological evolution of Valmalenco's main stream was modelled by means of a numerical solver – Basement. A starting point was the reorganization of the cross-sectional geometry of Mallero river. A thorough understanding of the way in which the software works was needed in order to find a balance between simplification of the geometry and a stably working model. This led to the use of numerous iterations until the computation was carried out until its final time instant and reasonable river bed profiles were obtained. Further, a calibration of the model was performed to the historical records of the flood event of 1987. For the purpose, estimated water and sediment discharges were used as upstream boundary conditions for the model and the results compared to the measurements of river bed and water surface elevation. As calibration parameters, the friction coefficients of the channel and the sediment grain size distribution were varied until the best possible approximation was obtained. Choices related to the sediment grain size distribution were made on the basis of existing measurements. In turn, the friction coefficients were linked to the sediment sizes by means of the Manning-Strickler relationship. The outcome of this procedure was a calibrated model representing the flood event in a proper way. Although there was a significant underestimation of the river bed aggradation at some sections, the former was quite accurately captured at the critical locations near Garibaldi bridge. Calibrated model geometry as well as granulometry served as a base point for the production of the following integrated model.

Further, a complete scenario chain was attempted. A return period of 100 years served as a definition of the intensity of the event and therefore, the boundary conditions used for the different models were based on this value. In order to overcome the inconsistency between the temporal and spatial scales of the different models, a key concept of the modelling approach was the spatial

separation between supply and transport through a break-point, chosen within the catchments. This led to the twofold effect of 1) modelling sediment supply upstream of the break-point on a sub-basin level, while downstream the river stream was modelled with typical cross-section resolution; 2) time evolution of the sediment discharge was artificially created from the bulk sediment volume in order to serve as an upstream boundary condition for the hydro-morphological model. As the Gavrilovic approach was adopted as the most applicable for the region of interest, a major flaw was introduced in the process chain. The sediment volume obtained was representative of one year and therefore not applicable to a short duration event scenario. For this reason it was decided to downscale the computation by varying some of its parameters. Namely, in terms of rainfall depth, values representative of an event were computed on the basis of Depth-Duration-Frequency curve for a return period of 100 years. Further, in order to take into account seasonal variation of the state of vegetation as well as temperature, the respective parameters were varied in accordance to the four seasons. The results obtained showed the expected variability in sediment volume, with the highest value being that for the summer season. This volume was further used as a boundary condition in the morphological model and for the purpose, it was artificially distributed in time as a proportion of the water discharge. With this set up, a new aggradation pattern was developed for the particular scenario. As this showed bed elevation level over the real bank elevations at a particular section, it was considered that bed level could increase up to the elevation of the lower bank. On the basis of this assumption, outflow was obtained at one critical section – the one relevant to Garibaldi bridge. For this section, several time instants were chosen for which corresponding bed elevation and water discharge were extracted from Basement and used as input for a quasi-steady approximation in another software (HEC-RAS) in order to describe an outflow discharge curve, which represented the final outcome of the scenario.

From the development of the scenario, it was evident that the creation of a complete process chain for a flood scenario was indeed possible. The assumptions adopted during the process were discussed in the light of the limitations posed by the different models. In fact, a simple sensitivity analysis on the sediment boundary condition revealed that the downstream end of the river was unaffected by a change in volume of the solid mass. This implies that the largest effect on water surface elevation would originate from sediment that is already present in the bed before the event, at least for the duration of this particular case. It is however expected that for longer durations, there would be a sensible effect also on the downstream end of the river. However, an important outcome of this work was the implementation of an approach to deal with the missing interface between sediment yield from the slopes and its consequent transport in the streams. Downscaling the Gavrilovic formula furnished solid volumes for a short-term intense event rather than yearly values.

In this sense, the phenomenological chain developed here may be generalized and implemented in different case studies where the model would be highly sensitive to external sediment forcing. On the other hand, another interpretation of these results is the evident need for a more thorough investigation in the long-term time distribution of sediment yield in the streams. The present scenario definition is, however, concluded at this point, stimulating further work on the case study. The obtained outflow hydrograph presents an opportunity to be exploited in a further flood risk analysis. Its possible implementation in a 2-D computational software could be a powerful tool to predict the spatial and temporal distribution of the calculated volume of water in the town of Sondrio. The resulting hazard map could be used in combination with vulnerability and exposure assessment to obtain a flood risk map for an event of particular intensity.

Appendix A

Gavrilovic computations

Table A-1 Choice of values for Gavrilovic coefficients. Definitions translated from Italian from the original DUSAF description provided by Regione Lombardia.

COD_TOT	Ξ	Π	Φ	
511	0	0	0	Riverbeds and artificial waterways
332	0.95	0.6	0.2	Debris accumulations and lithoid outcrops deprived of vegetation
335	0	0	0	Glaciers and permanent snowfields
333	0.6	0.95	0.4	Sparse vegetation
5121	0	0	0	Natural reservoirs
3221	0.5	0.95	0.25	Bushes
3211	0.75	0.8	0.35	Natural grassland of high altitude with absence of tree and shrub species
5122	0	0	0	Artificial reservoirs
3121	0.15	0.8	0.05	Coniferous forests of medium and high density
3241	0.1	0.95	0.2	Scrub with a significant presence of shrubs and tall trees
131	1	0.5	0.2	Quarries
3122	0.3	0.95	0.1	Coniferous forests of low density
3212	0.45	0.8	0.2	Natural grassland of high altitude with presence of sparse tree and shrub species
2311	0.6	0.95	0.35	Grassland in the absence of tree and shrub species
31311	0.2	0.8	0.1	Mixed forests of medium and high density (ceduo)
2312	0.4	0.95	0.35	Grassland with sparse presence of tree and shrub species
1122	0.03	0.2	0	Nucleiforme residential area (30-50%)
31321	0.3	0.8	0.15	Mixed forests of low density (ceduo 0 cut more regularly)
331	0.9	1.8	0.8	Beaches, dunes and stony riverbeds
1123	0.01	0.95	0.03	Sparse residential area (10-30%)
1221	0	0	0	Road networks
12123	0	0	0	Technological facilites
3222	0.1	1.3	0.65	bank vegetation

31312	0.1	0.8	0.1	Mixed forests of medium and high density (fustaia)
12122	0	0	0	Public and private facilities
31121	0.35	0.8	0.15	Deciduous forests of low density (ceduo)
1422	0.05	0.1	0.1	Campsites and tourist facilities and accomodation
134	1	1.2	0.8	Degraded areas not used and not vegetated
1121	0.05	0.1	0	Discontinuous residential area (50-80 %)
1421	0	0	0	Sports facilities
1411	0.3	1.2	0.15	Parks and gardens
3113	0.5	1.8	0.8	Riparian formations
31111	0.25	0.8	0.15	Deciduous forests of medium and high density (ceduo)
12111	0	0	0	Industrial plants, commercial area
12124	0.3	1.5	0.1	Cemeteries
31112	0.25	0.8	0.1	Deciduous forests of medium and high density (fustaia)
133	0	0	0	Construction sites
314	0.2	0.8	0.15	Recent reforestation
31322	0.2	0.8	0.15	Mixed forests of low density
3242	0.45	0.95	0.25	Bushes in abandoned agricultural areas
221	0.55	0.8	0.3	Vineyeards
2111	0.6	0.9	0.2	Land subject to intensive cultivation, subjected to a system of rotation
222	0.1	0.8	0.25	Orchards and small fruit
2112	0.55	0.9	0.2	As 222 but with the presence of auxilliary wooden plants (olive trees)
2241	0.1	0.8	0.05	Poplar
1111	0	0	0	Dense residential area (>80% large residential buildings)
1112	0	0	0	Meidum dense residential area (>80% small residential buildings)
1222	0	0	0	Railway networks
12121	0	0	0	Hospital settlements
2115	0.6	0.8	0.25	Family agricultural gardens
1412	0.4	0.95	0.35	Uncultivated green areas

Table A-2 Values relative to the calculation of erosion yield by means of Gavrilovic formula on sub-basin and entire basin scales (Chapter II).

Basin ID	172	173	174	175	176	177	178	179	180	181	182	183	184	Alpe Gera	
t [°C]	8.79	-0.34	4.69	-0.63	2.01	0.25	-2.33	2.68	-2.84	-2.79	1.71	-3.67	-3.79	-3.79	
H [mm/y]	971.82	924.58	965.63	1154.62	1140.10	1313.89	1500.25	1433.90	1361.93	1416.73	965.34	1249.13	1119.89	1119.89	
A [km^2]	11.00	29.64	23.29	25.08	25.60	53.10	14.19	0.18	11.22	13.12	26.61	42.73	46.33	38.59	
O [km]	18.98	29.06	20.66	25.69	25.05	32.62	17.09	2.35	14.96	15.10	25.85	34.69	43.78	36.42	
ΔD [km]	0.52	1.71	0.96	1.46	1.07	1.15	0.83	0.08	0.88	0.88	0.93	1.17	1.19	0.82	
L [km]	5.14	13.89	4.82	8.67	3.82	11.03	5.44	0.40	4.35	4.67	6.54	9.25	7.47	7.72	
L_i [km]	6.21	53.98	39.02	28.44	30.34	93.67	42.47	0.02	5.31	16.46	55.88	33.65	65.55	46.95	
I [°]	24.67	34.10	35.21	27.94	29.29	29.74	31.68	20.59	33.29	31.90	29.91	27.43	24.38	24.79	
t [°C]	8.79	0.00	4.69	0.00	2.01	0.25	0.00	2.68	0.00	0.00	1.71	0.00	0.00	0.00	
T	0.99	0.32	0.75	0.32	0.55	0.35	0.32	0.61	0.32	0.32	0.52	0.32	0.32	0.32	
$\boxed{\Xi}$	0.26	0.59	0.24	0.59	0.48	0.53	0.74	0.37	0.65	0.59	0.44	0.59	0.60	0.60	
$\boxed{\Pi}$	0.71	0.78	0.81	0.76	0.75	0.76	0.71	1.08	0.53	0.53	0.74	0.51	0.52	0.52	
$\boxed{\Phi}$	0.14	0.22	0.13	0.21	0.17	0.18	0.23	0.26	0.16	0.17	0.14	0.15	0.18	0.18	
Z	0.93	2.77	1.19	2.45	2.03	2.25	3.09	1.90	2.04	1.81	1.84	1.61	1.60	1.62	
W	2726.07	4234.53	2967.07	4389.12	5700.39	4935.51	8083.38	7168.53	3955.06	3441.06	3944.62	2533.21	2258.74	2285.55	
R	0.21	0.68	0.57	0.49	0.50	0.57	0.82	0.10	0.22	0.40	0.70	0.33	0.65	0.44	ΣG [m^3]
G [m^3]	6,415	84,817	39,070	53,409	72,806	150,361	94,335	126	9,669	18,024	73,097	36,020	68,192	38,566	661,360
	Global routing coefficient														
A [km^2]	322.10														
O [km]	91.83														
ΔD [km]	1.90														
L [km]	80.34														
L_i [km]	464.79														
W.A	29992	125530.6	69113	110071	145943	262098	114688	1313.3	44369	45141	104967	108238	104646	88195.58	ΣG [m^3]
R_{global}	0.25														284,155

Table A-3 Computation of seasonal volumes of sediment yield by means of a downscaled Gavrilovic formula (Chapter IV).

Basin ID		172	173	174	175	176	177	178	179	180	181	182	183	184	Alpe gera	
H [mm/event]		170	170	170	170	170	170	170	170	170	170	170	170	170	170	
A [km^2]		11.00	29.64	23.29	25.08	25.60	53.10	14.19	0.18	11.22	13.12	26.61	42.73	46.33	38.59	
O [km]		18.98	29.06	20.66	25.69	25.05	32.62	17.09	2.35	14.96	15.10	25.85	34.69	43.78	36.42	
ΔD [km]		0.52	1.71	0.96	1.46	1.07	1.15	0.83	0.08	0.88	0.88	0.93	1.17	1.19	0.82	
L [km]		5.14	13.89	4.82	8.67	3.82	11.03	5.44	0.40	4.35	4.67	6.54	9.25	7.47	23.26	
L_i [m]		6.21	53.98	39.02	28.44	30.34	93.67	42.47	0.02	5.31	16.46	55.88	33.65	65.55	31.40	
I [°]		24.67	34.10	35.21	27.94	29.29	29.74	31.68	20.59	33.29	31.90	29.91	27.43	24.38	24.79	
Π		0.71	0.78	0.81	0.76	0.75	0.76	0.71	1.08	0.53	0.53	0.74	0.51	0.52	0.52	
Φ		0.14	0.22	0.13	0.21	0.17	0.18	0.23	0.26	0.16	0.17	0.14	0.15	0.18	0.18	
R		0.21	0.68	0.57	0.49	0.50	0.57	0.82	0.10	0.22	0.40	0.70	0.33	0.65	0.23	
t [°C]	Spring	9.58	2.09	6.22	1.86	4.02	2.58	0.45	4.57	0.04	0.08	3.78	0.00	0.00	0.00	
	Summer	18.55	10.25	14.83	9.98	12.38	10.78	8.43	12.99	7.97	8.02	12.11	7.21	7.10	6.55	
	Autumn	9.70	3.58	6.95	3.38	5.15	3.97	2.23	5.60	1.90	1.93	4.95	1.34	1.26	0.85	
	Winter	0.84	0.00	0.00	0.00	0.00	0.00	0.00	0.00	0.00	0.00	0.00	0.00	0.00	0.00	
T	Spring	1.03	0.56	0.85	0.53	0.71	0.60	0.38	0.75	0.32	0.33	0.69	0.32	0.32	0.32	
	Summer	1.40	1.06	1.26	1.05	1.16	1.09	0.97	1.18	0.95	0.95	1.15	0.91	0.90	0.87	
	Autumn	1.03	0.68	0.89	0.66	0.78	0.71	0.57	0.81	0.54	0.54	0.77	0.48	0.47	0.43	
	Winter	0.43	0.32	0.32	0.32	0.32	0.32	0.32	0.32	0.32	0.32	0.32	0.32	0.32	0.32	
Ξ	Spring/Autumn	0.26	0.59	0.24	0.59	0.48	0.53	0.74	0.37	0.65	0.59	0.44	0.59	0.60	0.62	
	Summer	0.21	0.47	0.19	0.47	0.39	0.42	0.59	0.29	0.52	0.47	0.35	0.47	0.48	0.49	
	Winter	0.31	0.70	0.29	0.71	0.58	0.63	0.89	0.44	0.78	0.71	0.53	0.71	0.73	0.74	
Z	Spring/Autumn	0.93	2.77	1.19	2.45	2.03	2.25	3.09	1.90	2.04	1.81	1.84	1.61	1.60	1.65	
	Summer	0.75	2.22	0.95	1.96	1.63	1.80	2.47	1.52	1.64	1.45	1.47	1.29	1.28	1.32	
	Winter	1.12	3.32	1.43	2.94	2.44	2.70	3.70	2.28	2.45	2.18	2.21	1.93	1.92	1.98	
W	Spring	495.90	1369.41	588.38	1091.99	1098.05	1079.50	1104.56	1045.95	503.32	429.83	921.87	344.75	342.88	358.58	
	Summer	482.30	1868.29	623.20	1532.37	1283.03	1401.86	2012.43	1186.44	1057.86	887.19	1093.00	706.79	698.30	705.06	
	Autumn	498.72	1665.57	617.48	1352.68	1215.71	1272.67	1647.46	1138.89	840.07	707.00	1029.21	526.90	515.00	487.77	
	Winter	271.44	1023.49	287.80	849.49	644.38	750.28	1204.07	582.76	648.96	542.78	554.53	453.19	450.72	471.37	ΣG [m^3]
G [m^3]	Spring	1167.02	27428.87	7747.69	13287.86	14024.36	32887.08	12890.39	18.43	1230.52	2251.44	17083.02	4902.10	10351.49	3222.72	140,881
	Summer	1135.02	37421.34	8206.20	18646.62	16386.93	42708.01	23485.52	20.90	2586.27	4647.09	20254.23	10049.92	21081.59	6336.64	199,158
	Autumn	1173.67	33360.87	8130.83	16460.04	15527.05	38772.10	19226.14	20.06	2053.83	3703.26	19072.20	7492.01	15547.92	4383.79	174,983
	Winter	638.79	20500.13	3789.66	10337.07	8230.09	22857.44	14051.72	10.27	1586.59	2843.08	10276.01	6443.98	13607.38	4236.37	110,297

Appendix B

Porosity calibration

Manual computation

Channel		Water		Sediment			
B [m]	20	Q [m^3/s]	100	d_s [m]	0.01	τ	41.7504
S_0 [-]	0.002	ρ [kg/m^3]	1000	s [-]	2.65	τ* [-]	0.257933
n [$s/m^{1/3}$]	0.04	g [m/s^2]	9.81			τ^*_c [-]	0.047
A [m^2]	54.06347	d [m]	2.703173				
P [m]	25.40635					Φ [-]	0.775012
R_h [m]	2.127951	Q_{target}	100			Q_{tc} [m^3/s]	0.062361

Δt [s]	6.786438
λ_p [-]	0.4
ΔQ_s [m^3]	0.124722

$$Q_w = \frac{1}{n} A \sqrt{S_0} R_h^{2/3}$$

(1) Water depth, d, found by iteration in order to obtain R_h for the following computation. (Goal seek)

$$\tau = \rho g R_H S_0$$

(2) Compute shear stress.

$$\tau * = \frac{\tau}{\rho g (s-1) d_s}$$

(3) Compute Shields' parameter.

$$\Phi = 8(\tau * - \tau_c^*)^{3/2}$$

$$Q_s = \Phi \sqrt{g(s-1)d_s^3}\,B$$

(4) Compute solid transport by means of Mayer-Peter-Muller formula

$$W = \frac{\Delta Q_s \Delta t}{(1-\lambda_p)}$$

(5) Compute deposited volume by means of the Exner equation.

W [m^3] = 1.410702

	Q_{tc} [m^3/s]	0.05893
$Q_{s,in} = 3Q_{tc}$	$Q_{s,in}$ [m^3/s]	0.17679
	ΔQ_s [m^3/s]	0.11786
	Δt [s]	6.78643833

		$\lambda_p = 0.4$	$\lambda_p = 40$
Δx [m]	z_{bed} [m]	z_{bed}	z_{bed}
0	1000	1000.0016	1000.0027
50	999.9	999.90	999.90
	dz	0.00160	0.00270
	W [m^3]	0.80000	1.35000

Appendix C

A Matlab code

```
close all
clear all
clc

importfile('outputfilename.dat')

nCS = % number of cross sections;
nTot = length(data(:,1));
dist = data(1:nCS,2);
time = data(1:nCS:nTot,1);
M = zeros(length(time)+1,length(dist)+1);
M(2:end,1) = time;
M(1,2:end) = dist;
M_t = cell(length(data(1,:)),1);

lbank = data(1:nCS,4)';
rbank = data(1:nCS,5)';

for j = 1:length(data(1,:))

    for i = 1:nCS

    col = data(i:nCS:end,j);
    M(2:end,i+1) = col;
    M_t(j) = {M};

    end
end

filename = 'Basement results.xlsx';
xlswrite(filename,M_t{3,1},'zbed')
xlswrite(filename,lbank,'lbank')
xlswrite(filename,rbank,'rbank')
xlswrite(filename,M_t{6,1},'mean bottom level')
xlswrite(filename,M_t{7,1},'WSE')
xlswrite(filename,M_t{8,1},'energy line')
xlswrite(filename,M_t{9,1},'Q')
xlswrite(filename,M_t{10,1},'Qnum')
xlswrite(filename,M_t{11,1},'C')
xlswrite(filename,M_t{12,1},'Qs')
xlswrite(filename,M_t{13,1},'Tau')
xlswrite(filename,M_t{14,1},'beta0')
xlswrite(filename,M_t{15,1},'betasub0')
xlswrite(filename,M_t{16,1},'sublayer thickness')
xlswrite(filename,M_t{17,1},'n sublayers')
```

```
plot(M_t{3,1}(1,2:end),M_t{3,1}(2,2:end),'-r',...
     M_t{3,1}(1,2:end),M_t{3,1}(end,2:end))
hold on
plot(M_t{3,1}(1,2:end),lbank,'--k',...
     M_t{3,1}(1,2:end),rbank,'--k')
hold on
legend('initial profile','final profile','lbank','rbank')
time_inst = nTot/nCS
disp('End of computation')
```

Note: The code has been developed on the basis of the output files from *Basement v2.3* of type "Matlab" as defined in the software. Due to differences in output formats of different versions of Basement, there is the possibility that the code is not compatible with older/newer versions of the software.

Bibliography

ASCE, 2008. *Sedimentation Engineering.* Reston, Virginia: American Society of Civil Engineers.

Ballio, F. et al., 2010. Evaluation of sediment yield from valley slopes: a case study. *WIT Transactions of Engineering Sciences,* Volume 67, pp. 149-160.

Bemporad, G. A. et al., 1997. A distributed approach for sediment yield evaluation in Alpine regions. *Journal of Hydrology,* Volume 197, pp. 370-392.

Brambilla, D., Longoni, L., Mazza, F. & Papini, M., 2011. Sediment yield from mountain slopes: a Gis Based automation of classic Gavrilovic method. *River Basin Management VI,* Volume 146.

Brambilla, D. et al., 2011. On Analysis Of Sediment Sources Toward Proper Characterization Of Hydro-geological Hazard For Mountain Environments. *International Journal of Safety and Security Engineering,* 1(4), pp. 424-438.

Chanson, H., 2004. *The Hydraulics of Open Channel Flow.* 2nd ed. Oxford, UK: Butterworth-Heinemann.

Crosta, G. B., Dal Negro, P. & Frattini, P., 2003. Soil slips and debris flows on terraced slopes. *Natural Hazards and Earth System Sciences,* Volume 3, pp. 31-42.

D'Amico, M. & Pregnolato, M., 2011. *Water Regime in the Alpine Space: Soil Erosion Study in the Adda River Basin,* s.l.: AdaptAlp.

De Michele, C., Rosso, R. & Mrulli, M. C., 2005. *Il regime delle precipitazioni intense sul territorio della Lombardia. Modello di previsione statistica delle precipitazioni di Forte Intensita e breve durata,* ARPA: DIIAR-CIMI, Politecnico di Milano.

De Vente, J. & Poesen, J., 2005. Predicting soil erosion and sediment yield at the basin scale: Scale issues and semi-quantitative models. *Earth-Science Reviews,* Volume 71, pp. 95-125.

Di Silvio, G., 1994. Floods and sediment dynamics in mountain rivers. In: G. Rossi, N. Harmancioglu & V. Yevjevic, eds. *Coping with floods.* Netherlands: Springer, pp. 375-392.

Elsayed, S. M., 2014. *Comparative study of different scenarios for the morhpological evolution in a river stream.* Lecco: MSc Thesis. Politecnico di Milano, Italy.

Euronews, 2014. *Heavy rains wreak havoc along Swiss-Italian border.* [Online]
Available at: http://www.euronews.com/2014/11/16/heavy-rains-wreak-havoc-along-swiss-italian-border/
[Accessed 24 11 2014].

European Floods Directive, 2007. Directive 2007/60/EC of the European Parliament and of the Council of 23 October 2007 on the assessment and management of flood risks.. *Official Journal of the European Union,* Volume 288, pp. 27-34.

Filippetti, P. & Zoppi, A. M., 2012. *Evoluzione morphologica di un alveo montano.* Lecco, Italy: MSc Thesis. Politecnico di Milano.

Francani, V., Gattinoni, P. & Rampazzo, R., 2011. Slope instability triggered by climate change in periglacial areas. *Italian Journal of Engineering Geology and Environment,* Том 2, pp. 39-62.

Gavrilovic, Z., 1976. Bujicni tokovi i erozija. *Gradevinski kalendar,* pp. 159-311.

Guzzetti, F., Crosta, G., Marchetti, M. & Reichenbach, P., 1992. *Debris flows triggered by the July, 17-19, 1987 storm in the Valtellina area (Northern Italy).* Bern, Proceedings Interpraevent, pp. 193-204.

Ismes & Cae, 1988a. *Lineamenti per un piano di intervento per la protezione della città di Sondrio. Rapporto di Associazione Temporanea di Imprese nell'ambito di "Piani di allarme connessi alla situazione di rischio idrometeorologico nella Val Malenco".*

Ismes & Cae, 1988b. *Modello di simulazione dell'inondazione in Sondrio. Rapporto di Associazione Temporanea di Imprese nell'ambito di "Piani di allarme per situazioni di rischio idrometeorologico del torrente Mallero".*

Italtekna, Bonifica, Spea & Lombardia Risorse, 1989. *Stima delle portate di piena centenarie, bacino del torrente Mallero. Report of temporary firm syndicate within 'Piano Programma di Ricostruzione e Sviluppo della Valtellina e delle zone adiacenti delle Provincie di Como, Bergamo e Brescia colpite dalle avversità atmosferiche dei mesi di luglio e agosto 1987.*

Italtekna, Bonifica, Spea & Lombardia Risorse, 1990. *Aspetti idraulici ed idrologici, studi idraulici e sul trasporto solido. Report of temporary firm syndicate within 'Piano Programma di Ricostruzione e Sviluppo della Valtellina e delle zone adiacenti delle Provincie di Como, Bergamo e Brescia colpite dalle avversità atmosferiche dei mesi di luglio e agosto 1987.*

Julien, P. Y. & Simons, D. B., 1985. Transport capacity of overland flow. *American Society of Agricultural Engineers,* 23(3), pp. 755-762.

Klaassen, G. J., 1997. *Flooding risks in mountain areas.* TU Delft, FRIMAR.

Mayhew, F., 2014. *Italy floods kill four as storm hits village festival.* [Online]
Available at: http://www.independent.co.uk/news/world/europe/italy-floods-kill-four-as-storm-hits-village-festival-9645041.html
[Accessed 16 08 2014].

Mazza, F., Longoni, L., Papini, M. & Brambilla, D., 2012. *A hybrid method (Monte Carlo/possibilistic approach) to evaluate soil erosion in Alpine valleys.* Riverside, California, 6th International Conference on River Basin Management.

Meusburger, K., 2010. *Soil erosion in the Alps - causes and risk assessment.* Basel: MSc thesis. University of Basel.

Molinari, D., Menoni, S. & Ballio, F., 2013. *Flood early warning systems.* Southhampton, UK: WIT Press.

Morgan, R. C. P., 2005. *Soil Erosion & Conservation.* 3rd ed. Oxford: Blackwell Publishing.

Overeem, A., Adri, B. & Iwan, H., 2008. Rainfall depth-duration-frequency curves and their uncertainties. *Journal of Hydrology,* Volume 348, pp. 124-134.

Radice, A. & Elsayed, S. M., 2014. Hydro-morphologic modelling for different calamitous scenarios in a mountain stream. In: S. A., G. de Cesare, M. J. Franca & M. Pfister, eds. *River Flow 2014.* London: Taylor & Francis Group, p. 1603–1610.

Radice, A. et al., 2012. On integrated sediment transport modelling for flash events in mountain environments.. *Acta Geophysica,* Volume 60, pp. 191-213.

Radice, A. & Rosatti, G., 2012. *Sulla modellazione idraulico-morfologica dei corsi d'acqua: il torrente Mallero e la propagazione dell'incertezza legata all'alimentazione solida.* Brescia, XXXIII Convegno di Idraulica e Costruzioni Idrauliche.

Radice, A. et al., 2012. Management of flood hazard via hydro-morphological river modelling. The case of the Mallero in Italian Alps. *Journal of Flood Risk Management,* 6(3), pp. 197 - 209.

Reid, S. C., Stuart, N. L., Berney, J. M. & Holden, J., 2007. The timing and magnitude of coarse sediment transport events within an upland, temperate gravel-bed river. *Geomorphology,* Volume 83, pp. 152-182.

Uboldi, F. et al., 2014. A spatial bootstrap technique for parameter estimation of rainfall annual maxima distribution. *Hydrology and Earth System Sciences,* Volume 18, p. 981–995.

UCLA, 2010. *Meteorology: Frequently, infrequently and never asked questions.* [Online] Available at: http://web.atmos.ucla.edu/~fovell/meteo/meteorology_FINAQ.html [Accessed 15 07 2014].

Wang, Z., Lee, J. H. W. & Melching, C. S., 2012. *River Dynamics and Integrated River Management.* 2nd ed. London: Springer.

Wohl, E. & Merritt, D., 2005. Prediction of mountain stream morphology. *Water resources research,* Volume 41.